

T-1307.

THE EFFECT OF SUBSURFACE GEOLOGIC STRUCTURE IN  
ELECTROMAGNETIC INDUCTION PROSPECTING

ARTHUR LAKES LIBRARY  
COLORADO SCHOOL OF MINES  
GOLDEN, COLORADO

By

Richard G. Geyer

ProQuest Number: 10795987

All rights reserved

INFORMATION TO ALL USERS

The quality of this reproduction is dependent upon the quality of the copy submitted.

In the unlikely event that the author did not send a complete manuscript and there are missing pages, these will be noted. Also, if material had to be removed, a note will indicate the deletion.



ProQuest 10795987

Published by ProQuest LLC (2019). Copyright of the Dissertation is held by the Author.

All rights reserved.

This work is protected against unauthorized copying under Title 17, United States Code  
Microform Edition © ProQuest LLC.

ProQuest LLC.  
789 East Eisenhower Parkway  
P.O. Box 1346  
Ann Arbor, MI 48106 – 1346

A thesis submitted to the Faculty and the Board of Trustees of the Colorado School of Mines in partial fulfillment of the requirements for the degree of Doctor of Philosophy.

Signed: Richard G. Geyer  
Richard G. Geyer

Golden, Colorado

Date: May 13, 1970

Approved: G. V. Keller  
Dr. G. V. Keller  
Thesis Advisor

ARTHUR LAKES LIBRARY  
COLORADO SCHOOL OF MINES  
GOLDEN, COLORADO

J. C. Hollister  
Prof. J. C. Hollister  
Head of Department

Golden, Colorado

Date: May 13, 1970

## ABSTRACT

Few subsurface geometric configurations have been studied in electromagnetic induction prospecting. In particular, geophysicists have usually considered only models of the earth which are flat and which consist of parallel regions of contrasting electrical conductivity.

In order to evaluate the electric and magnetic field over subsurface geologic structure, the earth is modeled by two conductive layers which are joined at an irregular interface. Maxwell's equations are then applied to obtain a set of integral equations for the electromagnetic field which are solved by using a perturbation technique.

After giving consideration both to generalized resistivity ranges for rocks of different lithology and age and to geologic structures which are of particular interest in petroleum and mineral exploration, horizontal electric field and apparent resistivity master curves are calculated. These curves demonstrate that for a given subsurface structure and resistivity contrast, the horizontal electric field anomaly is greater when the first layer is more conductive than the second layer than when the second layer is more conductive than the first layer. When the wavelength of the electromagnetic field is less than the width of a resistant anticlinal ridge, the horizontal electric field decreases over the ridge.

On the other hand, when the wavelength is much greater than the width of a resistant ridge, the horizontal electric field increases over that ridge.

If the resistivity contrast, electric field anomaly, and first-layer thickness are known, the depth to the crest of an anticlinal ridge may be ascertained. Similarly, overburden thickness determinations accurate to within 10 % can be made from electric field anomalies provided that the width of the subsurface structure is small relative to the depth to the structure.

ARTHUR LAKES LIBRARY  
COLORADO SCHOOL OF MINES  
GOLDEN, COLORADO

## TABLE OF CONTENTS

	Page
ABSTRACT . . . . .	iii
ILLUSTRATIONS . . . . .	vii
ACKNOWLEDGMENTS . . . . .	ix
INTRODUCTION . . . . .	1
FORMULATION OF INTEGRAL EQUATIONS . . . . .	5
Case of $\vec{H}$ -Field Polarization . . . . .	8
Case of $\vec{E}$ -Field Polarization . . . . .	20
SOLUTION OF THE INTEGRAL EQUATIONS . . . . .	28
Case of $\vec{H}$ -Field Polarization . . . . .	29
Case of $\vec{E}$ -Field Polarization . . . . .	37
TESTS ON NUMERICAL EVALUATION FOR $\vec{H}$ -FIELD POLARIZATION . . . . .	44
Fourier Inversion . . . . .	45
Asymptotic Behavior for Low Frequencies . . . . .	51
Asymptotic Behavior far from Subsurface Geologic Structure . . . . .	58
Asymptotic Behavior for Homogeneous Halfspace . . . . .	61
Resolution of Perturbation Technique . . . . .	61
NUMERICAL EXAMPLES FOR $\vec{H}$ -FIELD POLARIZATION . . . . .	66
Electric Field Master Curves for Anticline versus Syncline . . . . .	68

	Page
Electric Field Master Curves for Varying $\beta$ . . .	73
Frequency Sounding Electric Field Master Curves for Anticline and Syncline . . . . .	73
Apparent Resistivity Master Curves . . . . .	87
Master Curves for Depth to Subsurface Ridge . .	90
Master Curves for Overburden Thickness Determination . . . . .	91
CONCLUSIONS . . . . .	95
REFERENCES . . . . .	96

## ILLUSTRATIONS

Figure		Page
1.	Nonplanar region of contrasting conductivity . . . . .	3
2.	Fourier transform of $\text{sinc}^2$ function . . . . .	48
3.	Fourier transform of Gaussian function . . . . .	50
4.	Wavenumbers as a function of frequency and conductivity . . . . .	53
5.	Subsurface triangular ridge . . . . .	55
6.	Electric field anomalies over triangular ridge . . . . .	57
7.	Apparent resistivity anomalies over triangular ridge . . . . .	59
8.	Magneto-telluric curves far from subsurface geologic structure . . . . .	62
9. - 12.	Electric field master curves for anticline versus syncline . . . . .	69 - 72
13. - 16.	Electric field master curves for anticline for varying $\beta$ . . . . .	74 - 77
17. - 20.	Frequency sounding electric field master curves for anticline . . . . .	78 - 81
21. - 24.	Frequency sounding electric field master curves for syncline . . . . .	83 - 86
25.	Magneto-telluric curves with anticlinal ridge on second layer . . . . .	88
26.	Magneto-telluric curves with synclinal trough on second layer . . . . .	89
27.	Master curves for depth to subsurface ridge . . . . .	92
28.	Master curves for overburden thickness determination . . . . .	93

## TABLES

Table		Page
1	Comparison of analytic and digital inverse Fourier transform for triangle . . . . .	49
2	Comparison of analytic and digital inverse Fourier transform for Gaussian function . . . . .	50
3	Comparison of calculated apparent resistivity with true resistivity of a homogeneous halfspace for various values of $1/h_1 G_1$ . .	63
4	Generalized resistivity ranges for rocks of different lithology and age . . . . .	67

## ACKNOWLEDGMENTS

First and foremost, the author wishes to express his sincere gratitude for the inspiration and the guidance provided to him by Professor George V. Keller during the course of this investigation. Professor Keller contributed a great deal of help in giving many valuable suggestions and comments to make this completion possible.

Special thanks for support are also due to the National Defense Education Act Title IV fellowship program, to Texaco Oil Company, and to the United States Department of Interior under the Bonneville Power Administration Research Grant 88. Finally, the author is indebted to King Resources Company for the use of computer facilities.

Felicitas magna vitae est ne perturbationes habere.

--- Seneca

INTRODUCTION

Changes in the earth's magnetic field which originate above the earth's surface induce currents which flow beneath the earth's surface. Similarly, changes in the magnetic fields of controlled sources which are used by geophysicists in investigating the electrical properties of the earth's subsurface also induce currents which flow beneath the earth's surface. In either case, the induced currents have an associated magnetic field frequently called a secondary field, which the geophysicist may measure to explore anomalously conductive or anomalously resistive regions in the subsurface. Thus the geophysicist may map variations in the earth's electrical properties by measuring changes in the natural electromagnetic field or by measuring the distortion caused by the presence of a conductive earth in an electromagnetic field produced by a controlled source. Generally, the electromagnetic methods of geological exploration have been used most commonly in mining exploration, where the objective is to detect an anomaly in the electromagnetic field strength caused by a conductive ore body.

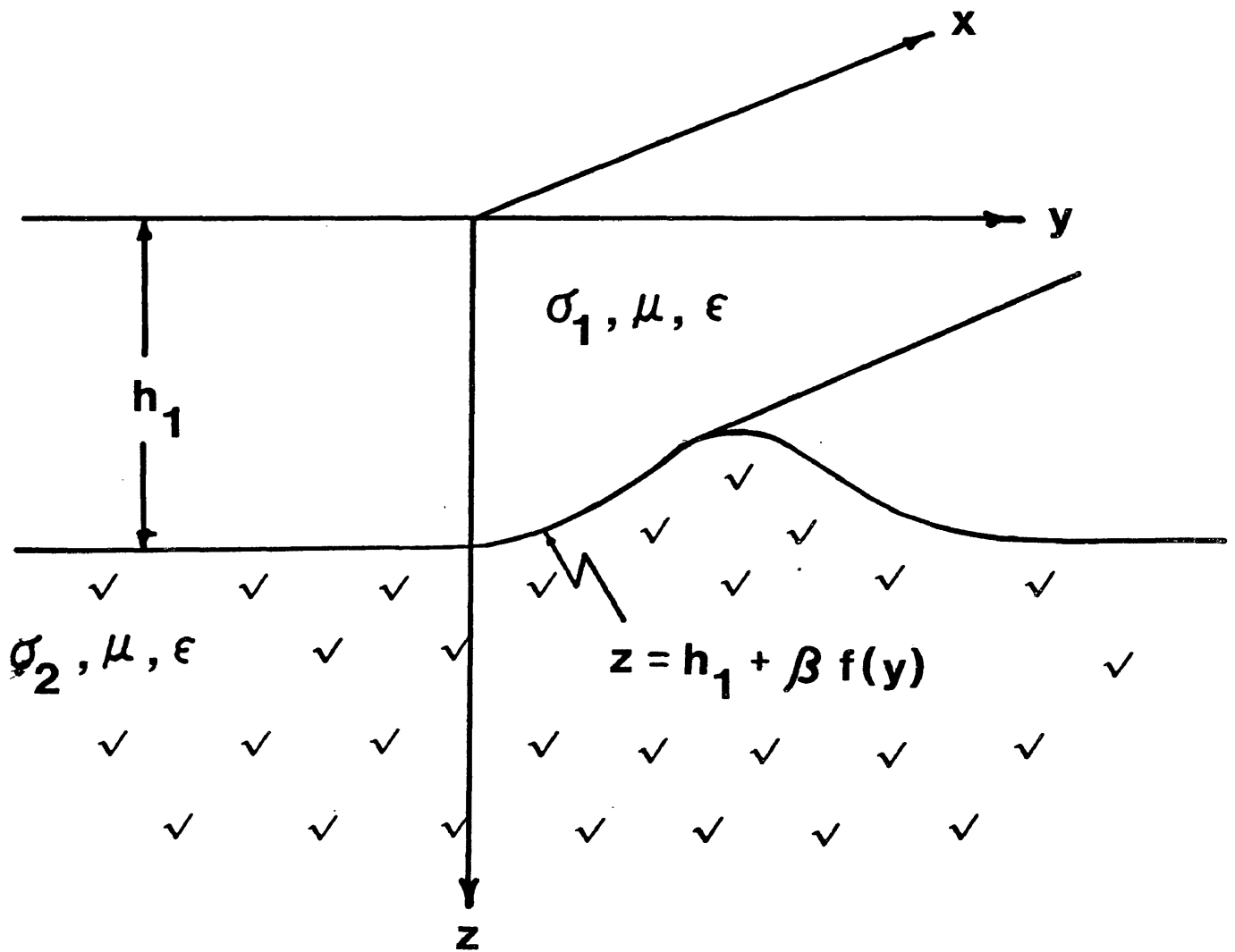
Only for relatively few configurations has the effect of subsurface geometry on the electromagnetic field been studied. Specifically, only cases of horizontally or vertically divided regions of contrasting conductivities (i.e., flat-lying geological horizons or vertical faults: Cagniard (1953), Van'ian (1965), Wait (1962), Weaver (1963)) have been solved quite generally mathematically.

Recently, Obukhov (1962, 1965, 1968), Dmitriev (1965, 1969), and Feinberg (1961) have outlined mathematical approaches for studying the effect of various types of irregularities in the surface of an insulating basement on the magnetotelluric field observed at the earth's surface. Mann (1964) outlines an approach for a basement surface which is sinusoidal in shape.

In this thesis the effect of an irregular subsurface horizon on the electromagnetic field and on the impedance measured at the earth's surface is investigated. The geometry considered is that of a conducting halfspace composed of two regions of differing electrical conductivities; these two layers are joined at a nonplanar interface. In particular, the effects of a subsurface anticline and syncline on the electromagnetic field and measured apparent resistivity are considered (see Figure 1).

The electromagnetic field is found for two polarizations which make either the incident magnetic or incident electric field parallel to the anticlinal ridge or synclinal trough. Formal solutions to the problem are obtained following procedures suggested by Obukhov (1962, 1965, 1969), Dmitriev (1965, 1969), Feinberg (1961), and Mann (1964). Throughout this investigation, the normally incident wave is assumed to be planar.

In order to evaluate the electric and magnetic field over subsurface geologic structure, a set of integral equations is formulated from Maxwell's equations for a rather general shape of the interface. A solution is found by a perturbation procedure. Numerical evaluation for the case of magnetic field polarization



**NONPLANAR REGION OF  
CONTRASTING CONDUCTIVITY**

**Figure 1**

is performed, and graphs of the electric field and of the apparent resistivity for various geometries, conductivity contrasts, and depths to the interface between the two layers are given.

FORMULATION OF INTEGRAL EQUATIONS

The behavior of an electromagnetic field in any medium is described by Maxwell's equations,

$$\nabla \cdot \vec{B} = 0 \quad \dots \dots \dots (1)$$

$$\nabla \cdot \vec{E} = s_t / \epsilon \quad \dots \dots \dots (2)$$

RMKS

$$\nabla \times \vec{H} = \vec{J}_t \quad \dots \dots \dots (3)$$

$$\nabla \times \vec{E} = - \partial \vec{B} / \partial t \quad \dots \dots \dots (4)$$

where  $\vec{B}$  is the magnetic induction field in webers per meter<sup>2</sup>,  $\vec{E}$  is the electric field in volts per meter,  $s_t$  is the total charge density in coulombs per meter<sup>3</sup>,  $\epsilon$  is the dielectric constant of free space ( $8.854 \times 10^{-12}$  farads per meter),  $\vec{H}$  is the magnetic field intensity in amperes per meter, and  $\vec{J}_t$  is the total current density in amperes per meter<sup>2</sup>.

In the problem at hand, all media are assumed to be charge-free; that is, there is no accumulation of free charge or polarization charge, or

$$s_t = s_f + s_p = 0$$

where  $s_f$  is the free-charge density and  $s_p$  is the polarization charge density. Thus equation (2) may be rewritten

$$\nabla \cdot \vec{E} = 0 \quad \dots \dots \dots (5)$$

Indeed, Jones (1964) has shown in quite straightforward fashion that there can be no permanent distribution of free charge in a linear homogeneous conductor with non-zero conductivity.

The constitutive equations for the conduction current density  $\vec{J}$  and the magnetic induction field  $\vec{B}$  for an electrically and magnetically linear isotropic medium are

$$\vec{J} = \sigma \vec{E} \quad \dots \dots \dots (6)$$

and

$$\vec{B} = \mu \vec{H} \quad \dots \dots \dots (7)$$

where  $\sigma$  is the electrical conductivity and  $\mu$  is the magnetic permeability. Similarly, the constitutive equation for an electrically linear isotropic medium expressing the relationship between the electric displacement field  $\vec{D}$  and the electric field  $\vec{E}$  is

$$\vec{D} = \epsilon \vec{E} \quad \dots \dots \dots (8)$$

In equation (3)  $\vec{J}_t$  represents the sum of conduction current density and displacement current density, that is,

$$\vec{J}_t = \vec{J} + \partial \vec{D} / \partial t$$

Hence equation (3) may be written

$$\nabla \times \vec{H} = \vec{J} + \partial \vec{D} / \partial t \quad \dots \dots \dots (9)$$

The wave equations satisfied by the electric and magnetic fields will now be considered. From equation (9),

$$\nabla \times \nabla \times \vec{H} = \nabla \times \vec{J} + \frac{\partial}{\partial t} \nabla \times \vec{D}$$

or since

$$\nabla \times \vec{J} = \sigma \nabla \times \vec{E} = -\sigma \partial \vec{B} / \partial t = -\mu \sigma \partial \vec{H} / \partial t \quad (7)$$

and

$$\nabla \times \vec{D} = -\epsilon \mu \partial \vec{H} / \partial t,$$

$$\nabla \times \nabla \times \vec{H} = -\mu \sigma \frac{\partial \vec{H}}{\partial t} - \epsilon \mu \frac{\partial^2 \vec{H}}{\partial t^2} \dots (10)$$

Now

$$\nabla \times \nabla \times \vec{H} = \nabla (\nabla \cdot \vec{H}) - \nabla^2 \vec{H}.$$

Use of Gauss' law (equation (1)) and equation (7) yields

$$\nabla \cdot \vec{B} = 0 = \nabla \cdot \mu \vec{H} = \mu \nabla \cdot \vec{H} + \vec{H} \cdot \nabla \mu$$

and since  $\nabla \mu$  is zero because homogeneity in  $\mu$  is assumed,

$$\nabla \cdot \vec{H} = 0$$

. Thus equation (10) may be rewritten

$$\nabla^2 \vec{H} = \mu \sigma \partial \vec{H} / \partial t + \epsilon \mu \partial^2 \vec{H} / \partial t^2 \dots (11)$$

In an exactly analogous manner it can be shown that

$$\nabla^2 \vec{E} = \mu \sigma \partial \vec{E} / \partial t + \epsilon \mu \partial^2 \vec{E} / \partial t^2 \dots (12)$$

Since experience has shown that the magnetotelluric field is quasi-periodic in the frequency range commonly used in electrical prospecting (Keller and Frischknecht, 1966) and since periodic sources are generally used in electrical prospecting, the electric and magnetic

fields may be represented as

$$\vec{E}_h = \vec{E} e^{i\omega t}$$

and

$$\vec{B}_h = \vec{B} e^{i\omega t}$$

where the subscript  $h$  merely denotes a harmonically varying field.

Substitution of the latter two equations into equations (11) and

(12) yield

$$\nabla^2 \vec{H} - i\omega\mu(\sigma + i\omega\epsilon)\vec{H} = 0 \quad \dots \dots (13)$$

and

$$\nabla^2 \vec{E} - i\omega\mu(\sigma + i\omega\epsilon)\vec{E} = 0 \quad \dots \dots (14)$$

The quantity  $i\omega\mu(\sigma + i\omega\epsilon)$  is designated as the constant  $\gamma^2$  for a fixed angular frequency  $\omega$ , i.e.,

$$\gamma^2 = i\omega\mu(\sigma + i\omega\epsilon) \quad \dots \dots (15)$$

where  $\gamma$  is called the propagation constant for the medium characterized by  $\mu$ ,  $\epsilon$ , and  $\sigma$ . A solution for equations (13) and (14) must now be sought which (a) satisfies the appropriate continuity conditions across the interface shown in Figure 1, (b) is independent of the  $x$ -coordinate, and (c) behaves properly at infinity.

Case of Magnetic Polarization --- The first case to be considered is that of  $\vec{H}$ -polarization. For  $\vec{H}$ -polarization, the direction of the magnetic field vector in the primary plane wave is taken parallel to the coordinate axis along which the properties of the medium are

invariant; that is, the incident  $\vec{H}$  field has the form

$$\vec{H}^{\text{incident}} = H_0 [\exp(-ikhz), 0, 0] \dots (16)$$

Note that expression (16) denotes a plane wave propagating in the  $+z$  direction. Similarly, for  $\vec{E}$ -polarization the incident  $\vec{E}$  field has the form

$$\vec{E}^{\text{incident}} = E_0 [\exp(-ikhz), 0, 0] \dots (17)$$

Equation (16) implies that it is only necessary to solve equation (13) for  $H_x$ . Then, by application of Ampere's law (equation (3)), there results

$$\begin{aligned} \nabla \times \vec{H} &\sim \begin{vmatrix} \hat{i}_x & \hat{i}_y & \hat{i}_z \\ \partial/\partial x & \partial/\partial y & \partial/\partial z \\ H_x & 0 & 0 \end{vmatrix} = \hat{i}_y \frac{\partial H_x}{\partial z} - \hat{i}_z \frac{\partial H_x}{\partial y} \\ &= (\sigma + i\omega\epsilon) (E_y \hat{i}_y + E_z \hat{i}_z) \end{aligned}$$

where  $\hat{i}_y$  and  $\hat{i}_z$  represent unit vectors in the  $y$  and  $z$  directions, respectively. Thus it is sufficient, for the case of  $\vec{H}$ -polarization, to solve equation (13) for  $H_x$  only and to derive  $E_y$  and  $E_z$  from equation (3). For  $\vec{E}$ -polarization equation (14) is solved for  $E_x$ , and then  $H_y$  and  $H_z$  are derived from equation (4). The solution for  $H_x$  will be presented in some detail and the observation made that the solution for  $E_x$  is entirely similar.

If the region  $z < 0$  is denoted as region 0, the region  $h_1 + \beta f(y) > z > 0$  as region 1, and the region  $z > h_1 + \beta f(y)$  as region 2, where region 0 contains air and where regions 1 and

2 contain conductive earth material, the equations for  $H_x$  in each region may be written as

$$\nabla^2 H_{0x} + \omega^2 \mu \epsilon H_{0x} = 0$$

$$\nabla^2 H_{1x} - i\omega\mu\sigma_1 H_{1x} = 0$$

$$\nabla^2 H_{2x} - i\omega\mu\sigma_2 H_{2x} = 0$$

or

$$\nabla^2 H_{0x} + k^2 H_{0x} = 0 \quad \dots (19)$$

$$\nabla^2 H_{1x} - \gamma_1^2 H_{1x} = 0 \quad \dots (20)$$

$$\nabla^2 H_{2x} - \gamma_2^2 H_{2x} = 0 \quad \dots (21)$$

where  $k^2 = \omega^2 \mu \epsilon$ ,  $\gamma_1^2 \equiv i\omega\mu\sigma_1$ , and  $\gamma_2^2 \equiv i\omega\mu\sigma_2$ .

In equations (20) and (21),  $\omega\epsilon \ll \sigma$ , which means that conduction currents are much greater than displacement currents in regions 1 and 2. The parameter  $\mu$  will be assumed to be equal to its free space value in all regions.

In order to solve equations (19), (20), and (21), a Fourier transform in the  $y$  coordinate of each equation is taken, and the resulting differential equation is then solved (see Obukhov, 1962, 1965, 1969 and Mann, 1964). Equations (19), (20), and (21) may be written in orthogonal Cartesian coordinates as

$$\partial^2 H_{0x} / \partial y^2 + \partial^2 H_{0x} / \partial z^2 + k^2 H_{0x} = 0 \quad \dots (19)$$

$$\partial^2 H_{1x} / \partial y^2 + \partial^2 H_{1x} / \partial z^2 - \gamma_1^2 H_{1x} = 0 \quad \dots (20)$$

$$\partial^2 H_{2x} / \partial y^2 + \partial^2 H_{2x} / \partial z^2 - \gamma_2^2 H_{2x} = 0 \quad \dots (21)$$

The Fourier transform of the  $n$ th spatial derivative of a function

$f(y, z)$  with respect to  $y$  is equal to  $(-i\xi)^n$  times the Fourier transform of  $f(y, z)$  with respect to  $y$  (Papoulis, 1962); hence

$$\int_{-\infty}^{\infty} \left\{ \frac{\partial^2 f(y, z)}{\partial y^2} \right\} = -\xi^2 F(\xi, z)$$

where  $F(\xi, z)$  is the Fourier transform of  $f(y, z)$  with respect to  $y$  and  $\xi$  is the spatial radian wavenumber in the  $y$  direction.

Hence the following transformed equations are obtained

$$-\xi^2 H_{0X}(\xi, z) + \partial^2 H_{0X}(\xi, z) / \partial z^2 + k^2 H_{0X}(\xi, z) = 0$$

$$-\xi^2 H_{1X}(\xi, z) + \partial^2 H_{1X}(\xi, z) / \partial z^2 - \gamma_1^2 H_{1X}(\xi, z) = 0$$

$$-\xi^2 H_{2X}(\xi, z) + \partial^2 H_{2X}(\xi, z) / \partial z^2 - \gamma_2^2 H_{2X}(\xi, z) = 0$$

or, more simply,

$$\frac{\partial^2 H_{0X}(\xi, z)}{\partial z^2} + (k^2 - \xi^2) H_{0X}(\xi, z) = 0 \quad \dots \quad (22)$$

$$\frac{\partial^2 H_{1X}(\xi, z)}{\partial z^2} - (\gamma_1^2 + \xi^2) H_{1X}(\xi, z) = 0 \quad \dots \quad (23)$$

$$\frac{\partial^2 H_{2X}(\xi, z)}{\partial z^2} - (\gamma_2^2 + \xi^2) H_{2X}(\xi, z) = 0 \quad \dots \quad (24)$$

Solutions to equations (22), (23), and (24) are exponentials, that

is, 
$$H_{0X}(\xi, z) = c_1 e^{\beta_0 z} + c_2 e^{-\beta_0 z}$$

where  $\beta_0 = (\xi^2 - k^2)^{\frac{1}{2}}$  and  $c_1$  and  $c_2$  are arbitrary constants.

Similarly,

$$H_{1X}(\xi, z) = c_3 e^{\beta_1 z} + c_4 e^{-\beta_1 z}$$

and

$$H_{2X}(\xi, z) = c_5 e^{\beta_2 z} + c_6 e^{-\beta_2 z}$$

where  $\mathcal{N}_1 = (\xi^2 + \sigma_1^2)^{\frac{1}{2}}$ ,  $\mathcal{N}_2 = (\xi^2 + \sigma_2^2)^{\frac{1}{2}}$  and  $c_3$ ,  $c_4$ ,  $c_5$ , and  $c_6$  are arbitrary constants. (Branches are taken such that  $\text{Re}(\mathcal{N}_0)$ ,  $\text{Re}(\mathcal{N}_1)$ , and  $\text{Re}(\mathcal{N}_2) \geq 0$  on real axis in  $\xi$ -plane for proper convergence of integrals.)

The solution for  $H_{0x}(y, z)$  in the upper halfspace consists of a primary term (the incident  $\vec{H}$  field) and a secondary term (the  $\vec{H}$  field due to the presence of the two layers). Because the secondary magnetic field in the upper halfspace (region 0) consists only of a reflected term (energy dissipated in the  $-z$  direction), the magnetic field in region 0 may be written as

$$H_{0x}(y, z) = H_0 e^{-ikz} + \frac{H_0}{2\pi} \int_{-\infty}^{\infty} A(\xi) e^{\mathcal{N}_0 z} e^{i\xi y} d\xi \dots (25)$$

For convenience, equation (25) will be normalized by the incident field strength  $H_0$  and it will be understood henceforth that  $H_{0x}$ ,  $H_{1x}$ , and  $H_{2x}$  represent the magnetic field strength components normalized by  $H_0$  in the upper halfspace, the first layer, and the second layer, respectively.

The magnetic field in region 1 (the first layer) consists of energy dissipated in both the  $+z$  and  $-z$  directions; hence the field present in the first layer is best written as

$$H_{1x}(y, z) = \frac{1}{2\pi} \int_{-\infty}^{\infty} [B(\xi) e^{\mathcal{N}_1 z} + C(\xi) e^{-\mathcal{N}_1 z}] e^{i\xi y} d\xi \dots (26)$$

Finally, in the second layer (region 2) there is only energy dissipated in the  $+z$  direction; thus

$$H_{2x}(y, z) = \frac{1}{2\pi} \int_{-\infty}^{\infty} D(\xi) e^{\mathcal{N}_2 z} e^{i\xi y} d\xi \dots (27)$$

In the derivations of the above solutions, the transform terms have been required to be bounded in the respective regions. Uniqueness of solution has been described by several authors including Sommerfeld (1964), Rellich (1943), Jones (1964), Morse and Feshbach (1953), and Stratton (1941). The solution indicated in equation (25) satisfies Sommerfeld's condition of radiation (Sommerfeld, 1964, p. 182-200) and, provided this solution satisfies the continuity conditions at the surface of the earth, "we may be then convinced that the unique solution of the mathematical problem is identical with the solution that is realized in nature" (Sommerfeld, 1964, p. 190). In like manner, provided that tangential boundary conditions in  $\vec{E}$  and  $\vec{H}$  are satisfied at the surface of the earth and at  $z = h_1 + \beta f(y)$ , uniqueness of solution in regions 1 and 2 (equations (26) and (27)) is assured (Stratton, 1941, p. 486-488). The unknown functions  $A(\xi)$ ,  $B(\xi)$ ,  $C(\xi)$ , and  $D(\xi)$  are to be determined by use of the boundary conditions. From equations (3) and (6),

$$E_{0y}(y, z) = -\frac{i}{\omega \epsilon} \partial H_{0x}(y, z) / \partial z$$

$$E_{0z}(y, z) = \frac{i}{\omega \epsilon} \partial H_{0x}(y, z) / \partial y$$

$$E_{1y}(y, z) = \frac{1}{\sigma_1} \partial H_{1x}(y, z) / \partial z$$

$$E_{1z}(y, z) = -\frac{1}{\sigma_1} \partial H_{1x}(y, z) / \partial y$$

$$E_{2y}(y, z) = \frac{1}{\sigma_2} \partial H_{2x}(y, z) / \partial z$$

$$E_{2z}(y, z) = -\frac{1}{\sigma_2} \partial H_{2x}(y, z) / \partial y$$

Use of equations (25), (26), and (27) then yields

$$E_{0y}(y, z) = \frac{-k}{\omega \epsilon} e^{-ikz} - \frac{i}{2\pi\omega\epsilon} \int_{-\infty}^{\infty} A(\xi) \mathcal{J}_0 e^{\mathcal{J}_0 z} e^{i\xi y} d\xi \quad \dots (28)$$

$$E_{0z}(y, z) = -\frac{1}{2\pi\omega\epsilon} \int_{-\infty}^{\infty} A(\xi) \xi e^{\mathcal{J}_0 z} e^{i\xi y} d\xi \quad \dots (29)$$

$$E_{1y}(y, z) = \frac{1}{2\pi\sigma_1} \int_{-\infty}^{\infty} [B(\xi) e^{\mathcal{J}_1 z} - C(\xi) e^{-\mathcal{J}_1 z}] \mathcal{J}_1 e^{i\xi y} d\xi \quad \dots (30)$$

$$E_{1z}(y, z) = \frac{-i}{2\pi\sigma_1} \int_{-\infty}^{\infty} [B(\xi) e^{\mathcal{J}_1 z} + C(\xi) e^{-\mathcal{J}_1 z}] \xi e^{i\xi y} d\xi \quad \dots (31)$$

$$E_{2y}(y, z) = -\frac{1}{2\pi\sigma_2} \int_{-\infty}^{\infty} D(\xi) \mathcal{J}_2 e^{-\mathcal{J}_2 z} e^{i\xi y} d\xi \quad \dots (32)$$

$$E_{2z}(y, z) = \frac{-i}{2\pi\sigma_2} \int_{-\infty}^{\infty} D(\xi) \xi e^{-\mathcal{J}_2 z} e^{i\xi y} d\xi \quad \dots (33)$$

To find A, B, C, and D the usual boundary conditions on the tangential electric and magnetic fields are applied. These boundary conditions are

$$\left. \begin{array}{l} H_{0x} = H_{1x} \\ E_{0y} = E_{1y} \end{array} \right\} \quad \text{at } z = 0 \quad \dots (34)$$

$$\left. \begin{aligned} H_{1x} &= H_{2x} \\ \vec{n} \times \vec{E}_1 &= \vec{n} \times \vec{E}_2 \end{aligned} \right\} \text{ at } z = h_1 + \beta f(y) \dots (35)$$

where  $\vec{n}$  is the unit normal to the interface  $z = h_1 + \beta f(y)$ . (Application of Stoke's theorem and the divergence theorem demonstrates that continuity in the tangential components of  $\vec{H}$  implies continuity in the normal component of the total current density. A similar application shows that continuity in the tangential components of  $\vec{E}$  implies continuity in the normal component of the magnetic induction field  $\vec{B}$ .) As Kaplan (1952, p. 100 - 104) shows, the unit normal  $\vec{n}$  to the surface between the two layers may be expressed as the normalized gradient vector of the function

$$g(y, z) \triangleq z - h_1 - \beta f(y)$$

That is,

$$\vec{n} \sim (0, n_y, n_z) = (0, -\beta \frac{df(y)}{dy}, 1) \cdot [1 + \beta^2 (\frac{df}{dy})^2]^{-1/2} \dots (36)$$

Substitution of equations (25), (26), (28), and (30) into equations (34) yields

$$1 + \frac{1}{2\pi} \int_{-\infty}^{\infty} A(\xi) e^{i\xi y} d\xi = \frac{1}{2\pi} \int_{-\infty}^{\infty} [B(\xi) + C(\xi)] e^{i\xi y} d\xi \dots (37)$$

$$-\frac{k}{\omega \epsilon} - \frac{i}{2\pi \omega \epsilon} \int_{-\infty}^{\infty} A(\xi) \eta_0 e^{i\xi y} d\xi = \frac{1}{2\pi \sigma_1} \int_{-\infty}^{\infty} [B(\xi) - C(\xi)] \eta_1 e^{i\xi y} d\xi \dots (38)$$

If use is made of the identity (Papoulis, 1962, p. 37)

$$1 \longleftrightarrow 2\pi \delta(\xi)$$

where  $\longleftrightarrow$  denotes the Fourier transform, and if Fourier transforms of both sides of equations (37) and (38) are taken, the

following algebraic equations in  $B(\xi)$  and  $C(\xi)$  result,

$$2\pi \delta(\xi) + A(\xi) = B(\xi) + C(\xi)$$

$$-\frac{k\sigma}{\omega \epsilon} 2\pi \delta(\xi) - \frac{i\sigma_1}{\omega \epsilon} A(\xi) \mathcal{J}_0 = [B(\xi) - C(\xi)] \mathcal{J}_1$$

or

$$B(\xi) = \frac{1}{2} \left[ 2\pi \delta(\xi) \left( 1 - \frac{k\sigma_1}{\omega \epsilon \mathcal{J}_1} \right) + A(\xi) \left( 1 - \frac{i\sigma_1 \mathcal{J}_0}{\omega \epsilon \mathcal{J}_1} \right) \right] \dots (39)$$

$$C(\xi) = \frac{1}{2} \left[ 2\pi \delta(\xi) \left( 1 + \frac{k\sigma_1}{\omega \epsilon \mathcal{J}_1} \right) + A(\xi) \left( 1 + \frac{i\sigma_1 \mathcal{J}_0}{\omega \epsilon \mathcal{J}_1} \right) \right] \dots (40)$$

Similarly, substitution of equations (26), (27), (30), (31), (32), and (33) into equations (35) yields

$$\begin{aligned} & \int_{-\infty}^{\infty} \left[ B(\xi) e^{\mathcal{J}_1 [h_1 + \beta f(y)]} + C(\xi) e^{-\mathcal{J}_1 [h_1 + \beta f(y)]} \right] e^{i\xi y} d\xi \\ &= \int_{-\infty}^{\infty} D(\xi) e^{-\mathcal{J}_2 [h_1 + \beta f(y)]} e^{i\xi y} d\xi \end{aligned}$$

$$- \frac{i n_y}{2 \pi \sigma_1} \int_{-\infty}^{\infty} [B(\xi) e^{\beta_1 [h_1 + \beta f(y)]} + C(\xi) e^{-\beta_1 [h_1 + \beta f(y)]}] \xi e^{i \xi y} d\xi$$

$$- \frac{n_z}{2 \pi \sigma_1} \int_{-\infty}^{\infty} [B(\xi) e^{\beta_1 [h_1 + \beta f(y)]} - C(\xi) e^{-\beta_1 [h_1 + \beta f(y)]}] \beta_1 e^{i \xi y} d\xi$$

$$= - \frac{i n_y}{2 \pi \sigma_2} \int_{-\infty}^{\infty} D(\xi) \xi e^{-\beta_2 [h_1 + \beta f(y)]} e^{i \xi y} d\xi$$

$$+ \frac{n_z}{2 \pi \sigma_2} \int_{-\infty}^{\infty} D(\xi) \beta_2 e^{-\beta_2 [h_1 + \beta f(y)]} e^{i \xi y} d\xi$$

The latter two equations may be simplified to yield

$$\begin{aligned} & \pi \left[ 1 - \left( \frac{\sigma_1}{i \omega \epsilon} \right)^{1/2} \right] e^{h_1 \beta_1} e^{\beta \beta_1 f(y)} + \pi \left[ 1 + \left( \frac{\sigma_1}{i \omega \epsilon} \right)^{1/2} \right] e^{-h_1 \beta_1} e^{-\beta \beta_1 f(y)} \\ & + \frac{1}{2} \int_{-\infty}^{\infty} A(\xi) \left[ \left( 1 + \frac{\sigma_1 \beta_0}{i \omega \epsilon \beta_1} \right) e^{h_1 \beta_1} e^{\beta \beta_1 f(y)} \right. \\ & \quad \left. + \left( 1 - \frac{\sigma_1 \beta_0}{i \omega \epsilon} \right) e^{-h_1 \beta_1} e^{-\beta \beta_1 f(y)} \right] e^{i \xi y} d\xi \\ & = \int_{-\infty}^{\infty} D(\xi) e^{-h_1 \beta_2} e^{-\beta \beta_2 f(y)} e^{i \xi y} d\xi \dots (41) \end{aligned}$$

and

$$-n_z \left\{ \pi \left[ 1 - \left( \sigma_1 / i\omega \epsilon \right)^{1/2} \right] e^{h_1 \gamma_1} e^{\beta \gamma_1 f(y)} \right.$$

$$\left. - \pi \left[ 1 + \left( \frac{\sigma_1}{i\omega \epsilon} \right)^{1/2} \right] e^{-h_1 \gamma_1} e^{-\beta \gamma_1 f(y)} \right\} \gamma_1$$

$$- \frac{i n_y}{2} \int_{-\infty}^{\infty} A(\xi) \left\{ \left[ 1 + \frac{\sigma_1 \gamma_0}{i\omega \epsilon \gamma_1} \right] e^{h_1 \gamma_1} e^{\beta \gamma_1 f(y)} \right.$$

$$\left. + \left[ 1 - \frac{\sigma_1 \gamma_0}{i\omega \epsilon \gamma_1} \right] e^{-h_1 \gamma_1} e^{-\beta \gamma_1 f(y)} \right\} \xi e^{i\xi y} d\xi$$

$$- \frac{n_z}{2} \int_{-\infty}^{\infty} A(\xi) \left\{ \left[ 1 + \frac{\sigma_1 \gamma_0}{i\omega \epsilon \gamma_1} \right] e^{h_1 \gamma_1} e^{\beta \gamma_1 f(y)} \right.$$

$$\left. - \left[ 1 - \frac{\sigma_1 \gamma_0}{i\omega \epsilon \gamma_1} \right] e^{-h_1 \gamma_1} e^{-\beta \gamma_1 f(y)} \right\} \gamma_1 e^{i\xi y} d\xi$$

$$= - i n_y \frac{\sigma_1}{\sigma_2} \int_{-\infty}^{\infty} \xi D(\xi) e^{-\gamma_2 h_1} e^{-\beta \gamma_2 f(y)} e^{i\xi y} d\xi$$

$$+ n_z \frac{\sigma_1}{\sigma_2} \int_{-\infty}^{\infty} D(\xi) \gamma_2 e^{-h_1 \gamma_2} e^{-\beta \gamma_2 f(y)} e^{i\xi y} d\xi$$

... (42)

For convenience the following notation will be adopted

$$\lambda \triangleq \sigma_1 / \sigma_2$$

$$P \triangleq \left( 1 + \frac{\sigma_1 \mathcal{J}_0}{i\omega \epsilon \mathcal{J}_1} \right) e^{h_1 \mathcal{J}_1}$$

$$Q \triangleq \left( 1 - \frac{\sigma_1 \mathcal{J}_0}{i\omega \epsilon \mathcal{J}_1} \right) e^{-h_1 \mathcal{J}_1}$$

$$R \triangleq \pi \left[ 1 - (\sigma_1 / i\omega \epsilon)^{1/2} \right] e^{h_1 \mathcal{J}_1}$$

$$S \triangleq \pi \left[ 1 + (\sigma_1 / i\omega \epsilon)^{1/2} \right] e^{-h_1 \mathcal{J}_1}$$

so that equations (41) and (42) may be rewritten in the following manner:

$$\begin{aligned} & R e^{\beta \mathcal{J}_1 f(y)} + S e^{-\beta \mathcal{J}_1 f(y)} \\ & + \frac{1}{2} \int_{-\infty}^{\infty} A(\xi) \left[ P e^{\beta \mathcal{J}_1 f(y)} + Q e^{-\beta \mathcal{J}_1 f(y)} \right] e^{i\xi y} d\xi \\ & = \int_{-\infty}^{\infty} D(\xi) e^{-h_1 \mathcal{J}_2} e^{-\beta \mathcal{J}_2 f(y)} e^{i\xi y} d\xi \quad \dots (43) \end{aligned}$$

and

$$\begin{aligned}
& -n_z \left[ R e^{\beta \alpha_1 f(y)} - S e^{-\beta \alpha_1 f(y)} \right] \alpha_1 \\
& - \frac{i n_y}{2} \int_{-\infty}^{\infty} A(\xi) \left[ P e^{\beta \alpha_1 f(y)} + Q e^{-\beta \alpha_1 f(y)} \right] \xi e^{i \xi y} d\xi \\
& - \frac{n_z}{2} \int_{-\infty}^{\infty} A(\xi) \left[ P e^{\beta \alpha_1 f(y)} - Q e^{-\beta \alpha_1 f(y)} \right] \alpha_1 e^{i \xi y} d\xi \\
& = -i n_y \lambda \int_{-\infty}^{\infty} \xi D(\xi) e^{-h_1 \alpha_2} e^{-\beta \alpha_2 f(y)} e^{i \xi y} d\xi \\
& \quad + n_z \lambda \int_{-\infty}^{\infty} D(\xi) \alpha_2 e^{-h_1 \alpha_2} e^{-\beta \alpha_2 f(y)} e^{i \xi y} d\xi \dots (44)
\end{aligned}$$

Equations (43) and (44) are simultaneous integral equations of the first kind for  $A(\xi)$  and  $D(\xi)$  (Hildebrand, 1965, p. 222 - 223).

Case of Electric Polarization --- When the incident wave is given by equation (17), a similar procedure may be used to formulate a set of integral equations; that is, the counterpart of equation (25) for the case of electric polarization is

$$E_{0x}(y, z) = E_0 e^{-i k z} + \frac{E_0}{2\pi} \int_{-\infty}^{\infty} A^*(\xi) e^{\alpha_0 z} e^{i \xi y} d\xi \dots (45)$$

Again, for convenience, normalization by  $E_0$  will be assumed and it will be understood henceforth that  $E_{0x}$ ,  $E_{1x}$ , and  $E_{2x}$  represent

normalized electric field components. Thus

$$E_{1x}(y, z) = \frac{1}{2\pi} \int_{-\infty}^{\infty} [B^*(\xi) e^{\lambda_1 z} + C^*(\xi) e^{-\lambda_1 z}] e^{i\xi y} d\xi \dots (46)$$

$$E_{2x}(y, z) = \frac{1}{2\pi} \int_{-\infty}^{\infty} D^*(\xi) e^{-\lambda_2 z} e^{i\xi y} d\xi \dots (47)$$

From equations (4) and (7),

$$H_{0y}(y, z) = -\frac{1}{i\omega\mu} \partial E_{0x}(y, z) / \partial z$$

$$H_{0z}(y, z) = \frac{1}{i\omega\mu} \partial E_{0x}(y, z) / \partial y$$

$$H_{1y}(y, z) = -\frac{1}{i\omega\mu} \partial E_{1x}(y, z) / \partial z$$

$$H_{1z}(y, z) = \frac{1}{i\omega\mu} \partial E_{1x}(y, z) / \partial y$$

$$H_{2y}(y, z) = -\frac{1}{i\omega\mu} \partial E_{2x}(y, z) / \partial z$$

$$H_{2z}(y, z) = \frac{1}{i\omega\mu} \partial E_{2x}(y, z) / \partial y$$

Use of equations (45), (46), and (47) in the latter expressions for the magnetic field yields

$$H_{0y}(y, z) = \frac{k}{\omega \mu} e^{-ikz} + \frac{i}{2\pi \omega \mu} \int_{-\infty}^{\infty} A^*(\xi) \mathcal{J}_0 e^{\mathcal{J}_0 z} e^{i\xi y} d\xi \dots (48)$$

$$H_{0z}(y, z) = \frac{1}{2\pi \omega \mu} \int_{-\infty}^{\infty} \xi A^*(\xi) e^{\mathcal{J}_0 z} e^{i\xi y} d\xi \dots (49)$$

$$H_{1y}(y, z) = \frac{i}{2\pi \omega \mu} \int_{-\infty}^{\infty} \left[ B^*(\xi) e^{\mathcal{J}_1 z} - C^*(\xi) e^{-\mathcal{J}_1 z} \right] \mathcal{J}_1 e^{i\xi y} d\xi \dots (50)$$

$$H_{1z}(y, z) = \frac{1}{2\pi \omega \mu} \int_{-\infty}^{\infty} \left[ B^*(\xi) e^{\mathcal{J}_1 z} + C^*(\xi) e^{-\mathcal{J}_1 z} \right] \xi e^{i\xi y} d\xi \dots (51)$$

$$H_{2y}(y, z) = \frac{-i}{2\pi \omega \mu} \int_{-\infty}^{\infty} D^*(\xi) \mathcal{J}_2 e^{-\mathcal{J}_2 z} e^{i\xi y} d\xi \dots (52)$$

$$H_{2z}(y, z) = \frac{1}{2\pi \omega \mu} \int_{-\infty}^{\infty} D^*(\xi) e^{-\mathcal{J}_2 z} \xi e^{i\xi y} d\xi \dots (53)$$

To find  $A^*$ ,  $B^*$ ,  $C^*$ , and  $D^*$ , the continuity conditions on the electric and magnetic fields must again be applied. These boundary conditions are

$$\left. \begin{aligned} E_{0x} &= E_{1x} \\ H_{0y} &= H_{1y} \end{aligned} \right\} \text{at } z = 0 \dots (54)$$

$$\left. \begin{aligned} E_{1x} &= E_{2x} \\ \hat{n} \times \vec{H}_1 &= \hat{n} \times \vec{H}_2 \end{aligned} \right\} \text{at } z = h_1 + \beta F(y) \dots (55)$$

Substitution of equations (45), (46), (48), and (50) into equations (40) yields

$$1 + \frac{1}{2\pi} \int_{-\infty}^{\infty} A^*(\xi) e^{i\xi y} d\xi = \frac{1}{2\pi} \int_{-\infty}^{\infty} [B^*(\xi) + C^*(\xi)] e^{i\xi y} d\xi \dots (56)$$

$$\frac{hk}{\omega\mu} + \frac{i}{2\pi\omega\mu} \int_{-\infty}^{\infty} A^*(\xi) \mathcal{J}_0 e^{i\xi y} d\xi = \frac{i}{2\pi\omega\mu} \int_{-\infty}^{\infty} [B^*(\xi) - C^*(\xi)] \mathcal{J}_1 e^{i\xi y} d\xi \dots (57)$$

By taking Fourier transforms of both sides of equations (56) and (57),  $B^*(\xi)$  and  $C^*(\xi)$  may be found. I.e.,

$$2\pi\delta(\xi) + A^*(\xi) = B^*(\xi) + C^*(\xi)$$

$$\frac{hk}{\omega\mu} 2\pi\delta(\xi) + \frac{i}{\omega\mu} A^*(\xi) \mathcal{J}_0 = \frac{i\mathcal{J}_1}{\omega\mu} [B^*(\xi) - C^*(\xi)]$$

Thus

$$B^*(\xi) = \frac{1}{2} \left[ 2\pi\delta(\xi) \left( 1 - \frac{ikh}{\mathcal{J}_1} \right) + A^*(\xi) \left( 1 + \frac{\mathcal{J}_0}{\mathcal{J}_1} \right) \right] \dots (58)$$

$$C^*(\xi) = \frac{1}{2} \left[ 2\pi\delta(\xi) \left( 1 + \frac{ikh}{\mathcal{J}_1} \right) + A^*(\xi) \left( 1 - \frac{\mathcal{J}_0}{\mathcal{J}_1} \right) \right] \dots (59)$$

Similarly, substitution into equation (55) of equations (46), (47), (50), (51), (52), and (53) leads to the following two equations

$$\begin{aligned} & - \int_{-\infty}^{\infty} \left[ B^*(\xi) e^{\lambda_1 [h_1 + \beta f(y)]} + C^*(\xi) e^{-\lambda_1 [h_1 + \beta f(y)]} \right] e^{i\xi y} d\xi \\ & = \int_{-\infty}^{\infty} D^*(\xi) e^{-\lambda_2 [h_1 + \beta f(y)]} e^{i\xi y} d\xi \end{aligned}$$

$$\frac{\eta y}{2\pi\omega\mu} \int_{-\infty}^{\infty} \left[ B^*(\xi) e^{\lambda_1 [h_1 + \beta f(y)]} + C^*(\xi) e^{-\lambda_1 [h_1 + \beta f(y)]} \right] \xi e^{i\xi y} d\xi$$

$$- \frac{i\eta z}{2\pi\omega\mu} \int_{-\infty}^{\infty} \left[ B^*(\xi) e^{\lambda_1 [h_1 + \beta f(y)]} - C^*(\xi) e^{-\lambda_1 [h_1 + \beta f(y)]} \right] \lambda_1 e^{i\xi y} d\xi$$

$$= \frac{\eta y}{2\pi\omega\mu} \int_{-\infty}^{\infty} D^*(\xi) e^{-\lambda_2 [h_1 + \beta f(y)]} \xi e^{i\xi y} d\xi$$

$$+ \frac{i\eta z}{2\pi\omega\mu} \int_{-\infty}^{\infty} D^*(\xi) \lambda_2 e^{-\lambda_2 [h_1 + \beta f(y)]} e^{i\xi y} d\xi$$

or, by substituting equations (58) and (59),

$$\begin{aligned} & \int_{-\infty}^{\infty} \left\{ \frac{1}{2} \left[ 2\pi\delta(\xi) \left( 1 - \frac{ik}{\lambda_1} \right) + A^*(\xi) \left( 1 + \frac{\lambda_0}{\lambda_1} \right) e^{(\xi^2 + \gamma_1^2)^{1/2} [h_1 + \beta f(y)]} \right. \right. \\ & \quad \left. \left. + \frac{1}{2} \left[ 2\pi\delta(\xi) \left( 1 + \frac{ik}{\lambda_1} \right) + A^*(\xi) \left( 1 - \frac{\lambda_0}{\lambda_1} \right) \right] e^{-(\xi^2 + \gamma_1^2)^{1/2} [h_1 + \beta f(y)]} \right\} \cdot e^{i\xi y} d\xi \\ & = \int_{-\infty}^{\infty} D^*(\xi) e^{-\lambda_2 h_1} e^{-\beta \lambda_2 f(y)} e^{i\xi y} d\xi \end{aligned}$$

and

$$\begin{aligned}
& \frac{n_y}{2\pi\omega\mu} \int_{-\infty}^{\infty} \left\{ \frac{1}{2} \left[ 2\pi\delta(\xi) \left(1 - \frac{ik}{\rho_1}\right) + A^*(\xi) \left(1 + \frac{\rho_0}{\rho_1}\right) \right] e^{(\xi^2 + \alpha_1^2)^{1/2} [h_1 + \beta f(y)]} \right. \\
& \quad \left. + \frac{1}{2} \left[ 2\pi\delta(\xi) \left(1 + \frac{ik}{\rho_1}\right) + A^*(\xi) \left(1 - \frac{\rho_0}{\rho_1}\right) \right] e^{-(\xi^2 + \alpha_1^2)^{1/2} [h_1 + \beta f(y)]} \right\} \cdot \xi e^{i\xi y} d\xi \\
& - \frac{in_z}{2\pi\omega\mu} \int_{-\infty}^{\infty} \left\{ \frac{1}{2} \left[ 2\pi\delta(\xi) \left(1 - \frac{ik}{\rho_1}\right) + A^*(\xi) \left(1 + \frac{\rho_0}{\rho_1}\right) \right] e^{(\xi^2 + \alpha_1^2)^{1/2} [h_1 + \beta f(y)]} \right. \\
& \quad \left. - \frac{1}{2} \left[ 2\pi\delta(\xi) \left(1 + \frac{ik}{\rho_1}\right) + A^*(\xi) \left(1 - \frac{\rho_0}{\rho_1}\right) \right] e^{-(\xi^2 + \alpha_1^2)^{1/2} [h_1 + \beta f(y)]} \right\} \cdot (\xi^2 + \alpha_1^2)^{1/2} e^{i\xi y} d\xi \\
& = \frac{n_y}{2\pi\omega\mu} \int_{-\infty}^{\infty} D^*(\xi) e^{-h_1 \rho_2} e^{-\beta \rho_2 f(y)} \xi e^{i\xi y} d\xi \\
& \quad + \frac{in_z}{2\pi\omega\mu} \int_{-\infty}^{\infty} D^*(\xi) \rho_2 e^{-h_1 \rho_2} e^{-\beta \rho_2 f(y)} e^{i\xi y} d\xi
\end{aligned}$$

The latter two equations may be simplified to yield

$$\begin{aligned}
& \pi \left[ 1 - \left( \frac{i\omega\epsilon}{\rho_1} \right)^{1/2} \right] e^{h_1 \alpha_1} e^{\beta \alpha_1 f(y)} + \pi \left[ 1 + \left( \frac{i\omega\epsilon}{\rho_1} \right)^{1/2} \right] e^{-h_1 \alpha_1} e^{-\beta \alpha_1 f(y)} \\
& + \frac{1}{2} \int_{-\infty}^{\infty} A^*(\xi) \left[ \left( 1 + \frac{\rho_0}{\rho_1} \right) e^{h_1 \rho_1} e^{\beta \rho_1 f(y)} \right. \\
& \quad \left. + \left( 1 - \frac{\rho_0}{\rho_1} \right) e^{-h_1 \rho_1} e^{-\beta \rho_1 f(y)} \right] e^{i\xi y} d\xi \\
& = \int_{-\infty}^{\infty} D^*(\xi) e^{-h_1 \rho_2} e^{-\beta \rho_2 f(y)} e^{i\xi y} d\xi \quad \dots (60)
\end{aligned}$$

and

$$\begin{aligned}
& - i n_z \left\{ \pi \left[ 1 - \left( \frac{i \omega \epsilon}{\sigma_1} \right)^{1/2} \right] e^{h_1 \delta_1} e^{\beta \delta_1 f(y)} \right. \\
& \quad \left. - \pi \left[ 1 + \left( \frac{i \omega \epsilon}{\sigma_1} \right)^{1/2} \right] e^{-h_1 \delta_1} e^{-\beta \delta_1 f(y)} \right\} \delta_1 \\
& + \frac{n_y}{2} \int_{-\infty}^{\infty} A^*(\xi) \left\{ \left( 1 + \frac{\delta_0}{\delta_1} \right) e^{h_1 \delta_1} e^{\beta \delta_1 f(y)} + \left( 1 - \frac{\delta_0}{\delta_1} \right) e^{-h_1 \delta_1} e^{-\beta \delta_1 f(y)} \right\} \\
& \quad \cdot \xi e^{i \xi y} d\xi \\
& - \frac{i n_z}{2} \int_{-\infty}^{\infty} A^*(\xi) \left\{ \left( 1 + \frac{\delta_0}{\delta_1} \right) e^{h_1 \delta_1} e^{\beta \delta_1 f(y)} - \left( 1 - \frac{\delta_0}{\delta_1} \right) e^{-h_1 \delta_1} e^{-\beta \delta_1 f(y)} \right\} \\
& \quad \cdot \delta_1 e^{i \xi y} d\xi \\
& = n_y \int_{-\infty}^{\infty} D^*(\xi) e^{-h_1 \delta_2} e^{-\beta \delta_2 f(y)} \xi e^{i \xi y} d\xi \\
& + i n_z \int_{-\infty}^{\infty} D^*(\xi) \delta_2 e^{-h_1 \delta_2} e^{-\beta \delta_2 f(y)} e^{i \xi y} d\xi \quad \dots \dots (61)
\end{aligned}$$

For ease of notation the following definitions are made

$$P^* \triangleq \left( 1 + \delta_0 / \delta_1 \right) e^{h_1 \delta_1}$$

$$Q^* \triangleq \left( 1 - \delta_0 / \delta_1 \right) e^{-h_1 \delta_1}$$

$$R^* \triangleq \pi \left[ 1 - \left( \frac{i \omega \epsilon}{\sigma_1} \right)^{1/2} \right] e^{h_1 \delta_1}$$

$$S^* \triangleq \pi \left[ 1 + \left( \frac{i \omega \epsilon}{\sigma_1} \right)^{1/2} \right] e^{-h_1 \delta_1}$$

With the above definitions equations (60) and (61) may be rewritten as

$$\begin{aligned}
& R^* e^{\beta \gamma_1 f(y)} + S^* e^{-\beta \gamma_1 f(y)} \\
& + \frac{1}{2} \int_{-\infty}^{\infty} A^*(\xi) \left[ P^* e^{\beta \gamma_1 f(y)} + Q^* e^{-\beta \gamma_1 f(y)} \right] e^{i\xi y} d\xi \\
& = \int_{-\infty}^{\infty} D^*(\xi) e^{-h_1 \gamma_2} e^{-\beta \gamma_2 f(y)} e^{i\xi y} d\xi \quad \dots (62)
\end{aligned}$$

$$\begin{aligned}
& -n_z \left[ R^* e^{\beta \gamma_1 f(y)} - S^* e^{-\beta \gamma_1 f(y)} \right] \gamma_1 \\
& - \frac{i n_y}{2} \int_{-\infty}^{\infty} A^*(\xi) \left[ P^* e^{\beta \gamma_1 f(y)} + Q^* e^{-\beta \gamma_1 f(y)} \right] \xi e^{i\xi y} d\xi \\
& - \frac{n_z}{2} \int_{-\infty}^{\infty} A^*(\xi) \left[ P^* e^{\beta \gamma_1 f(y)} - Q^* e^{-\beta \gamma_1 f(y)} \right] \gamma_1 e^{i\xi y} d\xi \\
& = i n_y \int_{-\infty}^{\infty} D^*(\xi) e^{-h_1 \gamma_2} e^{-\beta \gamma_2 f(y)} \xi e^{i\xi y} d\xi \\
& + n_z \int_{-\infty}^{\infty} D^*(\xi) \gamma_2 e^{-h_1 \gamma_2} e^{-\beta \gamma_2 f(y)} e^{i\xi y} d\xi \quad \dots (63)
\end{aligned}$$

Again, equations (62) and (63) are simultaneous integral equations of the first kind (Hildebrand, 1965) for  $A^*(\xi)$  and  $D^*(\xi)$ .

The problem now consists in finding solutions for  $A(\xi)$  and  $A^*(\xi)$ , for if  $A(\xi)$  and  $A^*(\xi)$  are known, then the solutions for the electromagnetic field in this problem are known for both electric and magnetic polarization and a given interface  $z = h_1 + \beta f(y)$ .

SOLUTION OF THE INTEGRAL EQUATIONS

Exact solutions of the equations of physics, such as equations (43), (44), (62), and (63) may be obtained for only a limited class of problems. For example, if the equation is the scalar Helmholtz equation, the method of separation of variables can be used in only 11 coordinate systems (Morse and Feshbach, 1953). If the surface upon which boundary conditions are to be satisfied is not one of these coordinate surfaces, or if the boundary conditions are not the simple Dirichlet or Neumann types, the method of separation fails. As Morse and Feshbach (1953) indicate, a similar situation exists if an integral equation formulation is employed. Indeed, even for the problems which can be solved exactly, it may be more convenient to employ approximate methods, for the evaluation of the exact solution may be much too complicated. Deviations from exactly soluble situations are referred to as perturbations. Perturbation techniques are well described in the literature (see Morse and Feshbach, 1953, p. 999 - 1106) and will only be reviewed briefly here.

Perturbation methods are particularly appropriate whenever the problem under consideration closely resembles one which is exactly solvable. The methods presume that one may change from the exactly solvable situation to the problem under consideration in a gradual fashion. The latter statement is usually expressed

analytically by requiring that the perturbation be a continuous function of a parameter  $\beta$ , which measures the strength of the perturbation. As Morse and Feshbach (1953, p. 1001) indicate, when using perturbation techniques to obtain the boundary conditions for the perturbation, one usually expands in power series with respect to  $\beta$  the unperturbed boundary conditions and neglects terms of order  $\beta^2$  or higher in the equations so obtained.

As Morse and Feshbach (1953) further indicate, a perturbation technique may involve deviations in the boundary surface(s) or boundary conditions (or both) from the exactly soluble form. For the present problem a perturbation method as described by Obukhov (1965, 1969), Dmitriev (1969), Davydov (1968), Feinberg (1961), and Mann (1964) will be used.

Case of Magnetic Polarization --- The perturbation parameter  $\beta$  in the above development has units of distance. When  $\beta/L \ll 1$ , where  $L$  is an appropriate linear dimension, a perturbation procedure with  $\beta$  as the small parameter may be used. That is, the following series expansions are valid for  $\beta/L \ll 1$ :

$$A(\xi) = A_0(\xi) + \beta A_1(\xi) + \beta^2 A_2(\xi) + \dots \quad (64)$$

$$D(\xi) = D_0(\xi) + \beta D_1(\xi) + \beta^2 D_2(\xi) + \dots \quad (65)$$

Similarly, from equation (36),

$$n_y = -\beta (df/dy) \cdot \left[ 1 + \beta^2 \left( \frac{df}{dy} \right)^2 \right]^{-1/2}$$

or

$$n_y = -\beta (df/dy) \left[ 1 - \frac{1}{2} \beta^2 (df/dy)^2 + \dots \right] \dots \dots (66)$$

and

$$n_z = 1 - \frac{1}{2} \beta^2 (df/dy)^2 + \dots \dots \dots (67)$$

$$e^{\beta x} = 1 + \beta x + \frac{1}{2} \beta^2 x^2 + \dots \dots \dots (68)$$

In equation (68), the symbol  $x$  stands for any quantity appearing in the exponent. If equations (64), (65), (66), (67), and (68) are substituted into equations (43) and (44) and if terms of the second order and higher are neglected in the substitution, there results

$$\begin{aligned} & R [1 + \beta \delta_1 f(y)] + S [1 - \beta \delta_1 f(y)] \\ & + \frac{1}{2} \int_{-\infty}^{\infty} [A_0(\xi) + \beta A_1(\xi)] \{ P [1 + \beta \delta_1 f(y)] + Q [1 - \beta \delta_1 f(y)] \} e^{i\xi y} d\xi \\ & - \int_{-\infty}^{\infty} [D_0(\xi) + \beta D_1(\xi)] \{ e^{-h_1 \delta_2} [1 - \beta \delta_2 f(y)] \} e^{i\xi y} d\xi \dots (69) \\ & = 0 \end{aligned}$$

and

$$\begin{aligned}
& -\gamma_1 \{R[1 + \beta\gamma_1 f(y)] - S[1 - \beta\gamma_1 f(y)]\} \\
& + \frac{i\beta}{2} \frac{df}{dy} \int_{-\infty}^{\infty} [A_0(\xi) + \beta A_1(\xi)] \{P[1 + \beta\gamma_1 f(y)] + Q[1 - \beta\gamma_1 f(y)]\} \xi e^{i\xi y} d\xi \\
& - \frac{1}{2} \int_{-\infty}^{\infty} [A_0(\xi) + \beta A_1(\xi)] \{P[1 + \beta\gamma_1 f(y)] - Q[1 - \beta\gamma_1 f(y)]\} \gamma_1 e^{i\xi y} d\xi \\
& - i\lambda\beta \frac{df}{dy} \int_{-\infty}^{\infty} \xi [D_0(\xi) + \beta D_1(\xi)] e^{-h_1 \gamma_2} [1 - \beta\gamma_2 f(y)] e^{i\xi y} d\xi \\
& - \lambda \int_{-\infty}^{\infty} [D_0(\xi) + \beta D_1(\xi)] \gamma_2 e^{-h_1 \gamma_2} [1 - \beta\gamma_2 f(y)] e^{i\xi y} d\xi \\
& = 0 \qquad \dots \dots (70)
\end{aligned}$$

Equations (69) and (70) may be rewritten as

$$\begin{aligned}
& R + S + \beta\gamma_1 f(y)(R - S) + \frac{1}{2} \int_{-\infty}^{\infty} A_0(\xi) [P + Q] e^{i\xi y} d\xi \\
& + \frac{\beta}{2} f(y) \int_{-\infty}^{\infty} A_0(\xi) [P - Q] \gamma_1 e^{i\xi y} d\xi + \frac{\beta}{2} \int_{-\infty}^{\infty} A_1(\xi) [P + Q] e^{i\xi y} d\xi \\
& + \frac{\beta^2}{2} f(y) \int_{-\infty}^{\infty} A_1(\xi) [P - Q] \gamma_1 e^{i\xi y} d\xi - \int_{-\infty}^{\infty} D_0(\xi) e^{-h_1 \gamma_2} e^{i\xi y} d\xi \\
& + \beta f(y) \int_{-\infty}^{\infty} D_0(\xi) \gamma_2 e^{-h_1 \gamma_2} e^{i\xi y} d\xi - \beta \int_{-\infty}^{\infty} D_1(\xi) e^{-h_1 \gamma_2} e^{i\xi y} d\xi \\
& + \beta^2 f(y) \int_{-\infty}^{\infty} D_1(\xi) \gamma_2 e^{-h_1 \gamma_2} e^{i\xi y} d\xi \\
& = 0 \qquad \dots \dots (71)
\end{aligned}$$

$$\begin{aligned}
& -\gamma_1 (R-S) - \gamma_1^2 \beta f(\gamma) (R+S) + \frac{i\beta}{2} \frac{df}{dy} \int_{-\infty}^{\infty} A_0(\xi) (P+Q) \xi e^{i\xi y} d\xi \\
& + \frac{i\beta^2}{2} \frac{df}{dy} \int_{-\infty}^{\infty} A_0(\xi) (P-Q) \mathcal{N}_1 \xi e^{i\xi y} d\xi \\
& + \frac{i\beta^2}{2} \frac{df}{dy} \int_{-\infty}^{\infty} A_1(\xi) (P+Q) \xi e^{i\xi y} d\xi + \frac{i\beta^3 f(\gamma)}{2} \frac{df}{dy} \int_{-\infty}^{\infty} A_1(\xi) (P-Q) \mathcal{N}_1 \xi e^{i\xi y} d\xi \\
& - \frac{1}{2} \int_{-\infty}^{\infty} A_0(\xi) (P-Q) \mathcal{N}_1 e^{i\xi y} d\xi - \frac{\beta f(\gamma)}{2} \int_{-\infty}^{\infty} A_0(\xi) (P+Q) \mathcal{N}_1^2 e^{i\xi y} d\xi \\
& - \frac{\beta}{2} \int_{-\infty}^{\infty} A_1(\xi) (P-Q) \mathcal{N}_1 e^{i\xi y} d\xi - \frac{\beta^2 f(\gamma)}{2} \int_{-\infty}^{\infty} A_1(\xi) (P+Q) \mathcal{N}_1^2 e^{i\xi y} d\xi \\
& - i\lambda\beta \frac{df}{dy} \int_{-\infty}^{\infty} D_0(\xi) e^{-h_1 \mathcal{N}_2} \xi e^{i\xi y} d\xi + i\lambda\beta^2 f(\gamma) \frac{df}{dy} \int_{-\infty}^{\infty} D_0(\xi) \mathcal{N}_2 e^{-h_1 \mathcal{N}_2} \xi e^{i\xi y} d\xi \\
& - i\lambda\beta^2 \frac{df}{dy} \int_{-\infty}^{\infty} D_1(\xi) e^{-h_1 \mathcal{N}_2} \xi e^{i\xi y} d\xi + i\lambda\beta^3 f(\gamma) \frac{df}{dy} \int_{-\infty}^{\infty} D_1(\xi) \mathcal{N}_2 e^{-h_1 \mathcal{N}_2} \xi e^{i\xi y} d\xi \\
& - \lambda \int_{-\infty}^{\infty} D_0(\xi) \mathcal{N}_2 e^{-h_1 \mathcal{N}_2} e^{i\xi y} d\xi + \lambda\beta f(\gamma) \int_{-\infty}^{\infty} D_0(\xi) \mathcal{N}_2^2 e^{-h_1 \mathcal{N}_2} e^{i\xi y} d\xi \\
& - \lambda\beta \int_{-\infty}^{\infty} D_1(\xi) \mathcal{N}_2 e^{-h_1 \mathcal{N}_2} e^{i\xi y} d\xi + \lambda\beta^2 f(\gamma) \int_{-\infty}^{\infty} D_1(\xi) \mathcal{N}_2^2 e^{-h_1 \mathcal{N}_2} e^{i\xi y} d\xi \\
& = 0
\end{aligned}$$

..... (72)

If, in the above two equations, second order terms are neglected and the terms are factored according to the various powers of  $\beta$  by which they are multiplied and the coefficients of each power of  $\beta$  are set equal to zero, the following simultaneous integral equations for  $A_0$ ,  $D_0$ ,  $A_1$ , and  $D_1$  result, which are somewhat easier to solve than equations (43) and (44).

$$\frac{1}{2} \int_{-\infty}^{\infty} A_0(\xi) (P+Q) e^{i\xi y} d\xi - \int_{-\infty}^{\infty} D_0(\xi) e^{-h_1 \lambda_2} e^{i\xi y} d\xi = - (R+S) \dots (73)$$

$$\begin{aligned} & \sigma_1 f(y) (R-S) + \frac{f(y)}{2} \int_{-\infty}^{\infty} A_0(\xi) (P-Q) \lambda_1 e^{i\xi y} d\xi \\ & + f(y) \int_{-\infty}^{\infty} D_0(\xi) \lambda_2 e^{-h_1 \lambda_2} e^{i\xi y} d\xi \\ = & -\frac{1}{2} \int_{-\infty}^{\infty} A_1(\xi) (P+Q) e^{i\xi y} d\xi + \int_{-\infty}^{\infty} D_1(\xi) e^{-h_1 \lambda_2} e^{i\xi y} d\xi. \end{aligned} \quad (74)$$

$$\begin{aligned} & \frac{1}{2} \int_{-\infty}^{\infty} A_0(\xi) (P-Q) \lambda_1 e^{i\xi y} d\xi + \lambda \int_{-\infty}^{\infty} D_0(\xi) \lambda_2 e^{-h_1 \lambda_2} e^{i\xi y} d\xi \\ = & -\sigma_1 (R-S) \end{aligned}$$

$$\begin{aligned} & -\sigma_1^2 f(y) (R+S) + \frac{i}{2} \frac{df}{dy} \int_{-\infty}^{\infty} A_0(\xi) (P+Q) \xi e^{i\xi y} d\xi \quad (75) \\ & - \frac{f(y)}{2} \int_{-\infty}^{\infty} A_0(\xi) (P+Q) \lambda_1^2 e^{i\xi y} d\xi - i\lambda \frac{df}{dy} \int_{-\infty}^{\infty} D_0(\xi) e^{-h_1 \lambda_2} \xi e^{i\xi y} d\xi \\ & + \lambda f(y) \int_{-\infty}^{\infty} D_0(\xi) \lambda_2^2 e^{-h_1 \lambda_2} e^{i\xi y} d\xi \\ = & \frac{1}{2} \int_{-\infty}^{\infty} A_1(\xi) (P-Q) \lambda_1 e^{i\xi y} d\xi + \lambda \int_{-\infty}^{\infty} D_1(\xi) \lambda_2 e^{-h_1 \lambda_2} e^{i\xi y} d\xi \end{aligned} \dots (76)$$

Equations (73), (74), (75), and (76) are in the standard form of Fourier inversion and may be solved by taking the Fourier transform of both sides of the equations. First of all,  $A_0$  and  $D_0$  in equations (73) and (75) can be found and then substituted into equations (74) and (76) to determine  $A_1$  and  $D_1$ . Then the solutions to equations (25), (26), (27), (28), (29), (30), (31), (32), and (33) will be completely specified for an arbitrary interface between the first and second layer. Upon Fourier transformation of both sides of equations (73) and (75), there results

$$\pi A_0(\xi)(P+Q) - 2\pi D_0(\xi) e^{-h_1 \mathcal{J}_2} = -2\pi \delta(\xi)(R+S)$$

and

$$\pi A_0(\xi)(P-Q)\mathcal{J}_1 + 2\pi\lambda D_0(\xi)\mathcal{J}_2 e^{-h_1 \mathcal{J}_2} = -2\pi \delta(\xi)\gamma_1(R-S)$$

or

$$\pi A_0(\xi)(P+Q)\lambda \mathcal{J}_2 - 2\pi\lambda D_0(\xi)\mathcal{J}_2 e^{-h_1 \mathcal{J}_2} = -2\pi\lambda \mathcal{J}_2 \delta(\xi)(R+S)$$

$$\pi A_0(\xi)(P-Q)\mathcal{J}_1 + 2\pi\lambda D_0(\xi)\mathcal{J}_2 e^{-h_1 \mathcal{J}_2} = -2\pi \delta(\xi)\gamma_1(R-S)$$

Thus .

$$A_0(\xi) = \frac{-2\delta(\xi) [\lambda \mathcal{J}_2 (R+S) + \gamma_1 (R-S)]}{[\mathcal{J}_1 (P-Q) + \lambda \mathcal{J}_2 (P+Q)]} \dots (77)$$

and

$$D_0(\xi) = \frac{\delta(\xi) [\mathcal{J}_1 (P-Q)(R+S) - \mathcal{J}_1 (P+Q)(R-S)]}{e^{-h_1 \mathcal{J}_2} [\mathcal{J}_1 (P-Q) + \lambda \mathcal{J}_2 (P+Q)]} \dots (78)$$

Substitution of equations (77) and (78) into equation (74) yields, after some algebraic manipulation,

$$\begin{aligned} & A_1(\xi) (P+Q) - 2 D_1(\xi) e^{-h_1 \mathcal{J}_2} \\ &= \frac{4 \mathcal{J}_1 F(\xi) \left(\frac{\sigma_1}{i\omega\epsilon}\right)^{1/2} (\lambda-1)}{\left\{ \lambda [\cosh(h_1 \mathcal{J}_1) + \left(\frac{\sigma_1}{i\omega\epsilon}\right)^{1/2} \sinh(h_1 \mathcal{J}_1)] + \lambda^{1/2} [\sinh(h_1 \mathcal{J}_1) + \left(\frac{\sigma_1}{i\omega\epsilon}\right)^{1/2} \cosh(h_1 \mathcal{J}_1)] \right\}} \end{aligned} \dots (79)$$

where  $F(\xi)$  is the Fourier transform of  $f(y)$ . Similarly, after substitution of equations (77) and (78) into equation (76), one obtains

$$A_1(\xi) (P-Q) \mathcal{J}_1 + 2 \lambda D_1(\xi) e^{-h_1 \mathcal{J}_2} \mathcal{J}_2 = 0 \dots (80)$$

Solving for  $D_1(\xi)$  in equation (80) yields

$$D_1(\xi) = - \frac{A_1(\xi) e^{h_1 \mathcal{J}_2}}{2 \lambda \mathcal{J}_2} (P-Q) \mathcal{J}_1 \dots (81)$$

Now, substitution of equation (81) into equation (79) gives the following solution for  $A_1(\xi)$ :

$$\begin{aligned} A_1(\xi) &= \frac{4 \mathcal{J}_1 \lambda \mathcal{J}_2 F(\xi) \left(\frac{\sigma_1}{i\omega\epsilon}\right)^{1/2} (\lambda-1)}{\left\{ \lambda [\cosh(h_1 \mathcal{J}_1) + \left(\frac{\sigma_1}{i\omega\epsilon}\right)^{1/2} \sinh(h_1 \mathcal{J}_1)] + \lambda^{1/2} [\sinh(h_1 \mathcal{J}_1) + \left(\frac{\sigma_1}{i\omega\epsilon}\right)^{1/2} \cosh(h_1 \mathcal{J}_1)] \right\} \cdot \\ &\quad \cdot [\lambda \mathcal{J}_2 (P+Q) + \mathcal{J}_1 (P-Q)] \end{aligned} \dots (82)$$

Equation (82) may be put in slightly different form, that is, if the following definitions are made,

$$G \triangleq e^{-h_1 \mathcal{J}_2} [\lambda \mathcal{J}_2 (P+Q) + \mathcal{J}_1 (P-Q)] / 2 \quad \dots (83)$$

$$Z_1 \triangleq \sinh(h_1 \delta_1) + \lambda^{1/2} \cosh(h_1 \delta_1) \quad \dots (84)$$

$$Z_2 \triangleq \lambda^{1/2} \sinh(h_1 \delta_1) + \cosh(h_1 \delta_1) \quad \dots (85)$$

and

$$\mathcal{K} \triangleq \frac{4 \pi \delta_1}{\left(\frac{i \omega \epsilon}{\sigma_1}\right)^{1/2} Z_1 + Z_2} \frac{\lambda - 1}{\lambda^{1/2}} \quad \dots (86)$$

then

$$A_1(\xi) = \left[ F(\xi) e^{-h_1 \mathcal{J}_2} / 2 \pi G \right] \lambda \mathcal{K} \mathcal{J}_2 \quad \dots (87)$$

Thus, from equations (81), (77), and (78), it may be written

$$D_1(\xi) = - \left[ F(\xi) / 4 \pi G \right] (P-Q) \mathcal{K} \mathcal{J}_1 \quad \dots (88)$$

$$A_0(\xi) = - \left[ \delta(\xi) / G \right] e^{-h_1 \mathcal{J}_2} [\lambda \mathcal{J}_2 (R+S) + \mathcal{J}_1 (R-S)] \quad \dots (89)$$

$$D_0(\xi) = \left[ \delta(\xi) / 2 G \right] [\mathcal{J}_1 (P-Q) (R+S) - \mathcal{J}_1 (P+Q) (R-S)] \quad \dots (90)$$

With equations (87) through (90), the electromagnetic field for the case of magnetic polarization is completely specified.

Case of Electric Polarization - - - An exactly analogous procedure may be used for the case of electric polarization, i.e.,

$$A^*(\xi) = A_0^*(\xi) + \beta A_1^*(\xi) + \beta^2 A_2^*(\xi) + \dots \dots \dots (91)$$

$$D^*(\xi) = D_0^*(\xi) + \beta D_1^*(\xi) + \beta^2 D_2^*(\xi) + \dots \dots \dots (92)$$

After substituting equations (91), (92), (66), (67), and (68) into equations (62) and (63) and after neglecting terms of the second order and higher, there results

$$\begin{aligned} & R^* [1 + \beta \alpha_1 f(y)] + S^* [1 - \beta \alpha_1 f(y)] \\ & + \frac{1}{2} \int_{-\infty}^{\infty} [A_0^*(\xi) + \beta A_1^*(\xi)] \{ P^* [1 + \beta \alpha_1 f(y)] + Q^* [1 - \beta \alpha_1 f(y)] \} e^{i\xi y} d\xi \\ & = \int_{-\infty}^{\infty} [D_0^*(\xi) + \beta D_1^*(\xi)] e^{-h_1 \alpha_2} [1 - \beta \alpha_2 f(y)] e^{i\xi y} d\xi \dots \dots (93) \\ & - \alpha_1 \{ R^* [1 + \beta \alpha_1 f(y)] - S^* [1 - \beta \alpha_1 f(y)] \} \\ & + \frac{i\beta}{2} \frac{df}{dy} \int_{-\infty}^{\infty} [A_0^*(\xi) + \beta A_1^*(\xi)] \{ P^* [1 + \beta \alpha_1 f(y)] + Q^* [1 - \beta \alpha_1 f(y)] \} \xi e^{i\xi y} d\xi \\ & - \frac{1}{2} \int_{-\infty}^{\infty} [A_0^*(\xi) + \beta A_1^*(\xi)] \{ P^* [1 + \beta \alpha_1 f(y)] - Q^* [1 - \beta \alpha_1 f(y)] \} \alpha_1 e^{i\xi y} d\xi \\ & = i\beta \frac{df}{dy} \int_{-\infty}^{\infty} [D_0^*(\xi) + \beta D_1^*(\xi)] e^{-h_1 \alpha_2} [1 - \beta \alpha_2 f(y)] \xi e^{i\xi y} d\xi \\ & + \int_{-\infty}^{\infty} [D_0^*(\xi) + \beta D_1^*(\xi)] \alpha_2 e^{-h_1 \alpha_2} [1 - \beta \alpha_2 f(y)] e^{i\xi y} d\xi \\ & \dots \dots (94) \end{aligned}$$

Equations (93) and (94) may be rewritten as

$$\begin{aligned}
 & R^* + S^* + \gamma_1 \beta f(y) (R^* - S^*) + \frac{1}{2} \int_{-\infty}^{\infty} A_0^*(\xi) (P^* + Q^*) e^{i\xi y} d\xi \\
 & + \frac{\beta f(y)}{2} \int_{-\infty}^{\infty} A_0^*(\xi) (P^* - Q^*) \mathcal{N}_1 e^{i\xi y} d\xi \\
 & + \frac{\beta}{2} \int_{-\infty}^{\infty} A_1^*(\xi) (P^* + Q^*) e^{i\xi y} d\xi \\
 & + \frac{\beta^2 f(y)}{2} \int_{-\infty}^{\infty} A_1^*(\xi) (P^* - Q^*) \mathcal{N}_1 e^{i\xi y} d\xi \\
 & - \int_{-\infty}^{\infty} D_0^*(\xi) e^{-h_1 \mathcal{N}_2} e^{i\xi y} d\xi \\
 & + \beta f(y) \int_{-\infty}^{\infty} D_0^*(\xi) \mathcal{N}_2 e^{-h_1 \mathcal{N}_2} e^{i\xi y} d\xi \\
 & - \beta \int_{-\infty}^{\infty} D_1^*(\xi) e^{-h_1 \mathcal{N}_2} e^{i\xi y} d\xi \\
 & + \beta^2 f(y) \int_{-\infty}^{\infty} D_1^*(\xi) \mathcal{N}_2 e^{-h_1 \mathcal{N}_2} e^{i\xi y} d\xi \\
 & = 0 \quad \dots \dots (95)
 \end{aligned}$$

$$\begin{aligned}
& -\gamma_1 (R^* - S^*) - \gamma_1^2 \beta f(y) (R^* + S^*) \\
& + \frac{i\beta}{2} \frac{df}{dy} \int_{-\infty}^{\infty} A_0^*(\xi) (P^* + Q^*) \xi e^{i\xi y} d\xi \\
& + \frac{i\beta^2}{2} f(y) \frac{df}{dy} \int_{-\infty}^{\infty} A_0^*(\xi) (P^* - Q^*) \mathcal{N}_1 \xi e^{i\xi y} d\xi \\
& + \frac{i\beta^2}{2} \frac{df}{dy} \int_{-\infty}^{\infty} A_1^*(\xi) (P^* + Q^*) \xi e^{i\xi y} d\xi \\
& + \frac{i\beta^3}{2} f(y) \frac{df}{dy} \int_{-\infty}^{\infty} A_1^*(\xi) (P^* - Q^*) \mathcal{N}_1 \xi e^{i\xi y} d\xi - \frac{1}{2} \int_{-\infty}^{\infty} A_0^*(\xi) (P^* - Q^*) \mathcal{N}_1 e^{i\xi y} d\xi \\
& - \frac{\beta f(y)}{2} \int_{-\infty}^{\infty} A_0^*(\xi) (P^* + Q^*) \mathcal{N}_1^2 e^{i\xi y} d\xi - \frac{\beta}{2} \int_{-\infty}^{\infty} A_1^*(\xi) (P^* - Q^*) \mathcal{N}_1 e^{i\xi y} d\xi \\
& - \frac{\beta^2 f(y)}{2} \int_{-\infty}^{\infty} A_1^*(\xi) (P^* + Q^*) \mathcal{N}_1^2 e^{i\xi y} d\xi - i\beta \frac{df}{dy} \int_{-\infty}^{\infty} D_0^*(\xi) e^{-h_1 \mathcal{N}_2 \xi} e^{i\xi y} d\xi \\
& + i\beta^2 f(y) \frac{df}{dy} \int_{-\infty}^{\infty} D_0^*(\xi) \mathcal{N}_2 e^{-h_1 \mathcal{N}_2 \xi} e^{i\xi y} d\xi - i\beta^2 \frac{df}{dy} \int_{-\infty}^{\infty} D_1^*(\xi) e^{-h_1 \mathcal{N}_2 \xi} e^{i\xi y} d\xi \\
& + i\beta^3 f(y) \frac{df}{dy} \int_{-\infty}^{\infty} D_1^*(\xi) \mathcal{N}_2 e^{-h_1 \mathcal{N}_2 \xi} e^{i\xi y} d\xi - \int_{-\infty}^{\infty} D_0^*(\xi) \mathcal{N}_2 e^{-h_1 \mathcal{N}_2 \xi} e^{i\xi y} d\xi \\
& + \beta f(y) \int_{-\infty}^{\infty} D_0^*(\xi) \mathcal{N}_2^2 e^{-h_1 \mathcal{N}_2 \xi} e^{i\xi y} d\xi - \beta \int_{-\infty}^{\infty} D_1^*(\xi) \mathcal{N}_2 e^{-h_1 \mathcal{N}_2 \xi} e^{i\xi y} d\xi \\
& + \beta^2 f(y) \int_{-\infty}^{\infty} D_1^*(\xi) \mathcal{N}_2^2 e^{-h_1 \mathcal{N}_2 \xi} e^{i\xi y} d\xi \\
& = 0
\end{aligned}$$

..... (96)

If in the above two equations second order terms are neglected and if the terms are factored according to the various powers of  $\beta$  by which they are multiplied and the coefficients of each power of  $\beta$  are set equal to zero, the following simultaneous integral equations for  $A_0^*$ ,  $D_0^*$ ,  $A_1^*$ , and  $D_1^*$  result, which are easier to solve than equations (62) and (63).

$$\frac{1}{2} \int_{-\infty}^{\infty} A_0^*(\xi) (P^* + Q^*) e^{i\xi y} d\xi - \int_{-\infty}^{\infty} D_0^*(\xi) e^{-h_1 \eta_2} e^{i\xi y} d\xi \dots (97)$$

$$= - (R^* + S^*)$$

$$\gamma_1 f(y) (R^* - S^*) + \frac{f(y)}{2} \int_{-\infty}^{\infty} A_0^*(\xi) (P^* - Q^*) \eta_1 e^{i\xi y} d\xi$$

$$+ f(y) \int_{-\infty}^{\infty} D_0^*(\xi) \eta_2 e^{-h_1 \eta_2} e^{i\xi y} d\xi = -\frac{1}{2} \int_{-\infty}^{\infty} A_1^*(\xi) (P^* + Q^*) e^{i\xi y} d\xi \dots (98)$$

$$+ \int_{-\infty}^{\infty} D_1^*(\xi) e^{-h_1 \eta_2} e^{i\xi y} d\xi$$

$$\frac{1}{2} \int_{-\infty}^{\infty} A_0^*(\xi) (P^* - Q^*) \eta_1 e^{i\xi y} d\xi + \int_{-\infty}^{\infty} D_0^*(\xi) \eta_2 e^{-h_1 \eta_2} e^{i\xi y} d\xi \dots (99)$$

$$= -\gamma_1 (R^* - S^*)$$

$$-\gamma_1^2 f(y) (R^* + S^*) + \frac{i}{2} \frac{df}{dy} \int_{-\infty}^{\infty} A_0^*(\xi) (P^* + Q^*) \xi e^{i\xi y} d\xi$$

$$- \frac{f(y)}{2} \int_{-\infty}^{\infty} A_0^*(\xi) (P^* + Q^*) \eta_1^2 e^{i\xi y} d\xi - i \frac{df}{dy} \int_{-\infty}^{\infty} D_0^*(\xi) e^{-h_1 \eta_2} \xi e^{i\xi y} d\xi \dots (100)$$

$$+ f(y) \int_{-\infty}^{\infty} D_0^*(\xi) \eta_2^2 e^{-h_1 \eta_2} e^{i\xi y} d\xi = \frac{1}{2} \int_{-\infty}^{\infty} A_1^*(\xi) (P^* - Q^*) \eta_1 e^{i\xi y} d\xi$$

$$+ \int_{-\infty}^{\infty} D_1^*(\xi) \eta_2 e^{-h_1 \eta_2} e^{i\xi y} d\xi$$

Equations (97), (98), (99), and (100) are in the standard form of the Fourier inversion and may be solved by taking the Fourier transform of both sides of the equations. First of all,  $A_0^*$  and

$D_0^*$  in equations (97) and (99) may be found and then substituted into equations (98) and (100) to determine  $A_1^*$  and  $D_1^*$ .

Then the solutions to equations (45), (46), (47), (48), (49), (50), (51), (52), and (53) will be completely specified for an interface of arbitrary shape between the first and second layers. Fourier transformation of both sides of equations (97) and (99) yields

$$\pi A_0^*(\xi) (P^* + Q^*) - 2\pi D_0^*(\xi) e^{-h_1 \mathcal{J}_2} = 2\pi \delta(\xi) (R^* + S^*)$$

and

$$\pi A_0^*(\xi) (P^* - Q^*) \mathcal{J}_1 + 2\pi D_0^*(\xi) \mathcal{J}_2 e^{-h_1 \mathcal{J}_2} = -2\pi \delta(\xi) \mathcal{J}_1 (R^* - S^*)$$

or

$$\pi A_0^*(\xi) (P^* + Q^*) \mathcal{J}_2 - 2\pi D_0^*(\xi) \mathcal{J}_2 e^{-h_1 \mathcal{J}_2} = -2\pi \mathcal{J}_2 \delta(\xi) (R^* + S^*)$$

$$\pi A_0^*(\xi) (P^* - Q^*) \mathcal{J}_1 + 2\pi D_0^*(\xi) \mathcal{J}_2 e^{-h_1 \mathcal{J}_2} = -2\pi \mathcal{J}_1 \delta(\xi) (R^* - S^*)$$

Thus

$$A_0^*(\xi) = \frac{-2\delta(\xi) [\mathcal{J}_2 (R^* + S^*) + \mathcal{J}_1 (R^* - S^*)]}{[\mathcal{J}_1 (P^* - Q^*) + \mathcal{J}_2 (P^* + Q^*)]} \dots \dots (101)$$

and

$$D_0^*(\xi) = \frac{\delta(\xi) [\mathcal{J}_1 (R^* + S^*) (P^* - Q^*) - \mathcal{J}_1 (R^* - S^*) (P^* + Q^*)]}{e^{-h_1 \mathcal{J}_2} [\mathcal{J}_2 (P^* + Q^*) + \mathcal{J}_1 (P^* - Q^*)]} \dots \dots (102)$$

Substitution of equations (101) and (102) into equation (98) yields, after some algebraic manipulation,

$$- A_1^*(\xi)(P^* + Q^*) + 2 D_1^*(\xi) e^{-h_1 \mathcal{J}_2} = 0 \quad \dots (103)$$

Similarly, substitution of equations (101) and (102) into equation (100) yields

$$\begin{aligned} & A_1^*(\xi)(P^* - Q^*) \mathcal{J}_1 + 2 D_1^*(\xi) \mathcal{J}_2 e^{-h_1 \mathcal{J}_2} \\ &= \frac{4 \sigma_1^2 F(\xi) (i\omega \epsilon / \sigma_1)^{1/2} (\lambda^{-1/2} - \lambda^{1/2})}{\left\{ \lambda^{1/2} [\sinh(h_1 \sigma_1) + (i\omega \epsilon / \sigma_1)^{1/2} \cosh(h_1 \sigma_1)] + [\cosh(h_1 \sigma_1) + (i\omega \epsilon / \sigma_1)^{1/2} \sinh(h_1 \sigma_1)] \right\}} \end{aligned} \quad \dots (104)$$

where  $F(\xi)$  is the Fourier transform of  $f(y)$ .  $D_1^*(\xi)$  may readily be found from equation (103):

$$D_1^*(\xi) = A_1^*(\xi)(P^* + Q^*) e^{h_1 \mathcal{J}_2} / 2 \quad \dots (105)$$

Now, substitution of equation (105) into equation (104) yields the following solution for  $A_1^*(\xi)$ :

$$\begin{aligned} A_1^*(\xi) = & \frac{-4 i \sigma_1 k F(\xi) (\lambda - 1)}{\left\{ (i\omega \epsilon / \sigma_1)^{1/2} [\sinh(h_1 \sigma_1) + \lambda^{1/2} \cosh(h_1 \sigma_1)] \right.} \\ & \left. + \lambda^{1/2} \sinh(h_1 \sigma_1) + \cosh(h_1 \sigma_1) \right\} [\mathcal{J}_1 (P^* - Q^*) + \mathcal{J}_2 (P^* + Q^*)] \lambda^{1/2} \end{aligned} \quad \dots (106)$$

Equation (106) may be put into slightly different form, that is, if the following additional definition is made,

$$G^* \triangleq e^{-h_1 \mathcal{J}_2} [\mathcal{J}_1 (P^* - Q^*) + \mathcal{J}_2 (P^* + Q^*)] / 2 \quad \dots (107)$$

then

$$A_1^*(\xi) = -i k F(\xi) e^{-h_1 \mathcal{J}_z} \mathcal{K} / 2\pi G^* \quad \dots (108)$$

Thus, from equations (105), (101), and (102),

$$D_1^*(\xi) = -i k F(\xi) \mathcal{K} (P^* + Q^*) / 4\pi G^* \quad \dots (109)$$

$$A_0^*(\xi) = \frac{-\delta(\xi) e^{-h_1 \mathcal{J}_z} [\mathcal{J}_1 (R^* - S^*) + \mathcal{J}_2 (R^* + S^*)]}{G^*} \quad \dots (110)$$

$$D_0^*(\xi) = \frac{\delta(\xi) [\mathcal{J}_1 (R^* + S^*) (P^* - Q^*) - \mathcal{J}_2 (R^* - S^*) (P^* + Q^*)]}{2 G^*} \quad \dots (111)$$

With equations (108) thru (111), the electromagnetic field for the case of electric field polarization is completely specified.

TESTS ON NUMERICAL EVALUATION FOR  $\vec{H}$  - FIELD POLARIZATION

Thus far the development has been quite general with respect to the shape of the interface assumed, and the electromagnetic field can be found that is associated with any interface with a small perturbation. It is the purpose of this investigation to study the effect of subsurface geologic structure for  $\vec{H}$  - field polarization, since this is one limiting case where the current density is perpendicular to the strike line of the subsurface structure. The electromagnetic field at the surface of the earth ( $z = 0$ ) is that which is of concern. Thus the following simplification of the field components can be made for the case of magnetic polarization. I.e.,

$$H_{0x}(y, 0) = 1 + \frac{1}{2\pi} \int_{-\infty}^{\infty} A(\xi) e^{i\xi y} d\xi \quad \dots \dots (112)$$

$$E_{0y}(y, 0) = -\frac{h}{\omega \epsilon} - \frac{i}{2\pi \omega \epsilon} \int_{-\infty}^{\infty} A(\xi) \eta_0 e^{i\xi y} d\xi \quad \dots \dots (113)$$

$$E_{0z}(y, 0) = -\frac{1}{2\pi \omega \epsilon} \int_{-\infty}^{\infty} A(\xi) \xi e^{i\xi y} d\xi \quad \dots \dots (114)$$

where  $A(\xi)$  is given by equation (64). In practice the geophysicist usually measures only the horizontal electric and magnetic fields. Normally a grounded wire, short relative to the wavelength of the field, is used in measuring the electric field in the earth.

Magnetic field components may be measured with a magnetometer. More commonly, however, the magnetic field components are measured with induction coils, which detect the time-rate of change of the magnetic induction. By the use of Faraday's law and Stoke's theorem the following expression is derived

$$EMF = - n A \partial B / \partial t$$

where  $n$  is the number of turns in the induction coil and  $A$  is the cross-sectional area of the coil. If the field is harmonic, the derivative in the above expression may be replaced by a multiplying term,  $i\omega$  :

$$EMF = -i\omega n A \mu_0 H \quad . . . (115)$$

where  $H$  in equation (115) is that magnetic field component which is perpendicular to the plane of the coil. Thus, a voltage is measured, rather than a magnetic field component.

Fourier Inversion - - - In the evaluation of the horizontal field components,  $H_{0x}$  and  $E_{0y}$ , in equations (112) and (113) it is observed that the essential numerical problem is that of inverse Fourier transformation. First, a complex function of spatial frequency, which depends on the electrical characteristics of the two-layered earth and on the nature of the interface between the layers, is generated for each case of interest. This complex function is then inverted to determine the anomalous electromagnetic field caused by the presence of subsurface geologic structure.

Because of the lack of both even symmetry of the real parts of the complex function to be inverted and odd symmetry of the imaginary parts of the complex function to be inverted, the inverted function is a complex function of  $y$ , possessing both an amplitude and phase factor (Papoulis, 1962, p. 11). Furthermore, because a finite number of sampled values of the function to be inverted are used, a few words might be said about the relationship between the true inverted continuous function and the digital inverted function.

Since the effects of sampling are well-documented and discussed in depth elsewhere (Papoulis, 1962; Bracewell, 1965; Gray, 1967), they will only be reviewed here. In general, the complex function of spatial frequency to be inverted for each case of interest in the problem at hand may be represented by  $W(\xi)$  and its continuous inverse by  $w(y)$ . In practice, a finite number  $N$  of equally-spaced digitized values of  $W(\xi)$  are inverted; these values may be represented as the following series with the Dirac comb function,

$$\begin{aligned}
 W_d(\xi) &= \sum_{n=-N}^N W(n\Delta\xi) \delta(\xi - n\Delta\xi) \\
 &= W(\xi) \sum_{n=-N}^N \delta(\xi - n\Delta\xi) \quad \dots (116)
 \end{aligned}$$

Transforming equation (116) yields the following equation

$$w_d(y) = w(y) * \frac{\sin(N + \frac{1}{2})y\Delta\xi}{\sin y\Delta\xi/2} \quad \dots (117)$$

Equation (117) implies that the inverse Fourier transform of the discrete function  $w_d(\xi)$  consisting of a finite number of equispaced sample values  $w(n\Delta\xi)$ ,  $n = -N, \dots, 0, \dots, N$ , of the continuous function  $w(\xi)$  is the convolution of the inverse transform of the continuous function with the periodic Fourier series kernel. Of course,

$$\lim_{N \rightarrow \infty} w_d(y) = w(y)$$

Qualitatively there are two effects on the inverted digital function,  $w_d(y)$ . A smearing effect due to truncation is produced, and since the Fourier - series kernel is periodic, the output of its convolution with the analytic continuous inverted function  $w(y)$  is a periodic function. Because the electric and magnetic fields on the surface of the earth are well-behaved functions and fairly smooth, the first effect is small. However, an inevitable consequence of sampling a function  $w(\xi)$  at equispaced intervals is an "aliasing" of  $w_d(y)$  about  $y_N = \pi/\Delta\xi$ . In this context the term alias is used to indicate a confusion of  $w_d(y)$  values at  $y_N = \pi/\Delta\xi$ .

A Fortran IV program for the Standard IC - 4000 computer was written for the inverse Fourier transformation. In order to test the program, the inverse Fourier transforms of two functions whose inverse Fourier transforms are well-known were digitally computed; that is, the inverse Fourier transforms of the following functions were calculated:

$$W_1(\xi) = \begin{cases} 1 - |\xi|/\xi_c, & |\xi| < \xi_c \\ 0 & , |\xi| \geq \xi_c \dots (118) \end{cases}$$

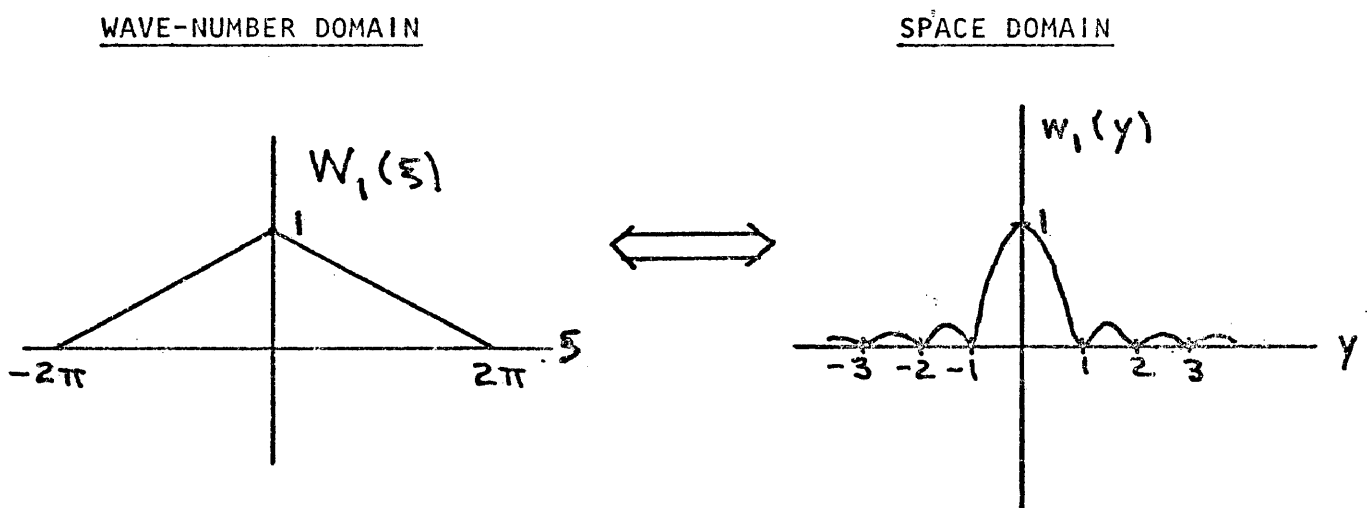
and

$$W_2(\xi) = \sqrt{\frac{\pi}{\alpha}} e^{-\xi^2/4\alpha} \dots (119)$$

The functions expressed by equations (118) and (119) are well-known in the theory of the Fourier integral. The function given by equation (118) is a triangular pulse in the spatial frequency domain whose analytic inverse Fourier transform is given by (Papoulis, 1962, p. 21 - 22),

$$W_1(\xi) \iff w_1(y) = \frac{2 \sin^2 \frac{\xi_c}{2} y}{\pi \xi_c y^2} \dots (120)$$

For convenience,  $\xi_c$  was chosen to be  $2\pi$  so that  $w_1(y) = \sin^2 \pi y / \pi^2 y^2$  reduces to a  $\text{sinc}^2$  function whose values are tabulated by Bracewell (1965, p. 368-372). The Fourier transform pair  $W_1(\xi) \iff w_1(y)$  is illustrated in Figure 3.



Fourier Transform of  $\text{Sinc}^2$  Function

Figure 2

The analytical inverse and digital inverse are compared in Table 1.

Table 1. Comparison of Analytic and Digital Inverse Fourier Transform  
of  $w_1(\xi)$

$y$	$\text{sinc}^2(y)$ (After Bracewell, 1965)	$w_1(y)$ (computed)
0.00	1.000	1.000
0.50	0.405	0.414
1.00	0.000	0.000
1.50	0.045	0.055
2.00	0.000	0.000
2.50	0.016	0.029
3.00	0.000	0.000

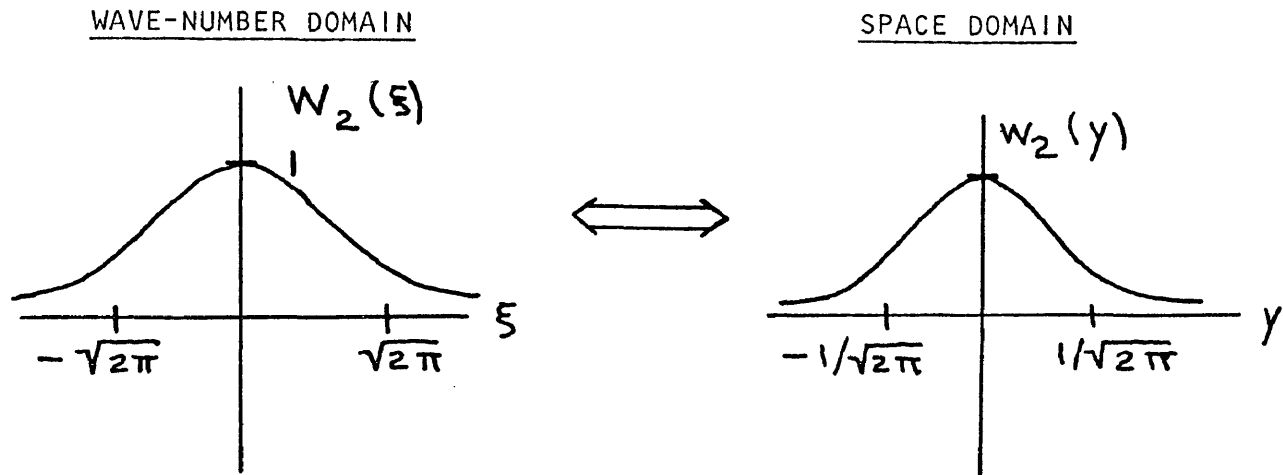
In the above test case  $N = 7$  and  $\Delta\xi = 1.042$ . The effects of sampling become more noticeable as  $y$  approaches the value  $\pi / \Delta\xi$ .

The function given by equation (119) is called a Gaussian function whose inverse is given by (Papoulis, 1962, p. 25),

$$W_2(\xi) \iff w_2(y) = e^{-\alpha y^2} \quad \dots (121)$$

For convenience,  $\alpha$  was chosen to be equal to  $\pi$  since values of  $\exp(-\pi y^2)$  are tabulated by Bracewell (1965, p. 368 - 372).

The Fourier transform pair  $W_2(\xi) \iff w_2(y)$  is illustrated in Figure 4.



Fourier Transform of Gaussian Function

Figure 3

The analytical inverse and the computed digital inverse are compared in Table 2.

Table 2. Comparison of Analytic and Digital Inverse Fourier Transform of  $w_2(\xi)$

y	$\exp(-\pi y^2)$ (After Bracewell, 1965)	$w_2(y)$ (computed)
0.00	1.000	0.994
0.50	0.456	0.461
1.00	0.043	0.042
1.50	0.001	0.000
2.00	0.000	0.002

In the above test case  $N = 7$  and  $\Delta\xi = 1.042$ , Both the effects of sampling and truncation become more noticeable as  $y$  approaches the value  $\pi/\Delta\xi$ , but because the second function is smoother than the first, the effects are less. This fact implies that the method will work better for smooth geometries, which is what would be expected.

Asymptotic Behavior for Low Frequencies - - - In order to gain some insight into the effect of subsurface structure on the electromagnetic field at the surface of the earth, an anticlinal ridge and a synclinal trough on the second layer are considered. The ridge might well be considered to be a basement ridge underlying sediments. Or the geologic section may be viewed as that of a local thinning or thickening of the first layer.

The study of such structures is important in the geologic interpretation of electromagnetic field data. Such a study should enable one to determine the effect of terrain on electromagnetic field data. It may also be of use in searching for subsurface anticlinal structures and stratigraphic traps in petroleum exploration (or dike-like features in mineral exploration), and for given resistivity contrasts, such a study may help in the determination of the geometry of a buried anticlinal ridge or synclinal trough.

Generally, the term wavenumber is often used to express relationships between effective depths of penetration, resistivity, and frequency of the field (Keller, 1966). In a conductive medium the wavenumber  $\gamma$ , neglecting displacement currents, is

$$\gamma = (i\omega\mu\sigma)^{1/2} = \left(\frac{\omega\mu\sigma}{2}\right)^{1/2} + i\left(\frac{\omega\mu\sigma}{2}\right)^{1/2}$$

so that in a medium having conductivity  $\sigma_1$ ,

$$\gamma_1 = \left( \frac{\omega \mu \sigma_1}{2} \right)^{1/2} + i \left( \frac{\omega \mu \sigma_1}{2} \right)^{1/2} = G_1 + i G_1$$

where  $G_1 = \left( \omega \mu \sigma_1 / 2 \right)^{1/2}$  is the real part of the radian wavelength.

The functional dependence of waves traveling in the  $+z$  direction is exponential, i.e.,  $e^{-\gamma z}$ . Thus

$$e^{-\gamma z} = e^{-\left( \frac{\omega \mu \sigma}{2} \right)^{1/2} z} e^{-i \left( \frac{\omega \mu \sigma}{2} \right)^{1/2} z}$$

Then the skin depth, that is, the distance within the conducting medium at which the amplitudes of the electric and magnetic field vectors are equal to  $1/e = 0.3679$  of their respective values at the surface, is

$$z_{\text{SKIN DEPTH}} \triangleq \left( \frac{2}{\omega \mu \sigma} \right)^{1/2} = 1/\text{Re}(\gamma), \quad \sigma \gg \omega \epsilon$$

At the skin depth the phase lags one radian for a plane wave in a uniform earth. Since the value of the skin depth gives an effective depth of penetration for the geophysicist's purposes, it is interesting to know its order or magnitude and in subsequent computations the skin depth will often be referred to.

Because the magnetic permeability of almost all rocks is very nearly that of free space, the wavenumber  $\gamma$  varies only with the resistivity of a medium and with the frequency of the field. Curves exhibiting the relationship between wavenumber, conductivity, and frequency are given in Figure 4.

In any theoretical investigation where numerical evaluations are performed, it is important to examine, if possible, limiting conditions. An examination of the asymptotic behavior of the fields provides a check on the numerical computations.

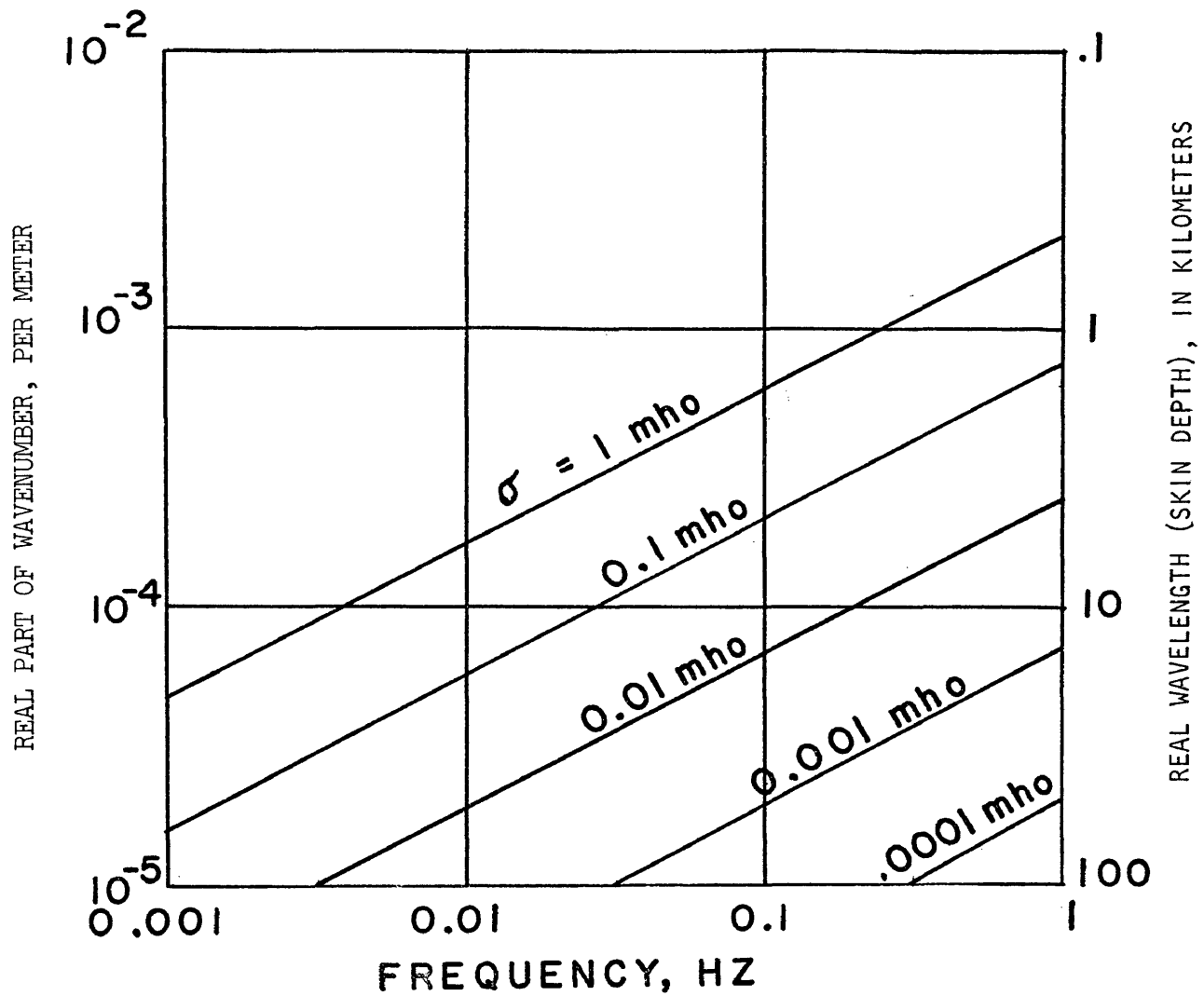


FIGURE 4. (After Keller and Frischknecht, 1966)

Wavenumbers as a function of frequency and conductivity for cases in which displacement currents can be neglected. A scale for converting wavenumbers to radian wavelengths or skin depths is shown to the right.

Several researchers have studied the limiting zero frequency (direct current) case of the problem at hand, including Berdichevskiy (1965), Neyman and Kalantarov (1948), Smirnov (1948), Sheynmann (1941, 1958), Kunetz and Chastenet deGery (1956), Utzman and Faire (1957), and Roy (1969). All of the above investigators considered only a perfectly insulating basement and made use of a Schwarz-Christoffel transformation to simplify boundary conditions for the direct current case. Berdichevskiy (1965) describes the transformations used for a hyperbolic anticline, a vertical step in the basement, and a vertical-sided insulating slab in the basement. Recently Roy (1969) considered the direct current case of a triangular-shaped ridge on a perfectly insulating basement (see Figure 5). Since a triangle has a Fourier transform (see Figure 2), the electromagnetic field over a buried triangular-shaped ridge may be computed using the mathematical procedure outlined above.

A Fortran IV program was written by the author for the Standard Computer Corporation IC-4000 computer in order to evaluate the horizontal components of the electric field ( $E_{0y}$ ) over a buried triangular-shaped anticlinal ridge. In order to check the numerical computations of the normalized horizontal component of the electric field (In this context the field values with subsurface structure present will be normalized with respect to the field values when no subsurface structure is present), the low-frequency behavior was examined and compared with Roy's computations for a given triangular-shaped ridge. In order to simulate low-frequency behavior the ratio of the real part of the radian wavelength in the first layer

# BASEMENT TRIANGULAR RIDGE

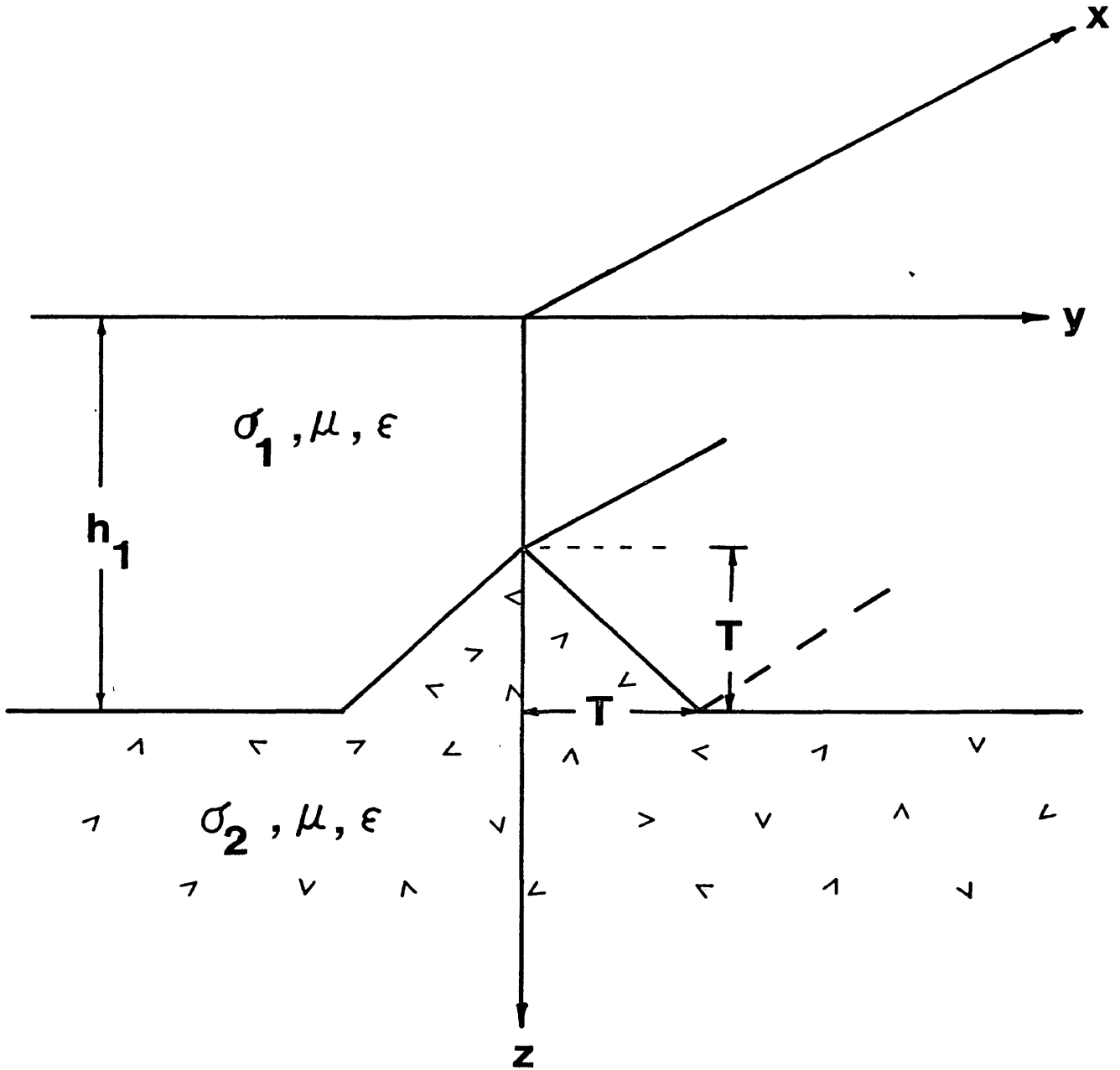


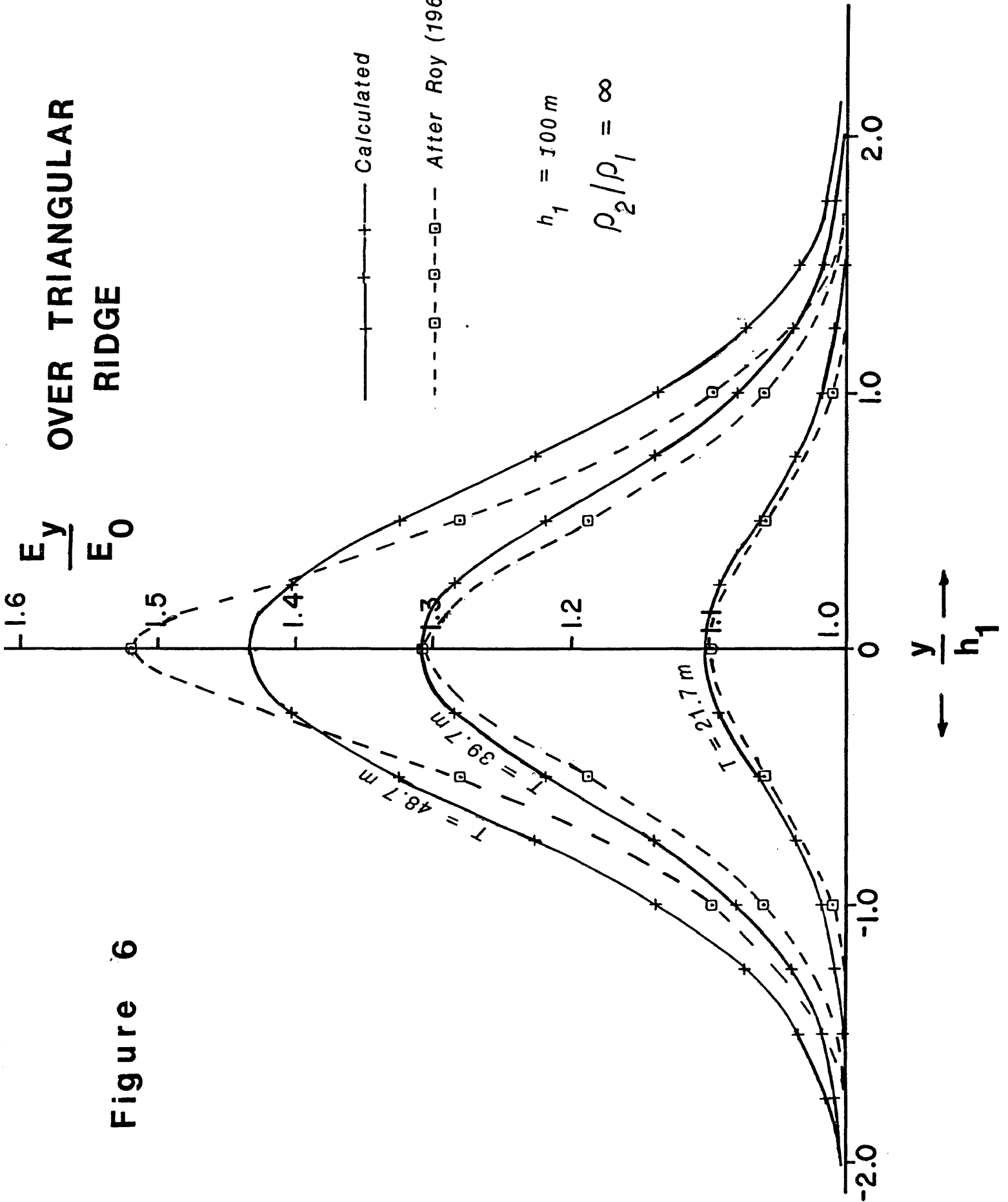
Figure 5

to the first-layer thickness ( $1/h_1 G_1$ ) was chosen to be equal to 100; this ratio corresponds for a first-layer resistivity of 100 ohm-meters and for a first-layer thickness of 100 meters to a frequency  $f$  of 0.253 Hertz. In order to simulate a perfectly insulating basement, a resistivity contrast  $\rho_2/\rho_1$  was chosen to be equal to  $10^6$ . Finally, the geometry for the computed triangular-shaped ridge was chosen so as to coincide with the triangular-shaped ridge used by Roy. Three test cases were run and the results are indicated in Figure 6. Figure 6 illustrates close agreement between Roy's results and computations for the horizontal component of the electric field at low frequencies. The fact that the rate of decay for the calculated anomaly is slightly less than that determined by Roy is due to aliasing. It is also seen that the effect of second and higher order terms is not negligible when the height of the ridge becomes greater than one-half the first layer thickness.

A Fortran IV program was also written for the Standard Computer Corporation IC - 4000 computer to evaluate the horizontal components of the magnetic field ( $H_{0x}$ ) at the surface over a buried triangular-shaped ridge. There are two approaches that might be taken in checking the computations for the horizontal magnetic field. One approach would be to use Ampere's law, which relates the current density to the magnetic field. With this approach the magnetic field component  $H_{1x}$  at some depth  $z$  in the first layer (given by equation (26)) and the electric field components  $E_{1z}$  and  $E_{1y}$  in the first layer would have to be computed. Knowledge of the

# OVER TRIANGULAR RIDGE

$$\frac{E y}{E_0}$$



Calculated

After Roy (1969)

$$h_1 = 100 \text{ m}$$

$$\rho_2 / \rho_1 = \infty$$

Figure 6

electric field components will yield the current density, given the layer resistivity. This current density can then be compared to that obtained merely by computing  $H_{0x}$  and  $H_{1x}$ .

Another approach for the present problem would be to compute the surface impedance. The surface impedance is defined as the ratio of the orthogonal field components, i.e.,

$$Z_o \cong E_{oy} / H_{ox}$$

(As Keller and Frischknecht (1966) indicate, there is a  $45^\circ$  phase difference between the magnetic and electric field intensities over a uniform earth.) If the surface impedance is known for a given frequency, the apparent resistivity can be computed. Grant and West (1965), Cagniard (1953), and Keller and Frischknecht (1966) give the following defining equation for apparent resistivity measured with the magneto-telluric method:

$$\rho_a = \frac{1}{\omega \mu} \left( \frac{E_{oy}}{H_{ox}} \right)^2 \dots \dots \dots (122)$$

Roy (1969) has tabulated apparent resistivity values over a buried triangular-shaped ridge for the direct current case. The same three test cases that were computed for the horizontal electric field for low-frequency behavior were used to evaluate apparent resistivity curves over a buried triangular-shaped anticlinal ridge. These results are compared with Roy's in Figure 7. Again, Figure 7 demonstrates close agreement.

#### Asymptotic Behavior far from Subsurface Geologic Structure - - -

At distances large relative to the first-layer thickness and relative

# TRIANGULAR RIDGE

$$\rho_1 = 1 \quad \Omega \text{ m}$$

$$\rho_2 / \rho_1 = \infty$$

$$h_1 = 100 \text{ m}$$

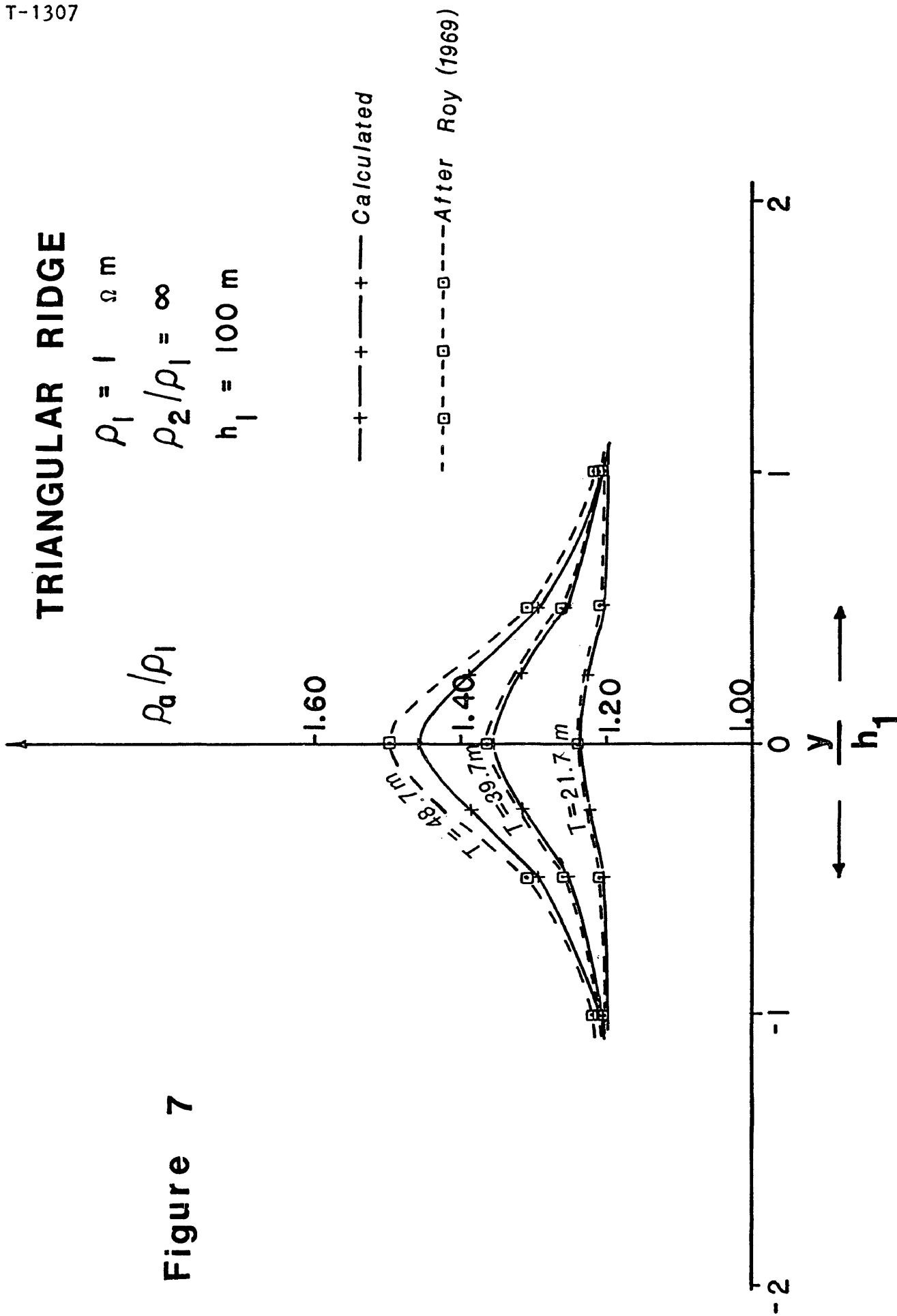


Figure 7

to the horizontal extent of the anticlinal ridge or trough, very little influence should be exerted on the electromagnetic field at the earth's surface due to the presence of the subsurface geologic structure. This statement is borne out by Figures 6 and 7.

A perhaps more realistic representation of an anticlinal ridge in cross-section is that portrayed by a Gaussian curve, that is, an anticlinal ridge on the second conducting layer may be simulated as a Gaussian curve in cross-sectional view. In reference to Figure 1,

$$\begin{array}{l} f(y) \\ \text{anticline} \end{array} = -e^{-\alpha y^2} \quad \dots \dots \dots (123)$$

so that the Fourier transform of  $f(y)$  is

$$f(y) \iff F(\xi) = -(\pi/\alpha)^{1/2} e^{-\xi^2/4\alpha}$$

or

$$F(2\pi f) = -(\pi/\alpha)^{1/2} e^{-\pi^2 f^2/\alpha}$$

where  $\xi$  is the wavenumber in radians per meter, and  $f$  is spatial frequency in cycles per meter. In a similar manner a synclinal interface may be simulated in cross-section by the function

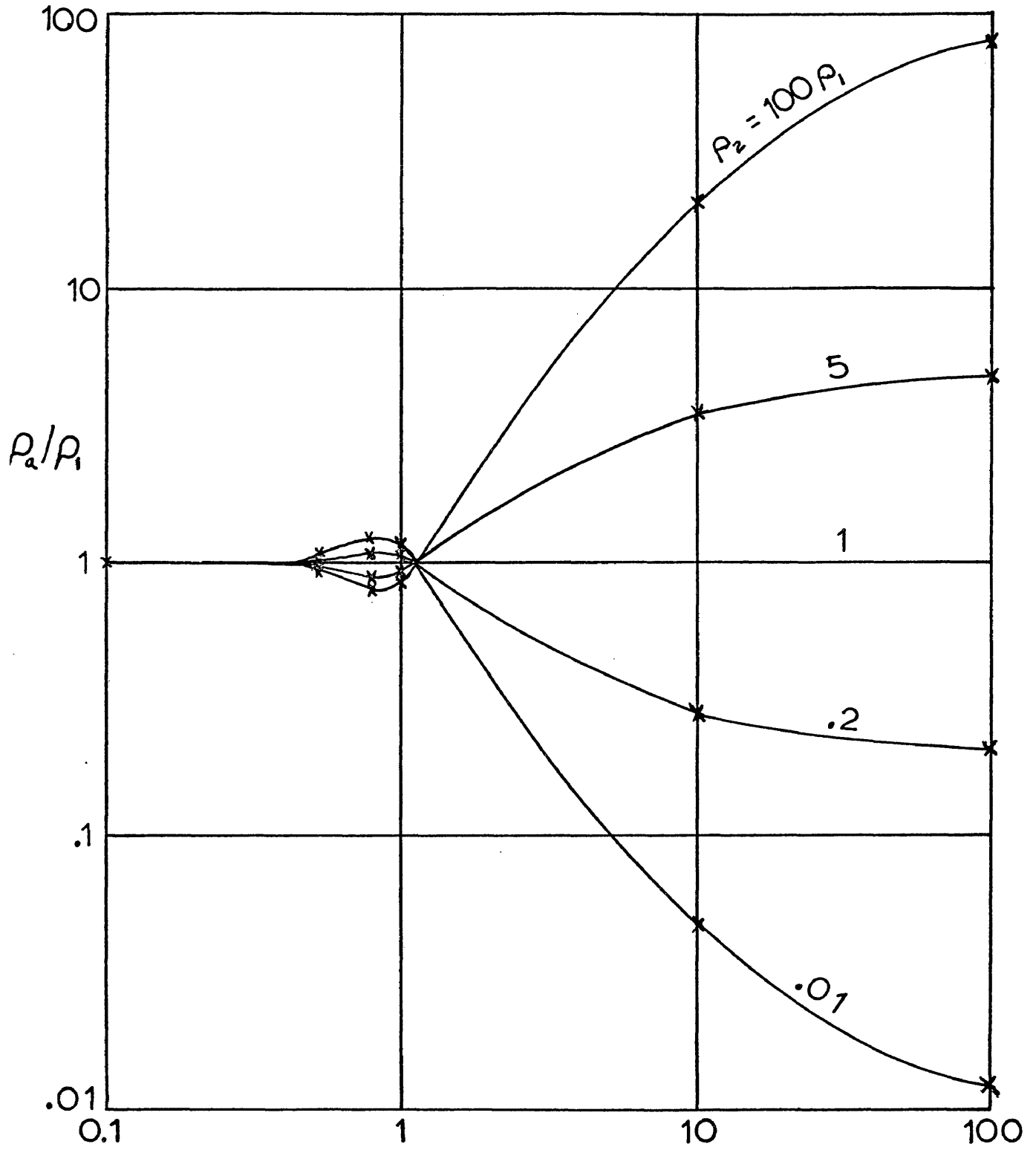
$$\begin{array}{l} f(y) \\ \text{syncline} \end{array} = e^{-\alpha y^2}$$

Indeed, far from a subsurface anticlinal ridge or synclinal trough apparent resistivity curves should be independent of the presence of the structure for any frequency and any resistivity

contrast between the two layers. Apparent resistivity curves were calculated over an anticlinal ridge for various ratios of radian wavelength to first-layer thickness, for  $h_1 = 500$  m,  $\beta/h_1 = 0.10$ ,  $y/h_1 = 40$ ,  $y_e = 25$  m ( $y_e$  is defined as the distance by which the Gaussian simulation of an anticline falls to  $1/e = 0.3679$  of its peak value), and for various resistivity contrasts. These curves are plotted in Figure 8. As Figure 8 illustrates, the apparent resistivity curves far from the subsurface anticlinal ridge reduce to two-layer resistivity curves for a flat earth (Keller and Frischknecht, 1966; Yungul, 1961).

Asymptotic Behavior for Homogeneous Halfspace - - - A final check which can be made on the numerical evaluations is to let the resistivity contrast be equal to one; in such a case the calculated apparent resistivity should always be equal to the true resistivity of the first layer regardless of the ratio of the radian wavelength to the first-layer thickness. A number of values for  $E_{0y}$  and  $H_{0x}$  and the apparent resistivity given by equation (122) were calculated for various ratios of the radian wavelength to the first-layer thickness ( $1/h_1 G_1$ ) and are given in Table 3. Table 3 indicates that the calculated results for the electric and magnetic fields yield apparent resistivities for a homogeneous halfspace which are in error by less than 0.003 %.

Resolution of Perturbation Technique - - - It has already been observed (see Figure 6) that when the magnitude of the perturbation



RATIO OF RADIANT WAVELENGTH TO FIRST-LAYER THICKNESS,  $1/h_1 G_1$

$h_1 = 500 \text{ m}$     $y_e = 25 \text{ m}$     $\beta = .10$

$Y = 20,000 \text{ m}$    **Figure 8**

Table 3. Comparison of Calculated Apparent Resistivity with True Resistivity of a Homogeneous Halfspace for Various Values of  $1/h_1 G_1$  (True Resistivity = 1000 ohm-meters)

$1/h_1 G_1$	$\rho_a$ (ohm-meters)	Error (%)
0.100	1000.0195	0.002
0.500	1000.0217	0.002
0.800	1000.0203	0.002
1.000	1000.0181	0.002
10.000	1000.0341	0.003

on the second layer is greater than one-half the first-layer thickness, the peak anomalous electric field value may be in error by as much as 10 %. In such cases, second and higher order terms become more important. In order to obtain greater accuracy in theoretical curve-matching higher order terms may be kept in expressions (64), (65), (66), (67), and (68). The second order term  $A_2(\xi)$  for magnetic polarization has been determined to be

$$\begin{aligned}
 A_2(\xi) = & \left\{ \frac{\lambda \gamma_1 (\sigma_1 / i\omega\epsilon)^{1/2} (\gamma_1^2 - \gamma_2^2) (\gamma_2 - \beta_2)}{\lambda \gamma_2 [\cosh(h, \gamma_1) + (\frac{\sigma_1}{i\omega\epsilon})^{1/2} \sinh(h, \gamma_1)] + \gamma_2 [\sinh(h, \gamma_1) + (\frac{\sigma_1}{i\omega\epsilon})^{1/2} \cosh(h, \gamma_1)]} \right\} F(\xi) * F(\xi) \\
 & - \left\{ \frac{\lambda \beta_2 \gamma_1 (\lambda - 1)^2 (\sigma_1 / i\omega\epsilon)^{1/2}}{\pi \left\{ \lambda [\cosh(h, \gamma_1) + (\sigma_1 / i\omega\epsilon)^{1/2} \sinh(h, \gamma_1)] + \lambda^{1/2} [\sinh(h, \gamma_1) + (\sigma_1 / i\omega\epsilon)^{1/2} \cosh(h, \gamma_1)] \right\}} \right\} \cdot \\
 & \quad \cdot F(\xi) * U_1(\xi) \\
 & - \left\{ \frac{\lambda (\lambda - 1) (\sigma_1 / i\omega\epsilon)^{1/2} \gamma_1}{\pi \left\{ \lambda [\cosh(h, \gamma_1) + (\sigma_1 / i\omega\epsilon)^{1/2} \sinh(h, \gamma_1)] + \lambda^{1/2} [\sinh(h, \gamma_1) + (\sigma_1 / i\omega\epsilon)^{1/2} \cosh(h, \gamma_1)] \right\}} \right\} \cdot \\
 & \quad \cdot F(\xi) * [U_2(\xi) + U_4(\xi)] \\
 & - \left\{ \frac{\lambda (\lambda - 1) (\sigma_1 / i\omega\epsilon)^{1/2} \gamma_1}{\pi \left\{ \lambda [\cosh(h, \gamma_1) + (\sigma_1 / i\omega\epsilon)^{1/2} \sinh(h, \gamma_1)] + \lambda^{1/2} [\sinh(h, \gamma_1) + (\sigma_1 / i\omega\epsilon)^{1/2} \cosh(h, \gamma_1)] \right\}} \right\} \cdot \\
 & \quad \cdot \left\{ \xi F(\xi) \right\} * [U_3(\xi) + U_5(\xi)] \\
 & \quad \dots (124)
 \end{aligned}$$

where

$$U_1(\xi) = \frac{\mathcal{J}_1 \mathcal{J}_2 F(\xi) (P-Q)}{[\lambda \mathcal{J}_2 (P+Q) + \mathcal{J}_1 (P-Q)]} \dots (125)$$

$$U_2(\xi) = \frac{\mathcal{J}_1 \mathcal{J}_2^2 F(\xi) (P-Q)}{[\lambda \mathcal{J}_2 (P+Q) + \mathcal{J}_1 (P-Q)]} \dots (126)$$

$$U_3(\xi) = \frac{\mathcal{J}_1 \xi F(\xi) (P-Q)}{[\lambda \mathcal{J}_2 (P+Q) + \mathcal{J}_1 (P-Q)]} \dots (127)$$

$$U_4(\xi) = \frac{\mathcal{J}_1^2 \mathcal{J}_2 F(\xi) (P+Q)}{[\lambda \mathcal{J}_2 (P+Q) + \mathcal{J}_1 (P-Q)]} \dots (128)$$

$$U_5(\xi) = \frac{\mathcal{J}_2 \xi F(\xi) (P+Q)}{[\lambda \mathcal{J}_2 (P+Q) + \mathcal{J}_1 (P-Q)]} \dots (129)$$

and  $*$  denotes convolution.

NUMERICAL EXAMPLES FOR  $\vec{H}$ -FIELD POLARIZATION

In order to illustrate the perturbing effect of subsurface geologic structure on two-layer magneto-telluric curves and in order to provide a better understanding of electric field anomalies caused by subsurface geologic structure, several examples have been evaluated. In choosing the examples to be studied, consideration was given to generalized resistivity ranges for rocks of different lithology and age (See Table 4).

As Keller and Frischknecht (1966, p. 39) indicate, conduction in near-surface rocks is almost entirely through the water-filling pore spaces in rocks. Conduction through mineral grains, however, is important at depth within the earth, where pore structures in the rock are closed by overburden pressure.

As Table 4 purports, there exists an indirect relationship between resistivity and lithology or geologic age in water-bearing rocks, since these two factors tend to control the porosity or water storage capacity of a rock. In Table 4 the vertical columns are arranged in a generally decreasing order of porosity from left to right. As Keller (1966) indicates, there are many exceptions to the ranges listed in the table, especially if metamorphism has decreased the porosity of normally porous rocks or if conductive minerals occur in high enough concentrations to lower the resistivity of otherwise resistant rocks.

Table 4. Generalized Resistivity Ranges (Ohm-meters) for Rocks of Different Lithology and Age (After Keller and Frischknecht, 1966)

Age	Marine Sedimentary Rocks	Terrestrial Sedimentary Rocks	Extrusive Rocks (basalt, rhyolite)	Intrusive Rocks (granite, gabbro)	Chemical Precipitates (limestones, salt)
Quaternary and Tertiary	1 - 10	15 - 50	10 - 200	500 - 2000	50 - 5000
Mesozoic	5 - 20	25 - 100	20 - 500	500 - 2000	100 - 10,000
Carboniferous Paleozoic	10 - 40	50 - 300	50 - 1000	1000-5000	200 - 100,000
Early Paleozoic	40 - 200	100 - 500	100 - 2000	1000-5000	10,000 - 100,000
Precambrian	100 - 2000	300 - 5000	200 - 5000	5000-20,000	10,000 - 100,000

In the numerical evaluation of type cases which are of particular interest in petroleum and mineral exploration, several descriptive parameters of the geologic section must be specified. These parameters are the thickness  $h_1$  of the first layer, the ratio  $1/h_1 \gamma_1$  of the radian wavelength to the first-layer thickness, the ratio  $\beta/h_1$  of the maximum magnitude of the perturbation on the second layer to the first-layer thickness, the relationship of the "width" of the structure relative to the first-layer thickness ( $2 y_e/h_1$ ), and the resistivity contrast  $\rho_2/\rho_1$  between the first and second layers. The ratio of the radian wavelength to the first-layer thickness gives an effective depth of penetration for any  $\omega\sigma_1$  product. Because the anticlinal ridge (or synclinal trough) is simulated in cross-section by a Gaussian-shaped curve, it is convenient to set  $\alpha$  in equation (123) equal to  $1/y_e^2$  so that a measure is obtained on the distance  $y$  at which the height of the anticline falls to  $1/e = 0.3679$  of its maximum deviation from the depth  $h_1$ . This distance is denoted by  $y_e$ . Knowledge of  $y_e$  gives a width parameter  $2y_e$  for the structural rise (or trough) on the second layer.

#### Electric Field Master Curves for Anticline versus Syncline - - -

Figures 9, 10, 11, and 12 illustrate the normalized horizontal electric field anomalies over an anticlinal ridge and synclinal trough of the same geometry at a depth  $h_1$  of 500 m and for  $1/h_1 \gamma_1 = 1.00$ . (Normalized phase values are always given in fractions of  $\pi$  radians.) Several resistivity contrasts are portrayed.

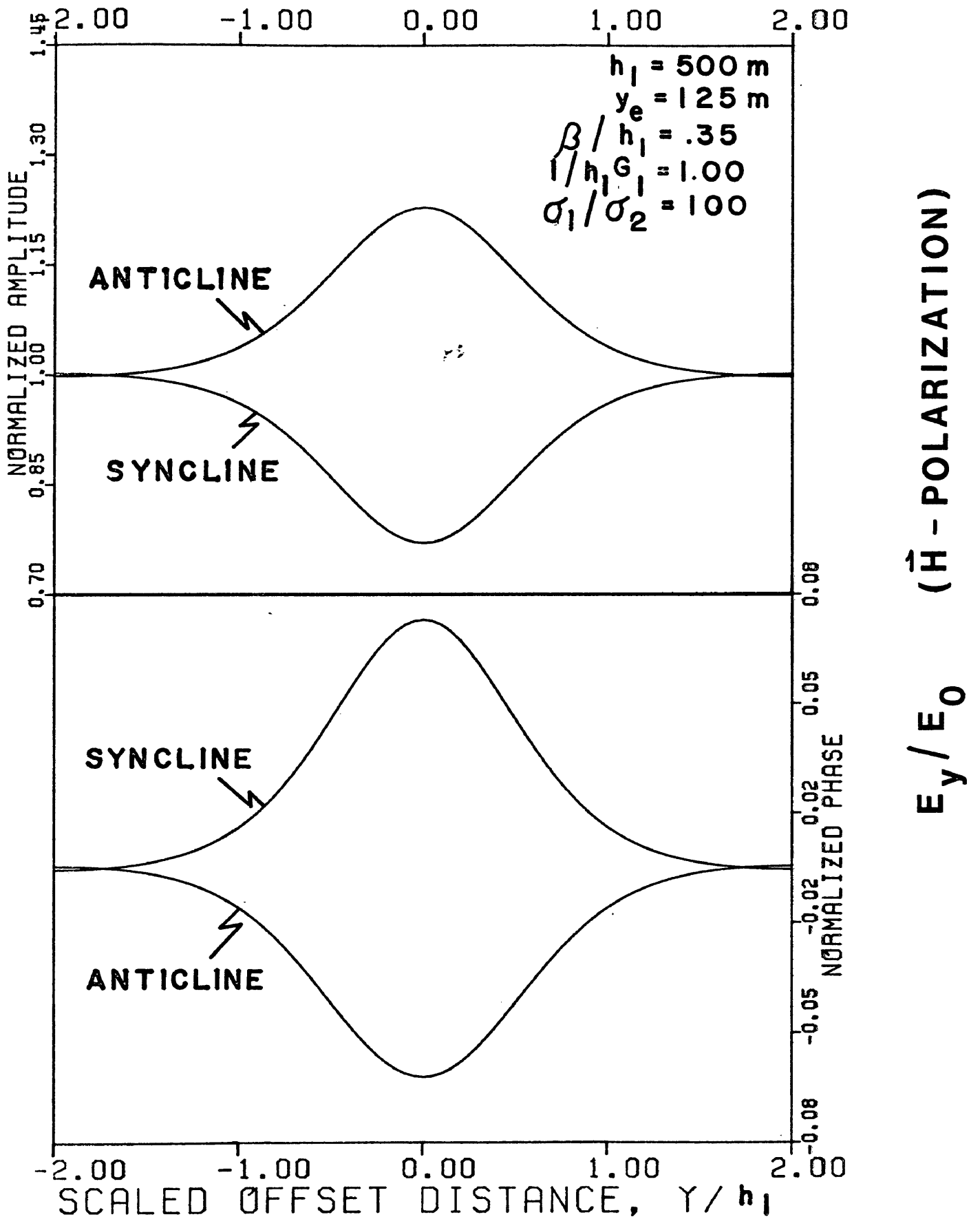


Figure 9

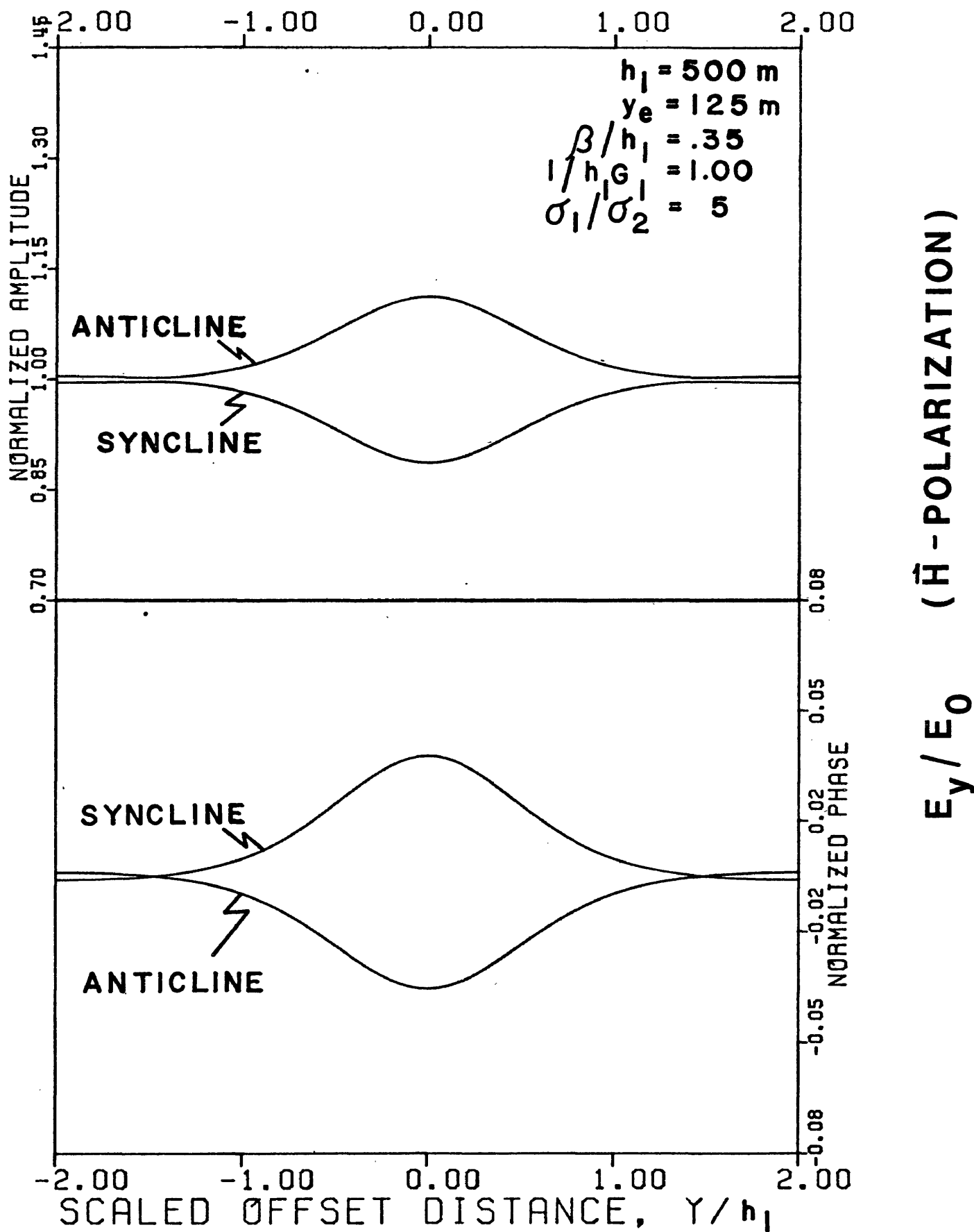


Figure 10

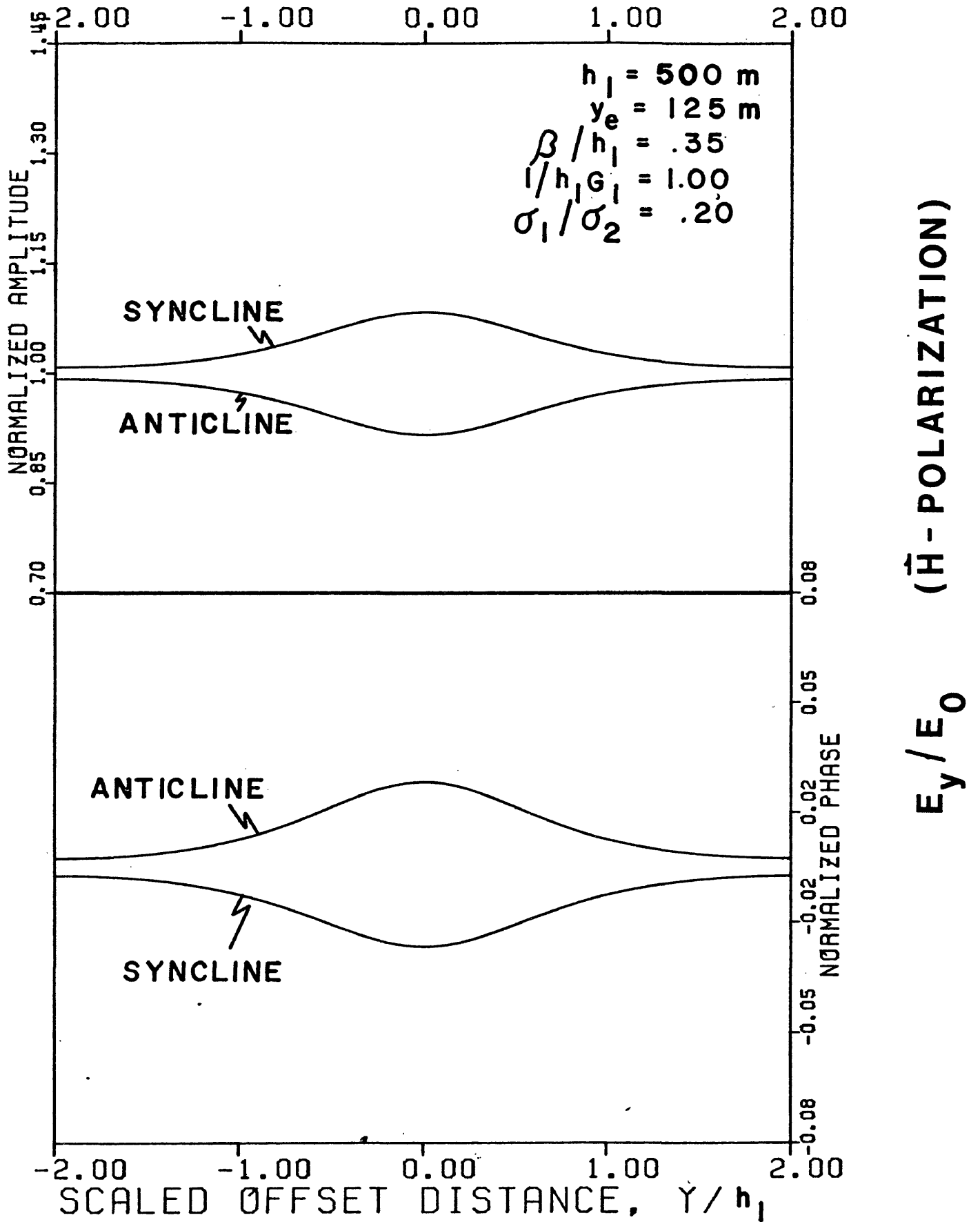


Figure 11

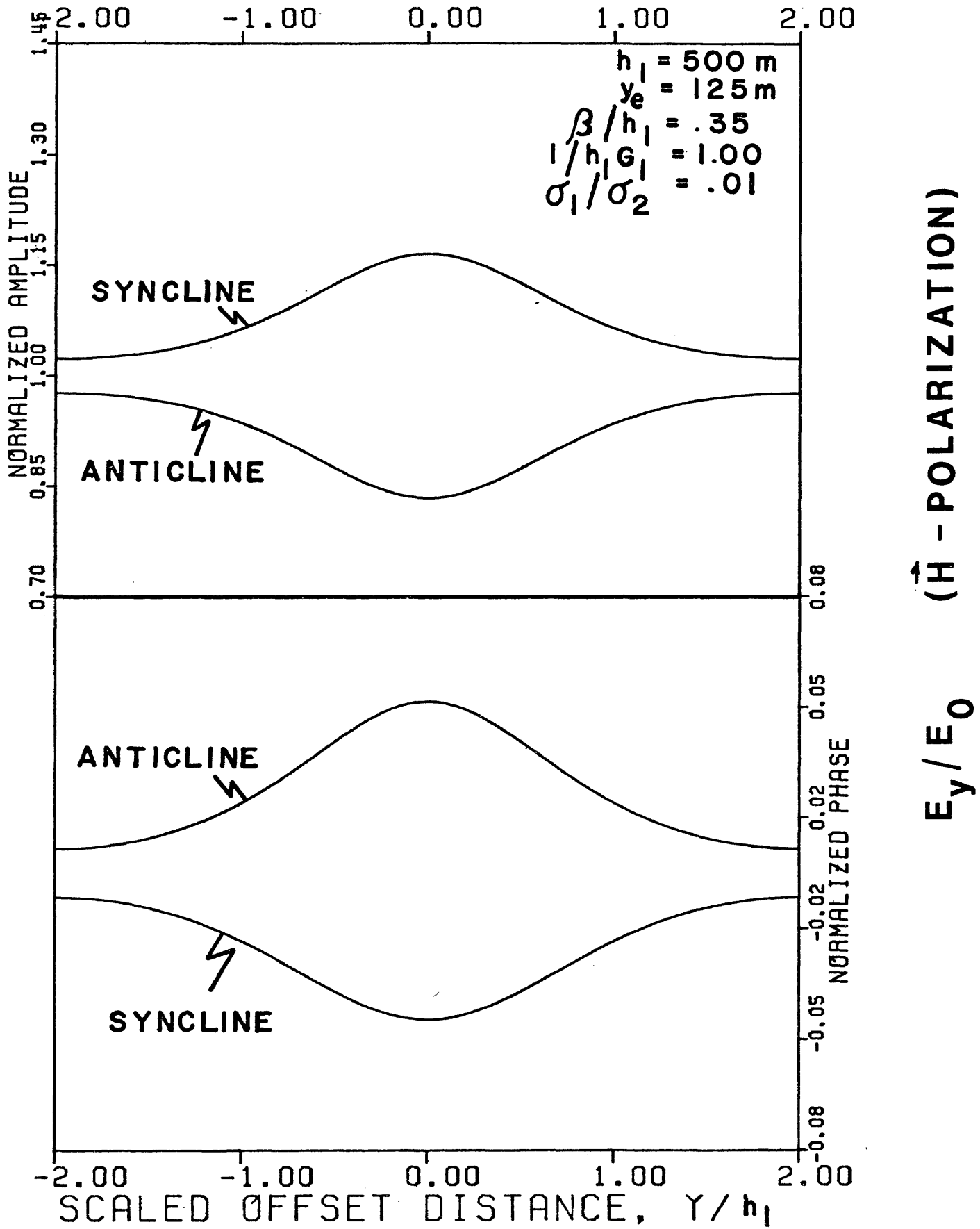


Figure 12

As one might expect, the horizontal electric field increases over a buried resistive ridge whereas it decreases over a buried conductive ridge. The converse is true in the case of a buried synclinal trough. It should be noted that the electric field anomalies are not symmetric for inverted resistivity contrasts given the same structure. For a given subsurface structure, the electric field anomaly is greater when the first layer is more conductive than the second layer than when the second layer is more conductive than the first layer.

Electric Field Master Curves for Anticline for Varying  $\beta$  - - -

Figures 13, 14, 15, and 16 illustrate the relative sensitivity of the horizontal electric field anomaly over an anticlinal ridge to changes in the height  $\beta$  of that ridge for various resistivity contrasts. It is observed that the horizontal electric field component anomaly is more sensitive for a given increase (or decrease) in the relative height of the ridge for larger resistivity contrasts.

Frequency Sounding Electric Field Master Curves for Anticline and

Syncline - - - Figures 17, 18, 19, and 20 portray the effect of changing the ratio of the radian wavelength in the first layer to the first-layer thickness for various resistivity contrasts over an anticlinal ridge. For a given first-layer electrical conductivity  $\sigma_1$ , first-layer thickness  $h_1$ , and ratio of first-layer real radian wavelength to first-layer thickness  $1/h_1 G_1$ , the frequency of the field is determined. It is interesting to note that when the radian wavelength in the first layer

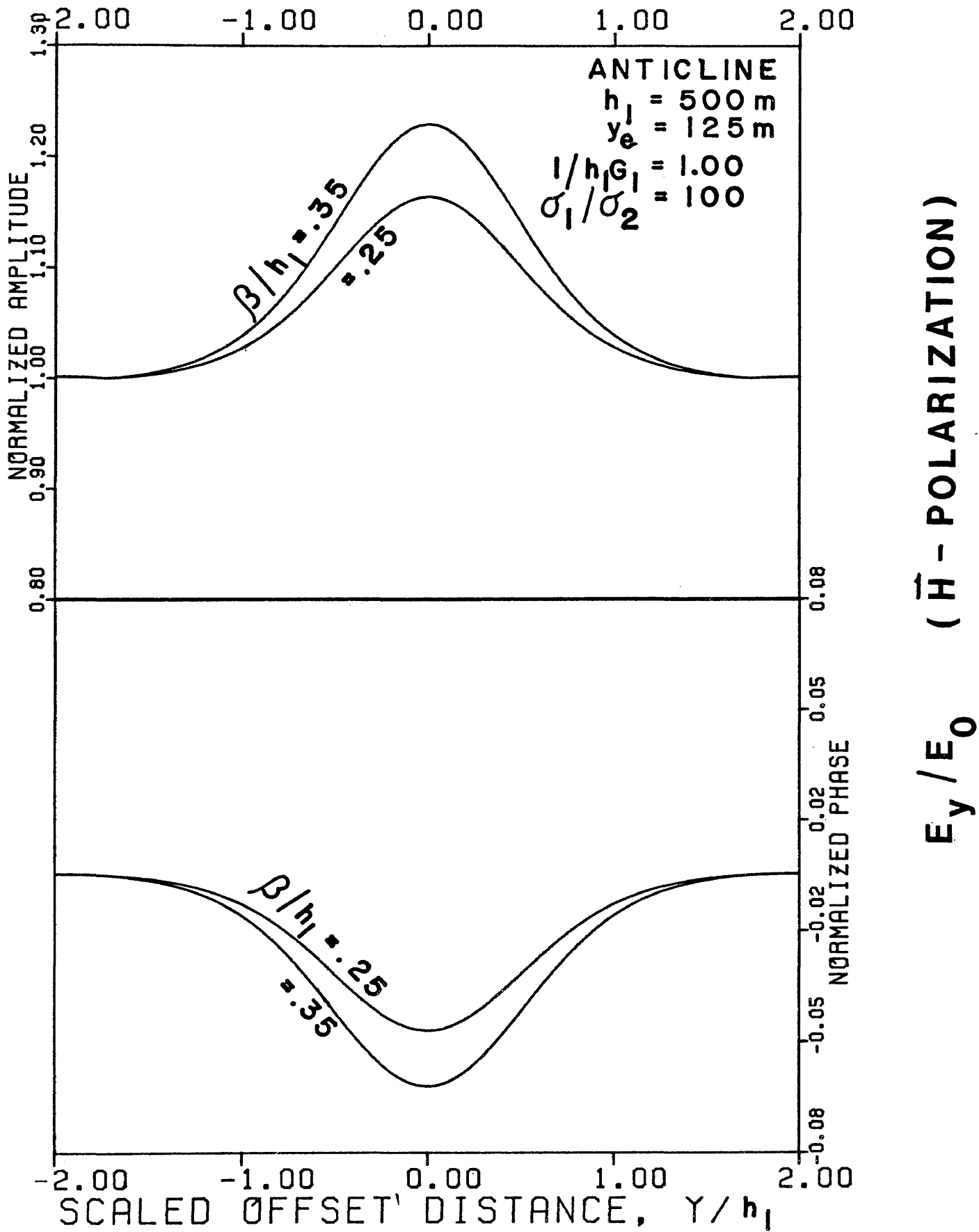


Figure 13

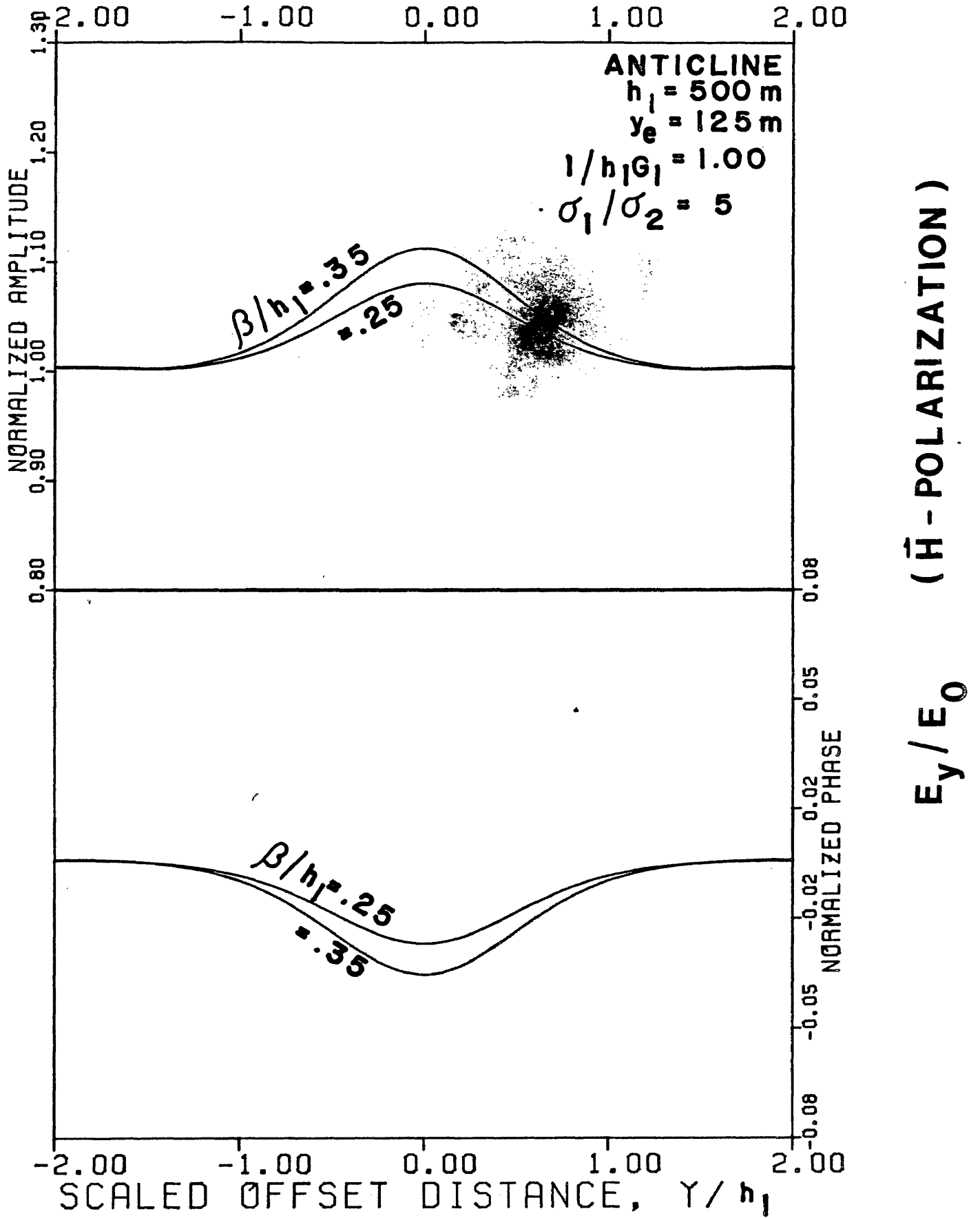


Figure 14

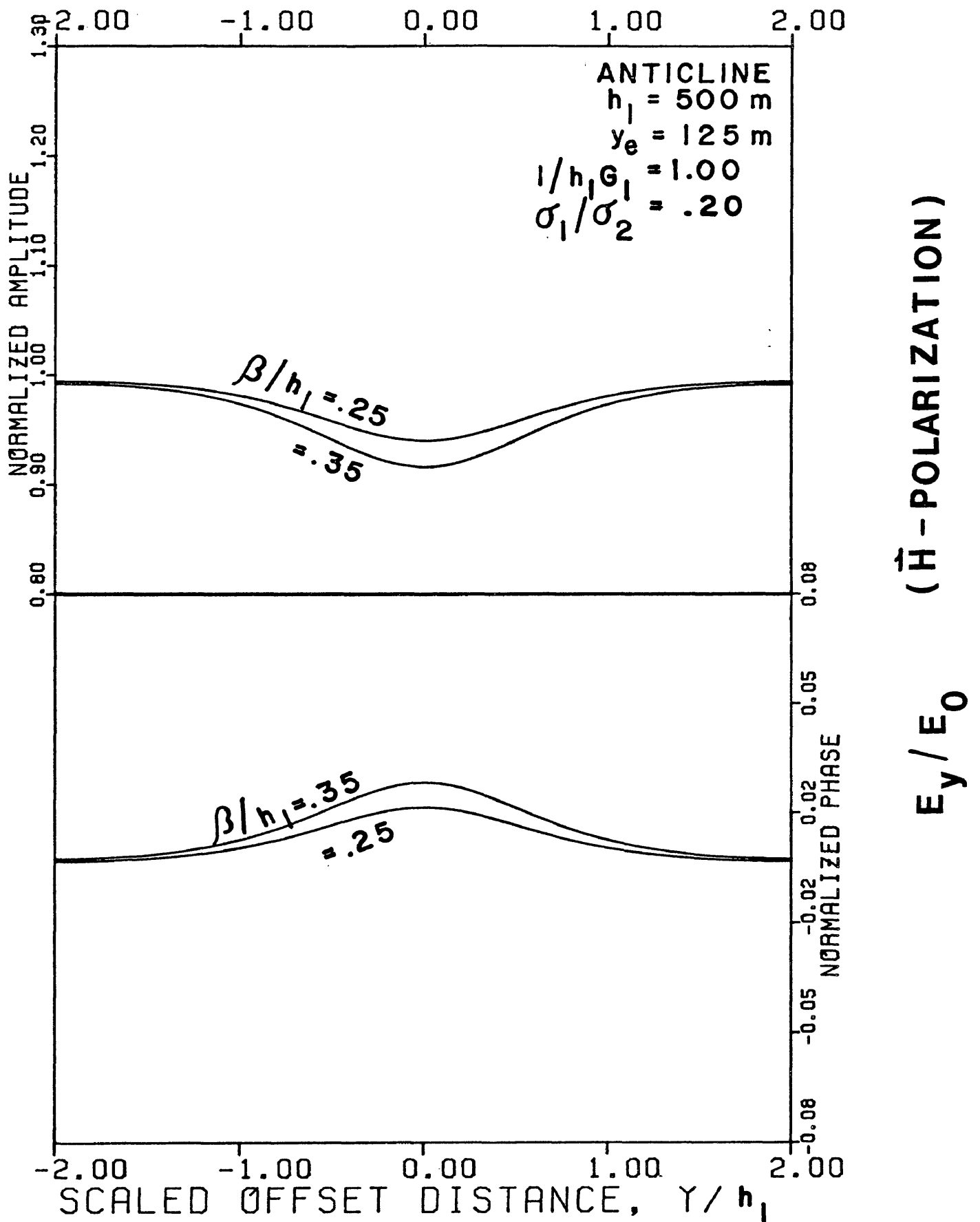


Figure 15

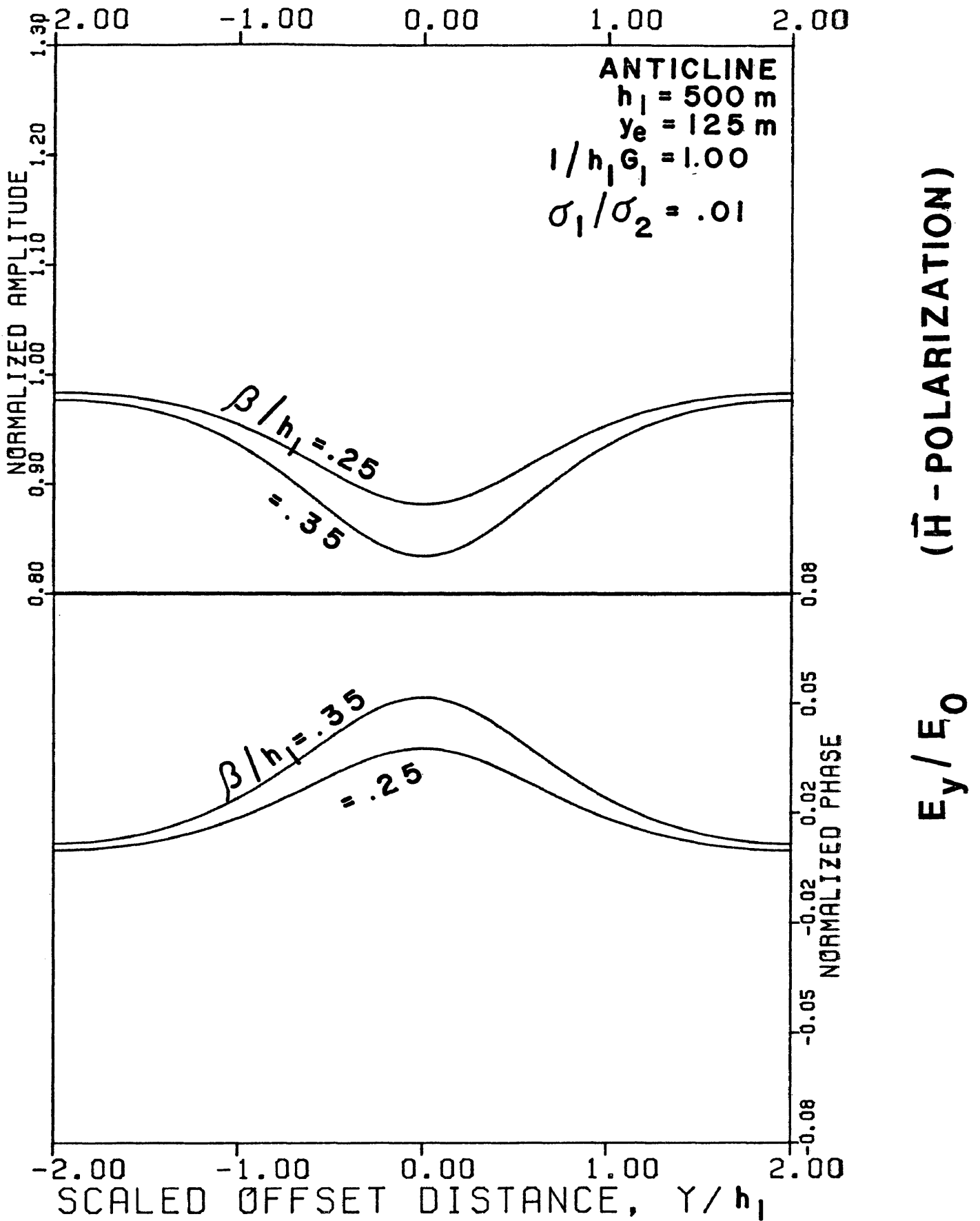


Figure 16

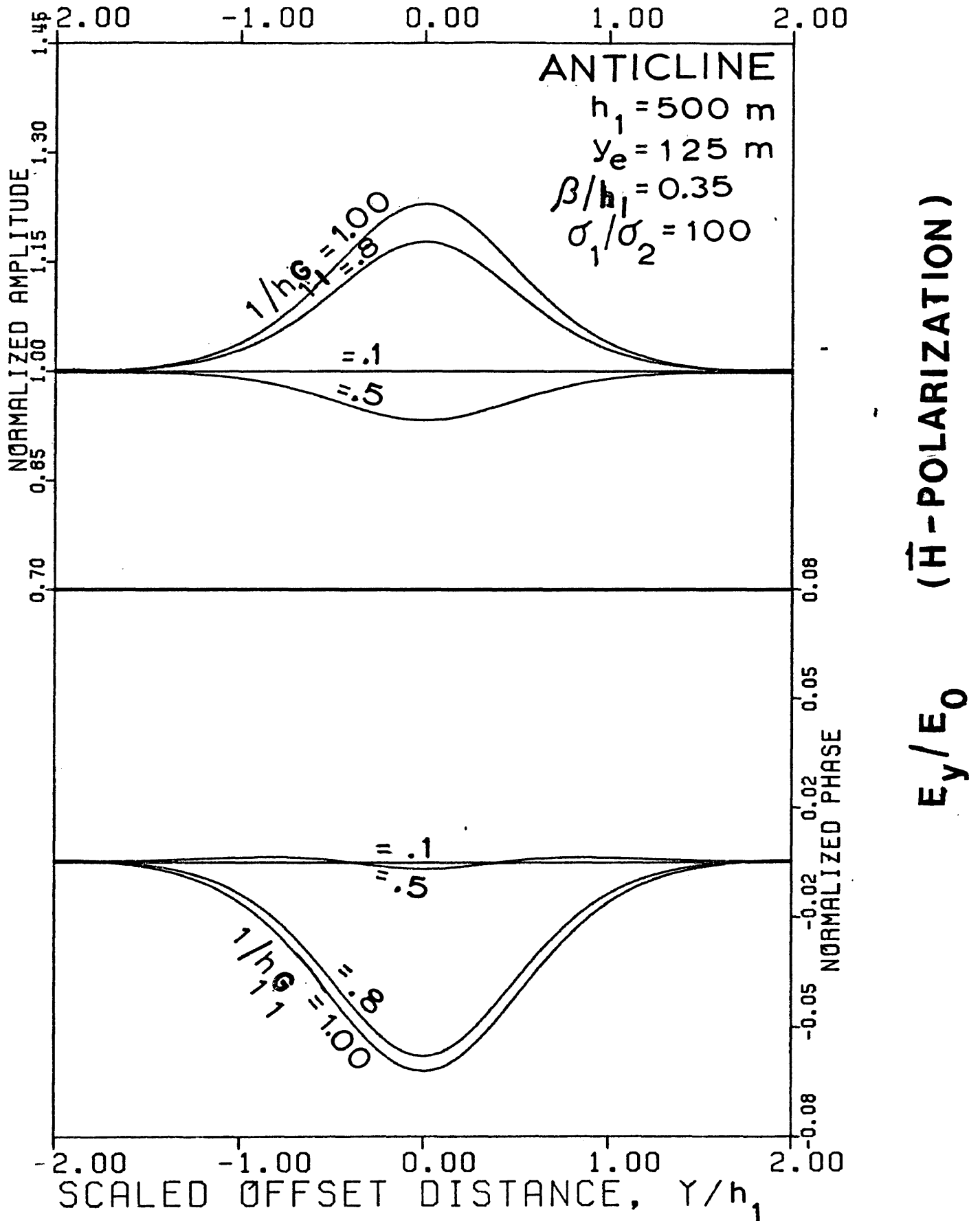


Figure 17

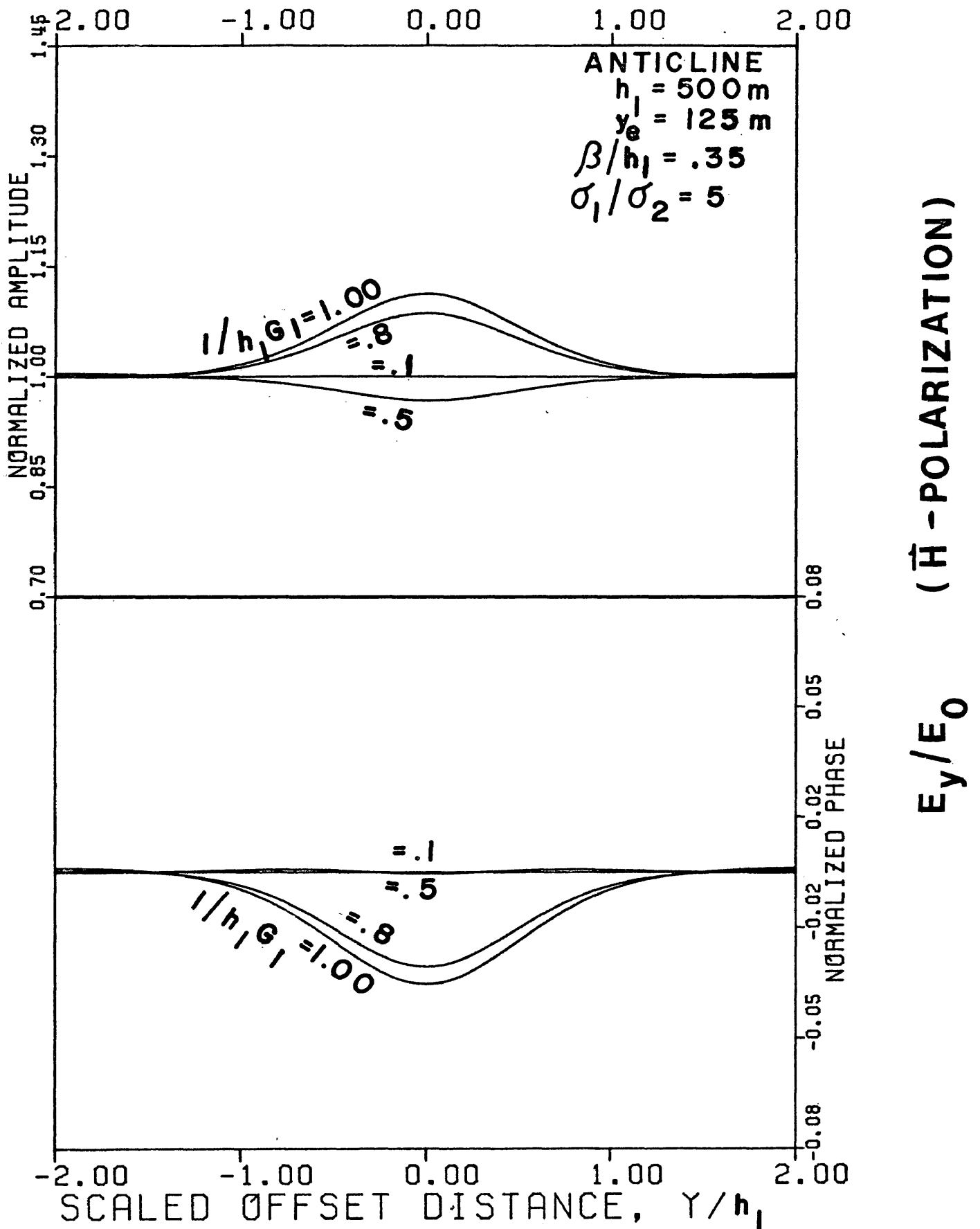


Figure 18

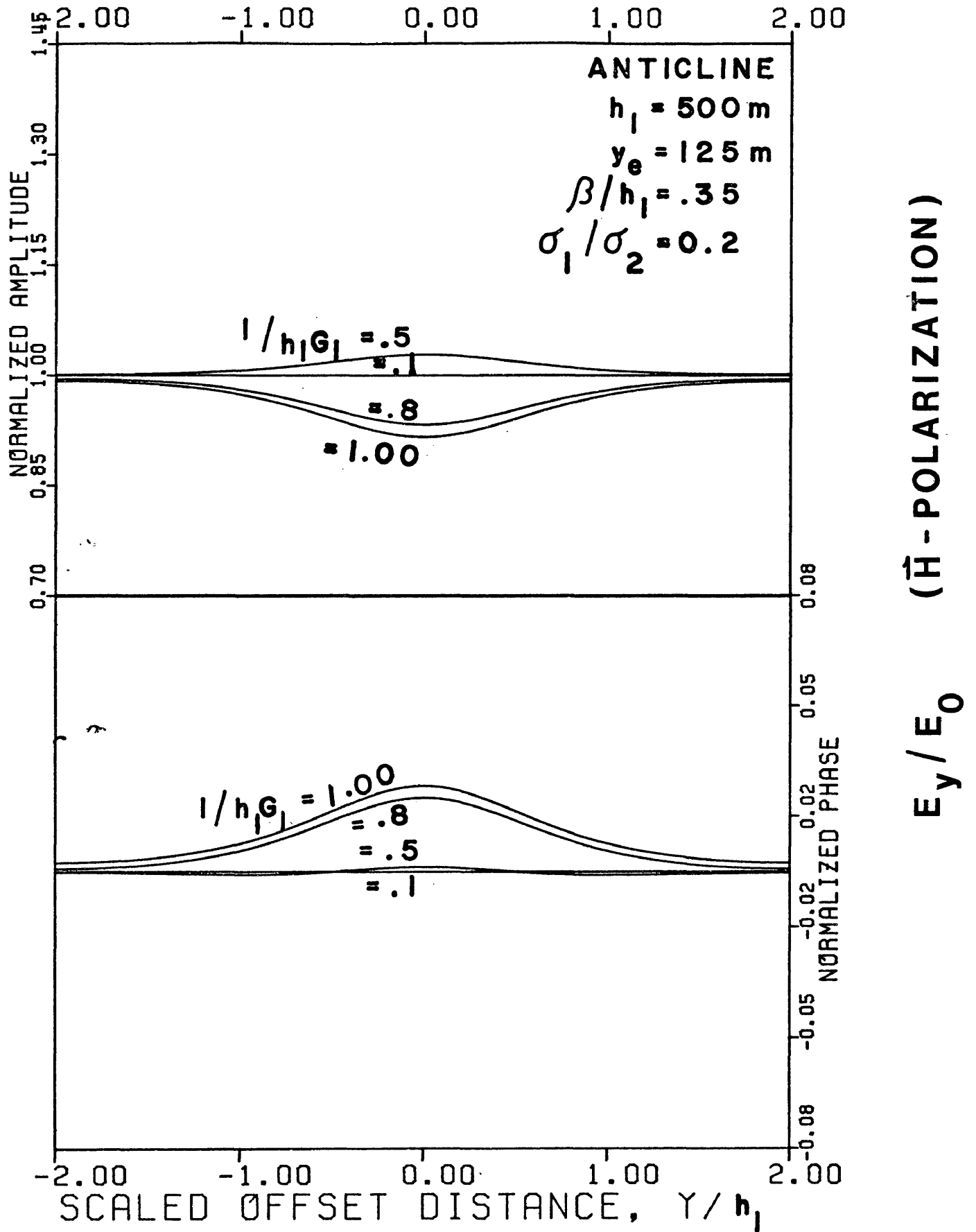


Figure 19

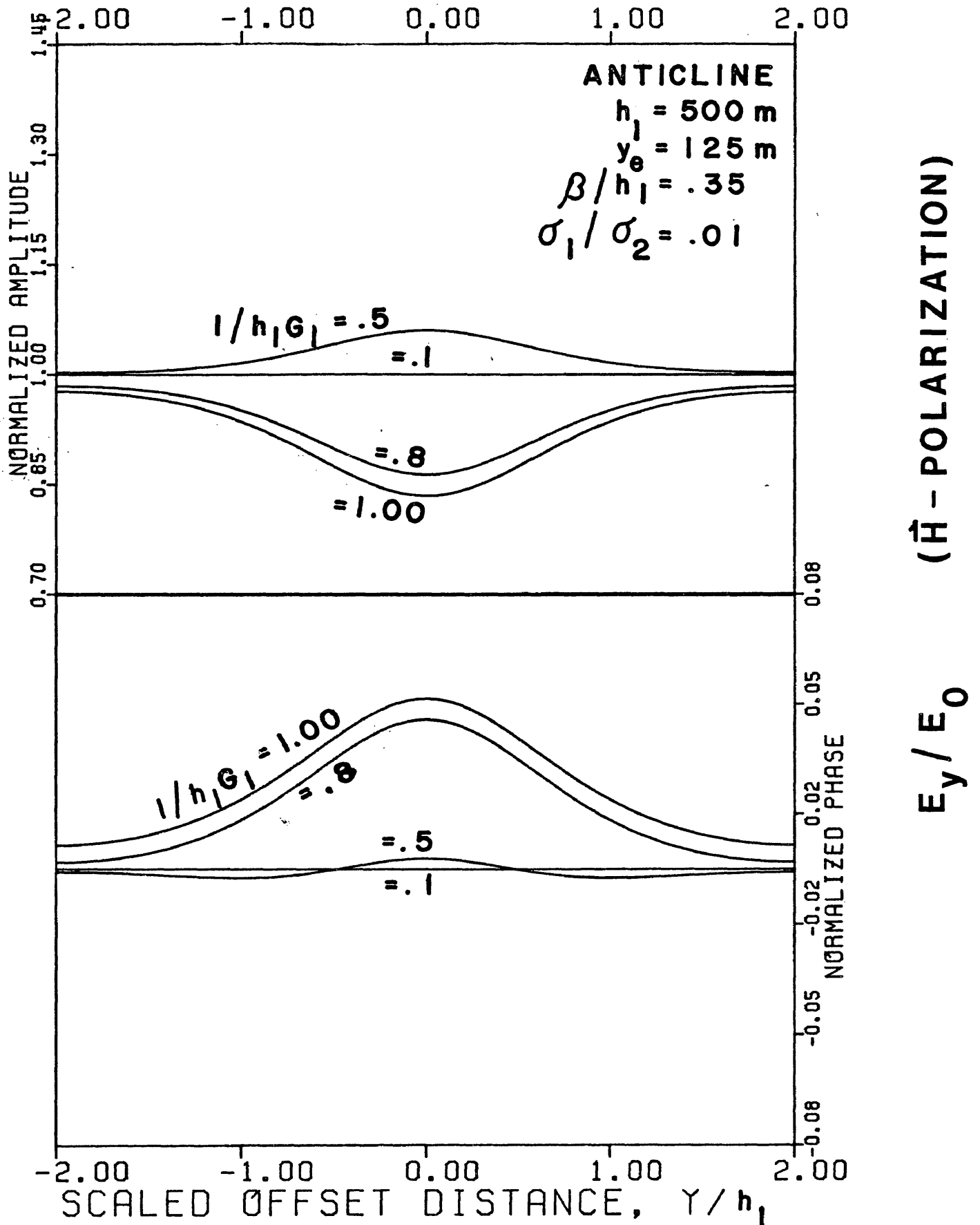


Figure 20

is less than the "effective width"  $2 y_e$ , the electric field decreases over a resistant anticlinal ridge. When the real radian wavelength in the first layer  $1/G_1$  is larger than the effective width  $2 y_e$ , however, the electric field increases over a resistant anticlinal ridge, approaching uniformly the direct current anomaly as  $1/h_1 G_1 \gg 1$ . On the other hand, the electric field increases over a buried conductive ridge when  $1/2 y_e G_1 < 1$  whereas the electric field decreases over a buried conductive ridge when  $1/2 y_e G_1 > 1$ . An increasing electric field over a buried conductive ridge when  $1/2 y_e G_1 < 1$  and a decreasing electric field over a buried resistive ridge when  $1/2 y_e G_1 < 1$  seems due to an interference phenomenon similar to that over a two-layered flat earth.

Figures 21, 22, 23, and 24 illustrate the effect of changing the ratio of the real radian wavelength in the first layer to the first-layer thickness for various resistivity contrasts over a synclinal trough. A very interesting feature in Figures 21 and 22 is that the electric field increases over a synclinal trough when  $1/h_1 G_1 < .8$ , decreases when  $.8 < 1/h_1 G_1 < 1.0$ , and again increases when  $1/h_1 G_1 \gg 1$  for the case where the first layer is more conductive than the second layer. On the other hand, when the first layer is much less conductive than the second (see Figures 23 and 24) the electric field over a synclinal trough decreases when  $0 < 1/h_1 G_1 < .5$ , increases when  $.5 < 1/h_1 G_1 < 1$ , and again decreases for  $1 \ll 1/h_1 G_1$ .

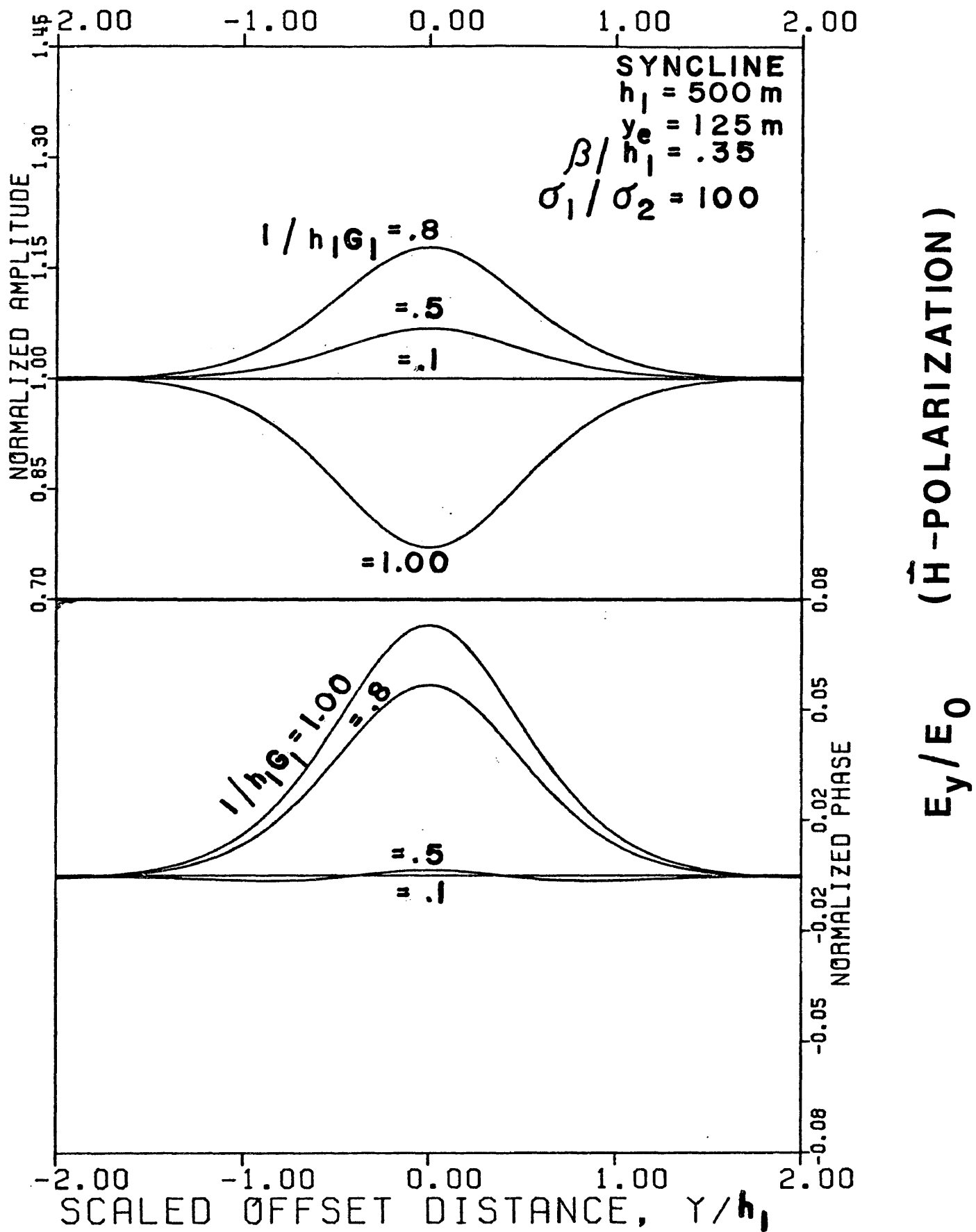
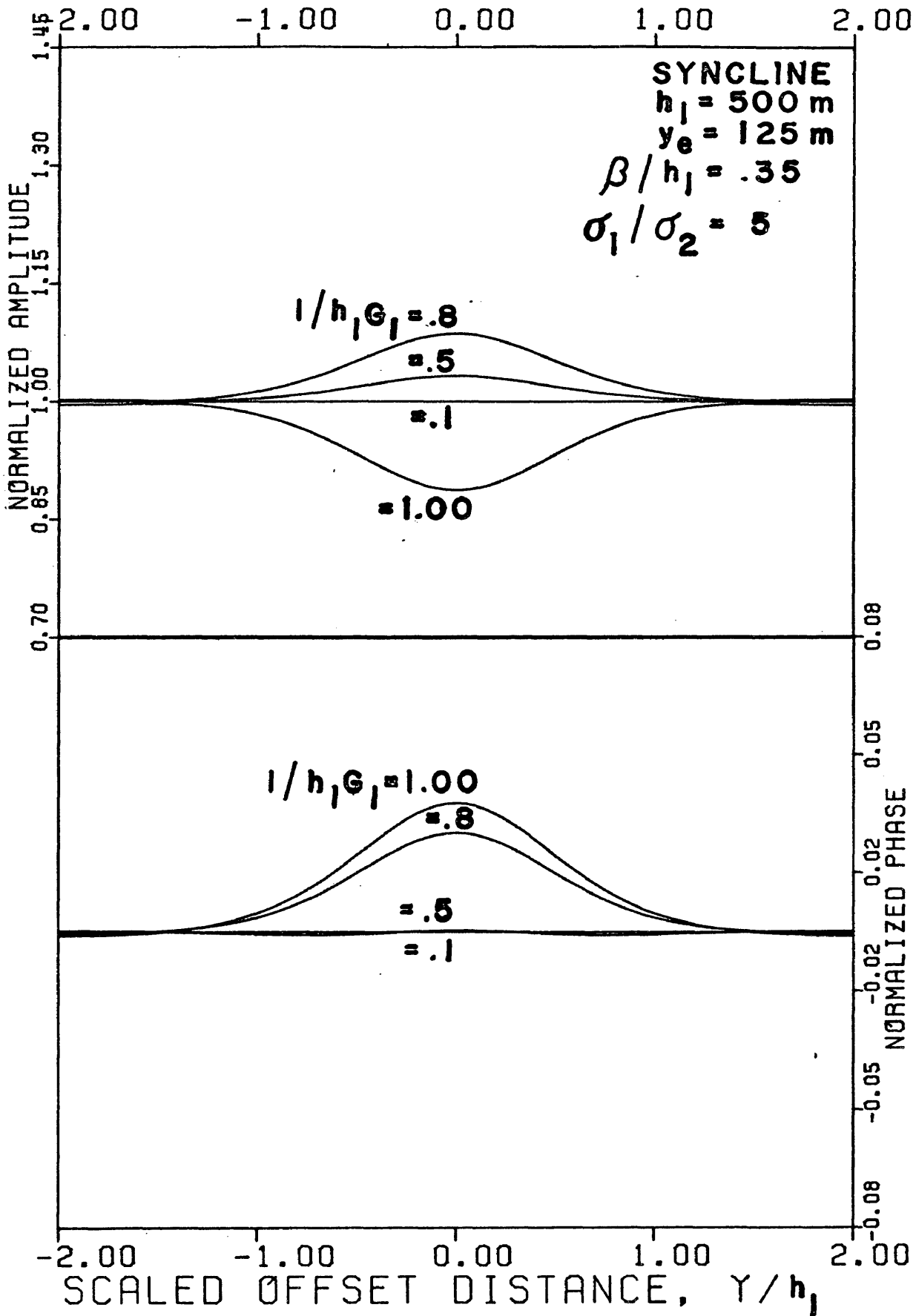
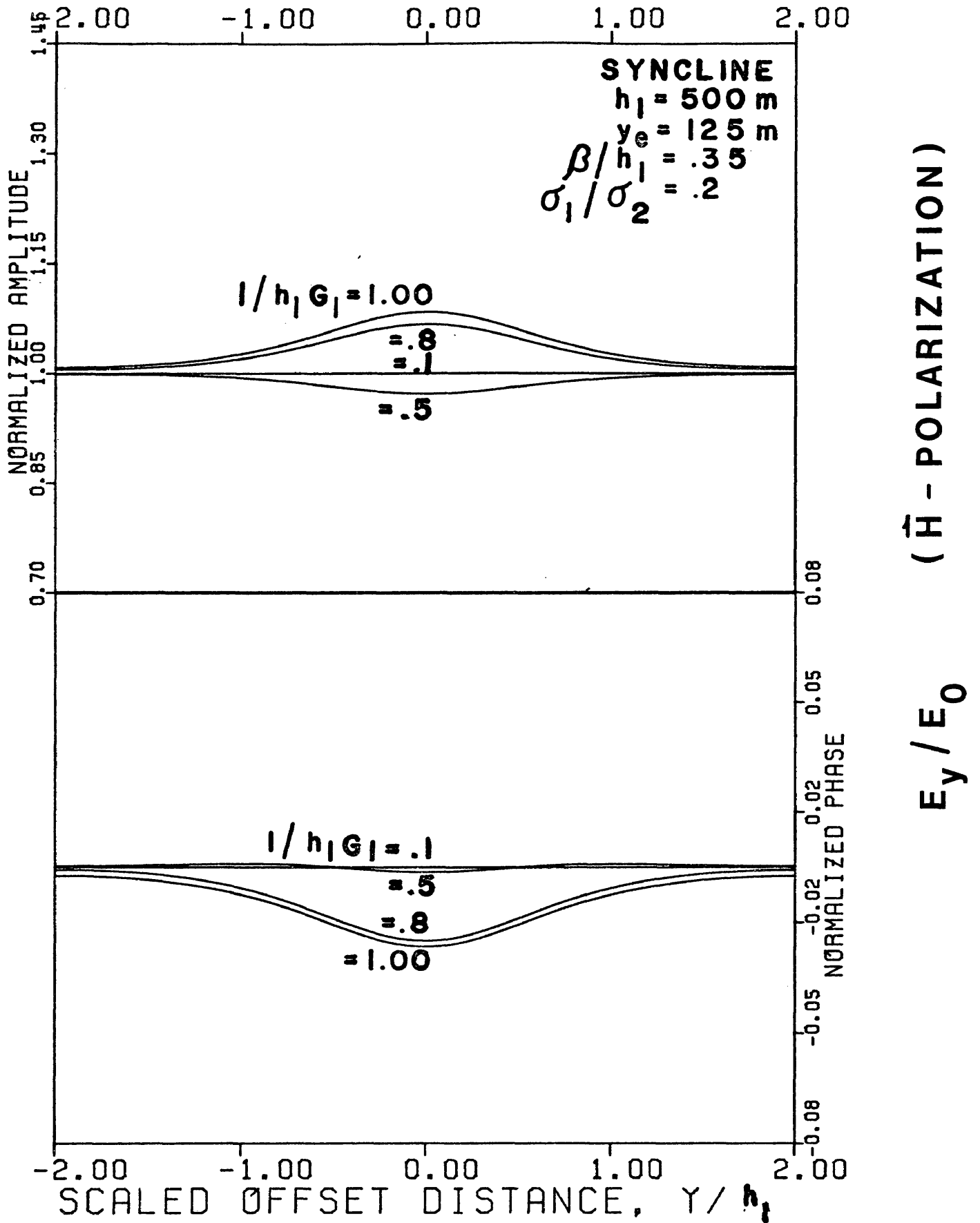


Figure 21



$E_y/E_0$  ( $\vec{H}$ -POLARIZATION)

Figure 22



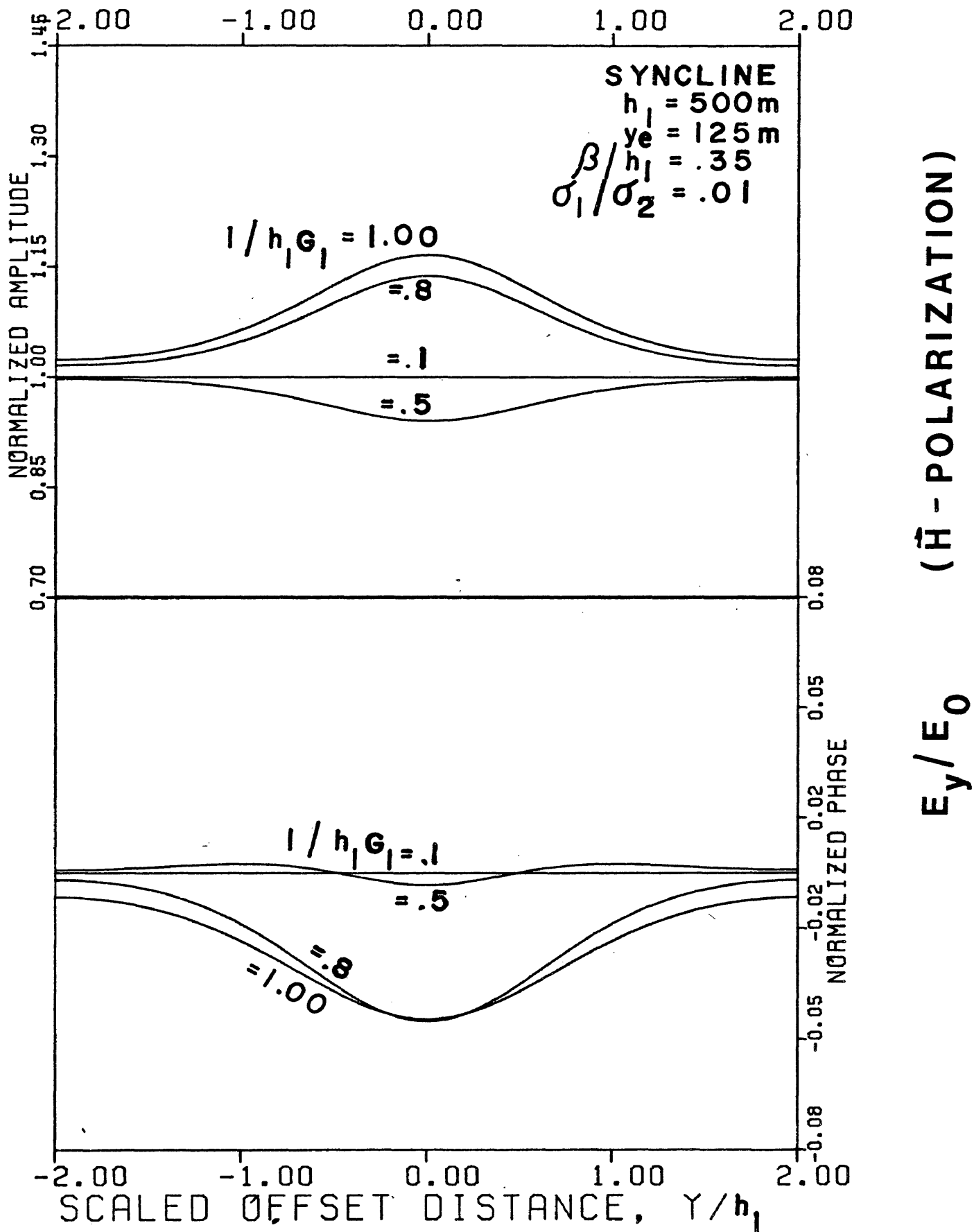
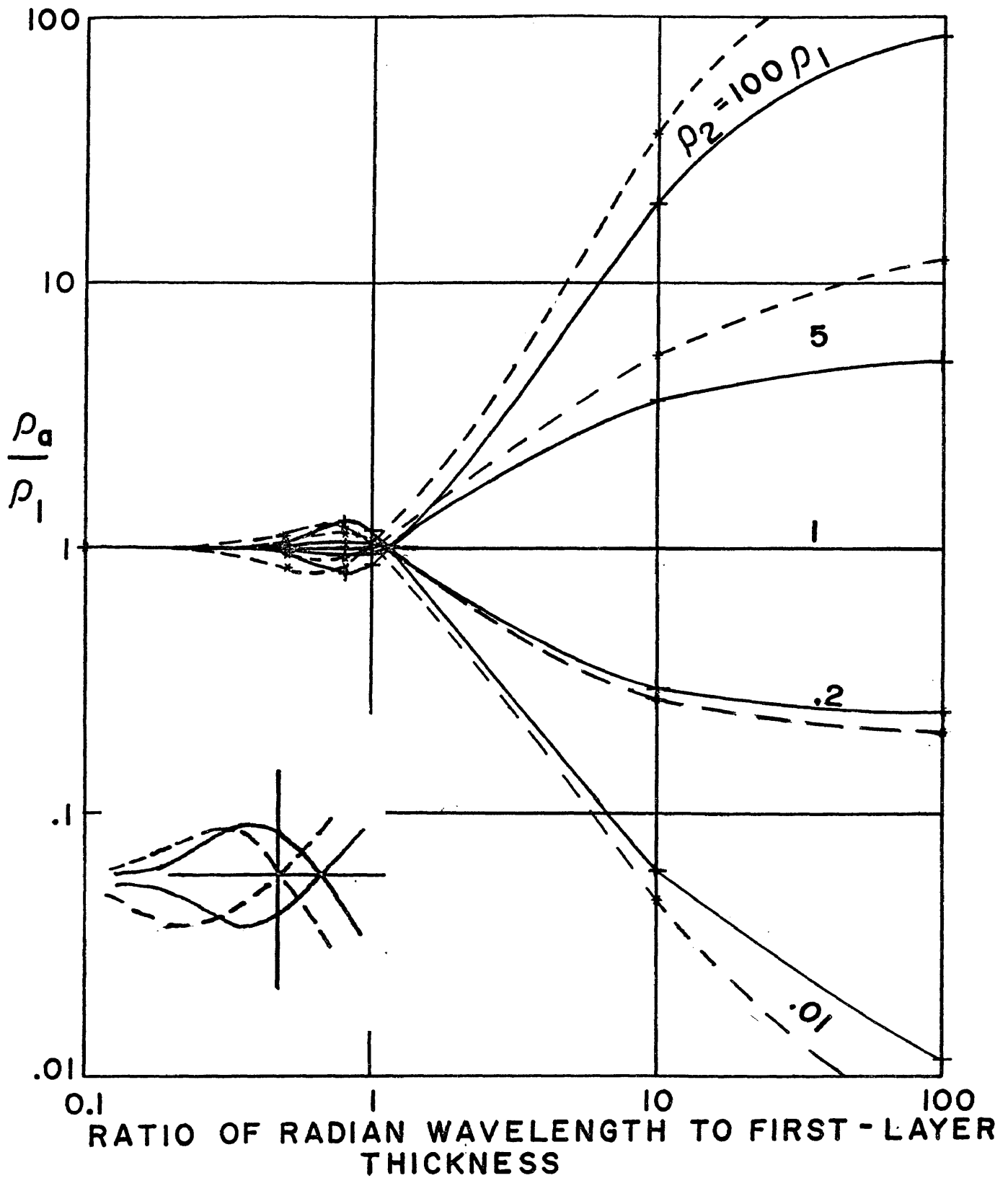


Figure 24

Thus a double interference phenomenon not characteristic of a frequency sounding over an anticlinal ridge is 'apparent.

Apparent Resistivity Master Curves - - - Figure 25 compares magneto-telluric apparent resistivity curves for a two-layered earth for the case where no subsurface structure is present and for the case where an anticlinal ridge is present on the second layer. The offset distance is zero, that is, the calculated apparent resistivities represent what would be measured directly over the axial plane of the ridge if the orthogonal electric and magnetic field components were measured for various  $\omega$  and equation (122) were used. It becomes apparent that the differences in apparent resistivity curves are subtle and, at best, would be somewhat difficult to ascertain in the field in searching for subsurface anticlines. As in the case of horizontal electric field anomalies the apparent resistivity curves are distorted in a nonsymmetric fashion for inverted resistivity contrasts. The intersection points along  $\rho_a/\rho_1 = 1$  are shifted toward the higher frequency range when an anticlinal ridge is present, and the increase in apparent resistivity due to the presence of the anticlinal ridge is greater when the second layer is more resistive than the first layer than the decrease in apparent resistivity when the second layer is more conductive than the first layer.

Figure 26 illustrates magneto-telluric apparent resistivity curves for a two-layered earth for the case where no subsurface



— TWO-LAYERED EARTH WITH NO STRUCTURE  
 - - - TWO-LAYERED EARTH WITH ANTICLINAL RIDGE ON SECOND LAYER

Figure 25

OFFSET DISTANCE = 0  
 $h_1 = 500$  m  
 $\beta / h_1 = .35$

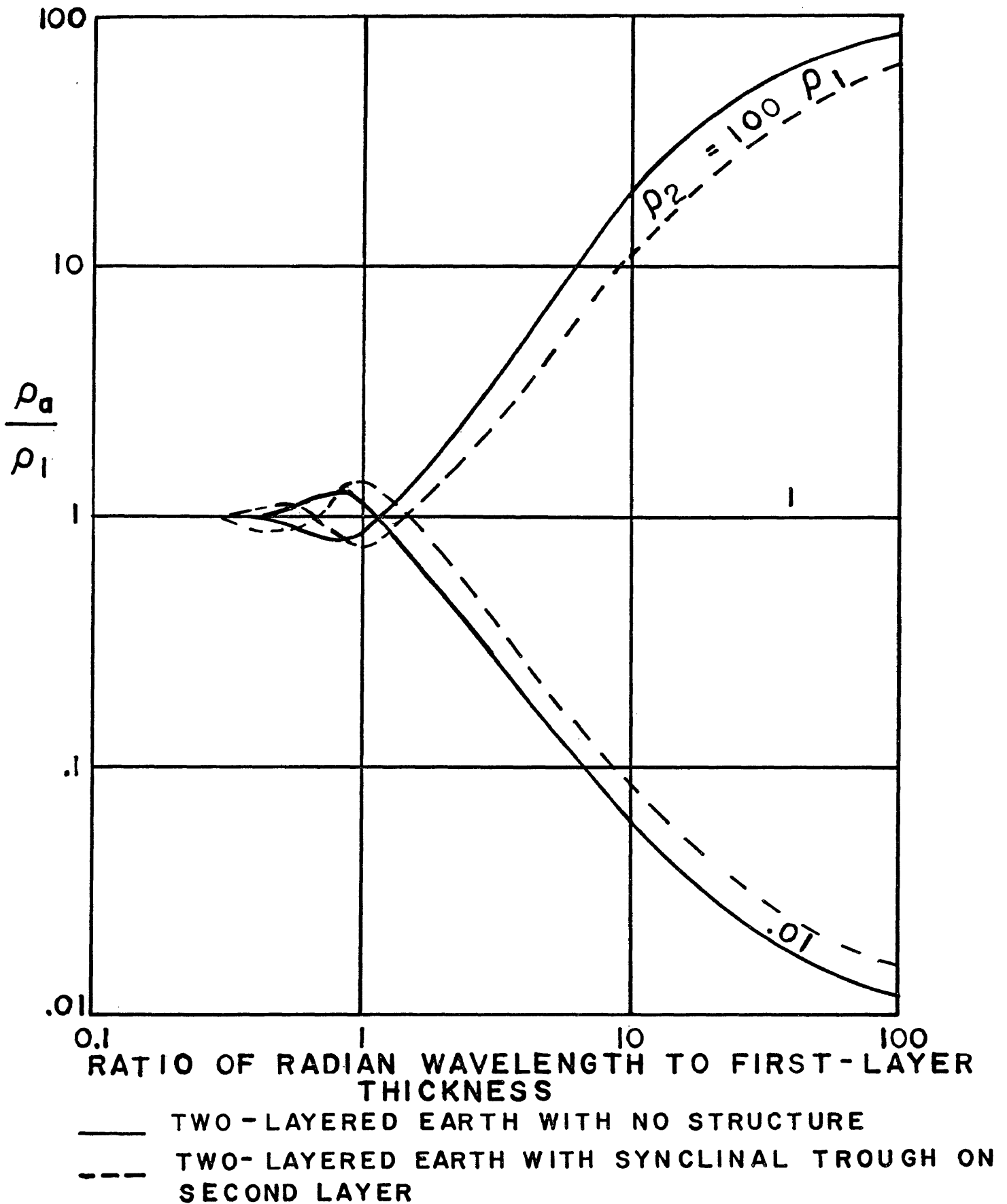


Figure 26

OFFSET DISTANCE = 0  
 $h_1 = 500 \text{ m}$   
 $\beta/h_1 = .35$

structure is present and for the case where a synclinal trough is present on the second layer. Again, the perturbing effect of the synclinal trough is more readily apparent in electric field master curves. An interesting double interference phenomenon is apparent when the ratio of the radian wavelength ( $1/\omega_1$ ) to the first-layer thickness approximately equals unity. The apparent resistivity curves are also distorted in a nonsymmetric fashion for inverted resistivity contrasts. In this case, however, the intersection points along  $\rho_a/\rho_1 = 1$  are shifted toward the lower frequency range with the presence of a synclinal trough (or with lateral thickening of the first layer). The decrease in apparent resistivity due to a lateral thickening of the first layer is greater when the first layer is more conductive than the second layer than the increase in apparent resistivity when the first layer is more resistive than the second layer.

Master Curves for Depth to Subsurface Ridge - - - One of the objectives of this study is to investigate the nature of the electric field and apparent resistivity anomalies over a given buried anticline or syncline, depicting the magnitude of the anomalies for various geometries and for various resistivity contrasts. Such an investigation should serve as a guide for both qualitative and quantitative interpretation in electromagnetic induction prospecting.

The inverse problem is also important; that is, given electric field and apparent resistivity anomalies, to obtain information

about the subsurface geologic structure. One parameter frequently sought in geophysical prospecting is the depth to the top of a buried structure. Many researchers have discussed the same problem in gravity and magnetic prospecting, including Bott and Smith (1958), Morse (1969), Smellie (1967), Henderson and Zietz (1948), Vacquier, Steenland, and Henderson (1951), and Peters (1949).

If the resistivity contrast, electric field anomaly, and first-layer thickness are known, the depth to the crest of an anticlinal ridge may be determined in electromagnetic induction prospecting. This determination is diagrammatically portrayed in Figure 27. The resistivity contrast  $\rho_2/\rho_1$  and first-layer thickness  $h_1$  may be obtained by standard galvanic or electromagnetic induction techniques where  $E_{\max}/E_0 = 1$  (Keller and Frischknecht, 1966). Then, given the peak anomaly, it is an easy matter to determine  $\beta$ , the height of the buried ridge. The depth to the top of the buried ridge is then equal to  $h_1 - \beta$ .

#### Master Curves for Overburden Thickness Determination - - -

Another important parameter frequently sought is overburden thickness. (See Figure 28.) If  $Y_{\frac{1}{2}}$  is designated as the horizontal distance by which the electric field anomaly over a buried ridge (or trough) decays to one-half of its peak value and if some control on the ratio  $2 y_e/h_1$  is obtained by frequency sounding (see Figures 17 - 24), an estimate of the overburden thickness  $h_1$  may be obtained. It is observed that knowledge of the effective

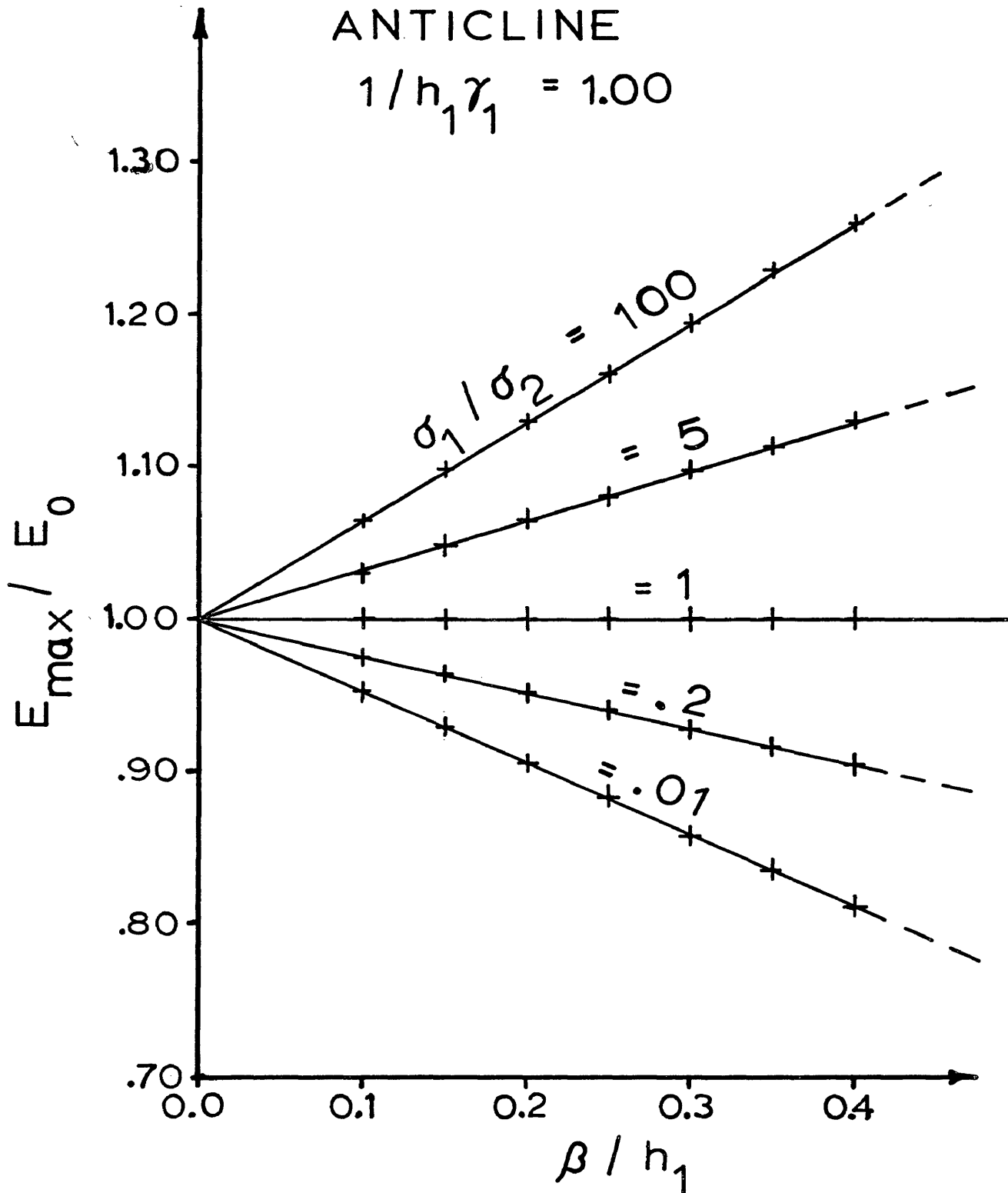


Figure 27

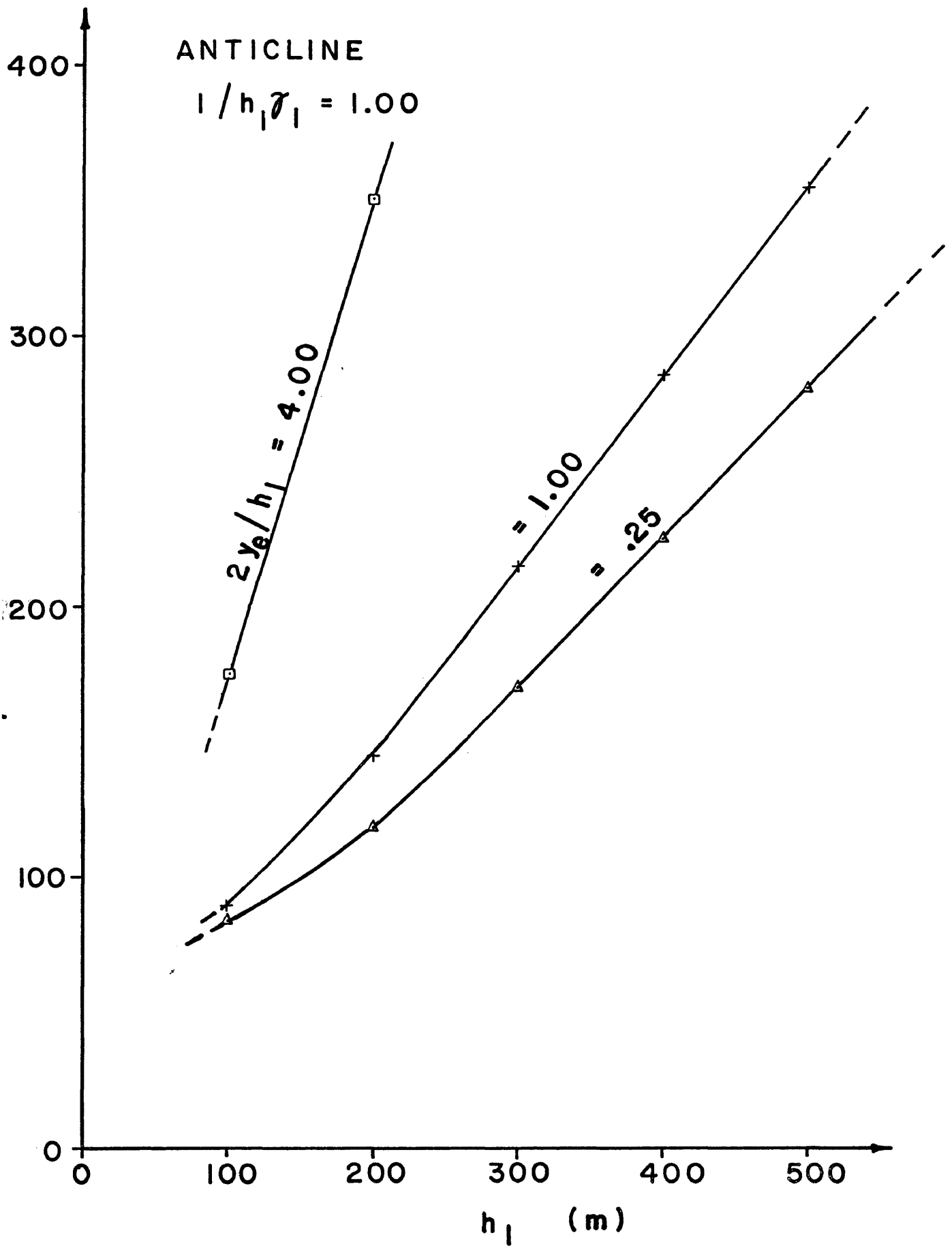


Figure 28

width  $2 y_e$  becomes less important provided that  $2 y_e/h_1$  is less than unity. In such a case, overburden thickness determinations will be in error by less than 15 % provided that the depth to the top of the structure is less than 500 meters. Curves such as those shown in Figure 28 may also be used to determine the effective width of an anomaly-producing geologic structure given an estimate of the overburden thickness.

CONCLUSIONS

Use of Fourier transformation and a perturbation technique presents a powerful method for solving problems in electromagnetic induction prospecting. Direct application of Fourier transformation coupled with a perturbation of the boundary conditions in this investigation has led to a formulation of the electromagnetic field for a two-layered earth with an interface having small perturbations of arbitrary shape. Although this research has concentrated on subsurface geologic structure, the same approach might be used for mapping surface terrain with electromagnetic inductive methods. The extension for geologic modeling purposes to a multi-layered earth with arbitrary interfaces between the layers is straightforward. In addition, a similar approach may be used for dipole excitation.

Both the electric field master curves and the apparent resistivity master curves which have been presented should prove to be of great utility in interpretation of subsurface geologic structure. Electric field master curves lend themselves more readily to quantitative interpretation. With the aid of the master curves, numerous inferences can be made with regard to resistivity contrasts, the geometry of the subsurface geologic structure, the depth of burial of the structure, and the overburden thickness.

REFERENCES

- Berdichevskiy, M. N., 1965, Electrical prospecting with the telluric current method (Translation): Colorado School Mines Quart., v. 60, no. 1, 216 p.
- Bott, M. H. P., and Smith, R. A., 1958, The estimation of the limiting depth of gravitating bodies: Geophys. Prosp., v. 6, no. 1, p. 1 - 10.
- Bracewell, R., 1965, The Fourier transform and its applications: New York, McGraw-Hill, Inc., 381 p.
- Cagniard, L., 1953, Basic theory of the magneto-telluric method of geophysical prospecting: Geophysics, v. 18, no. 3, p. 605 - 635.
- Davydov, V. M., 1968, Electromagnetic field of arbitrary source above gently sloping structures: Geologiya i Geofizika, no. 6, p. 83 - 92.
- de Hoop, A. T., 1958, Representation theorems for the displacement in an elastic solid and their application to elastodynamic diffraction theory: D. Sc. thesis, Technische Hogeschool, Delft.
- Dieter, K., Paterson, N. R., and Grant, F. S., 1969, IP and resistivity type curves for three-dimensional bodies: Geophysics, v. 34, no. 4, p. 615 - 632.

- Dmitriev, V. I., 1965, Method of calculating the magnetotelluric field in an inhomogeneous layer with wave-like perturbations of the lower surface: Prikl. Geofiz., v. 41, publ. by "Nedra", Moscow.
- \_\_\_\_\_, 1969, Calculation of the magnetotelluric field in a layer with an arbitrarily shaped flexure of the lower surface for the case of H-polarization: Prikl. Geofiz., v. 51, publ. by "Nedra", Moscow.
- Feinberg, E. L., 1961, Propagation of radio waves along real surfaces: in Propagation of radio Waves over the earth, ch. 2, publ. by Akad. Nauk. SSSR.
- Fuks, B. A., and Shabat, B. V., 1949, Funktsii kompleksno-go peremennogo (Functions of complex variable): GONTI.
- Grant, F. S., and West, G. F., 1965, Interpretation theory in applied geophysics: New York, McGraw-Hill, Inc., 584 p.
- Gray, R. L., 1965, The elements of linear filter theory: Special Notes of the Department of Geophysics, Colorado School of Mines, 145 p.
- Henderson, R. G., and Zietz, I., 1948, Analysis of total magnetic intensity anomalies produced by point and line sources: Geophysics, v. 13, p. 428 - 436.
- Hildebrand, F. B., 1965, Methods of applied mathematics: London, Prentice-Hall International, Inc., 362 p.
- Hv̄zdara, M., 1968, Electromagnetic induction in a halfspace with an oblique interface: Ceskoslovenska Akad. ved Studia Geophysica et Geodaetica, v. 12, p. 304 - 320.

- Jones, D. S., 1964, The theory of electromagnetism: New York, John Wiley and Sons, 641 p.
- Kaplan, W., 1959, Advanced calculus: Reading, Mass., Addison-Wesley, 679 p.
- Keller, G. V., and Frischknecht, F. C., 1966, Electrical methods in geophysical prospecting: New York, Pergamon Press, 519 p.
- Keller, G. V., 1968, Electrical prospecting for oil: Colorado School Mines Quart., v. 63, no. 2, 268 p.
- Knopoff, L., 1956, Diffraction of elastic waves: Jour. Acoust. Soc. Am., v. 28, p. 217 - 229.
- Knopoff, L., and Hudson, J. A., 1964, Transmission of Love waves past a continental margin: Jour. Geophys. Research, v. 69, p. 1649 - 1653.
- Kober, H., 1957, Dictionary of conformal representation: New York, Dover Inc., 208 p.
- Kunetz, G., and Chastenet deGery, J., 1956, La representation conforme et divers problemes de potentiel dans des milieux de "permeabilite" differente: Revue de l'Institut Francais du Petrole et Annales des Combustibles Liquides, v. 11, no. 10, p. 1179 - 1192.
- Mann, J. E., Jr., 1964, Magnetotelluric theory of the sinusoidal interface: Jour. Geophys. Research, v. 69, no. 16, p. 3517 - 3524.
- Morse, P. M., and Feshbach, H., 1953, Methods of theoretical physics, parts I and II, New York, McGraw-Hill, 1939 p.

- Morse, D. J., 1969, Some remarks concerning the Bott-Smith inequalities for depth determinations of gravitating bodies: Jour. Canadian Soc. Explor. Geophysics, v. 5, no. 1, p. 91 - 112.
- Neyman, L. R., and Kalantarov, P. L., 1948, Teoreticheskiye osnovy elektrotekhniki (Theoretical foundation of electrotechnics): v. 3, Gosenergoizdat.
- Obukhov, G. G., 1962, Computation of magnetotelluric fields in an inhomogeneous layer: Prikl. Geofiz., v. 35, Gostoptekhizdat.
- \_\_\_\_\_, 1965, Magnetotelluric fields over buried structures (E-polarization): Prikl. Geofiz., v. 46, publ. by "Nedra", Moscow.
- \_\_\_\_\_, 1969, Magnetotelluric fields over an uneven insulating basement surface: Prikl. Geofiz., v. 49, publ. by "Nedra", Moscow.
- Papoulis, A., 1962, The Fourier integral and its applications: New York, McGraw-Hill, 318 p.
- Peters, L. J., 1949, The direct approach to magnetic interpretation and its practical application: Geophysics, v. 14, p. 290 - 320.
- Rellich, F. 1943, Jahresber Deutschen Math. Vereinigung, v. 53 and 57.
- Roy, K. K., 1969, Theoretical and model investigations on electro-telluric field response of some geological inhomogeneities: Ph. D. thesis, Indian Institute of Technology, Kharagpur, India.

- Sheynmann, S. M., 1941, Elementy teorii elektrorazvedki anizotropnykh sred (The elements of the theory of electric prospecting of anisotropic mediums): Tr. VSEGEI, vyp. 9, 10, Gosgeolizdat.
- \_\_\_\_\_, 1958, O vozmozhnosti ispol'zovaniya poley telluricheskikh tokov i dalnikh radiostantsiy dlay geologicheskogo kartirovaniya (On the possibility of using telluric current fields and remote radio stations for geological mappings): Tr. Vses. in-ta metodiki i tekhniki razvedki, Gostoptekhizdat.
- Smellie, D. W., 1967, Elementary approximations in aeromagnetic interpretation: Mining geophysics, v. 2, p. 474 - 489.
- Smirnov, V. T., 1948, Kurs vyshey matematiki (A course of higher mathematics): GONTI.
- Sommerfeld, A., 1964, Partial differential equations in physics: New York, Academic Press, 335 p.
- \_\_\_\_\_, 1964, Electrodynamics: New York, Academic Press, 371 p.
- Stratton, J. A., 1941, Electromagnetic theory: New York, McGraw-Hill, 615 p.
- Utzman, R. V., and Faire, B., 1957, Influence de la non-cylindricite des structures sur le champ tellurique. Etude sur modeles pour les anticlinaux resistants: Rev. Inst. Francais du Petrole., v. 12, no. 2, p. 135 - 144.
- Vacquier, V., Steenland, N. C., Henderson, R. G., and Zietz, I., 1951, Interpretation of aeromagnetic maps (memoir 47): New York, Geol. Soc. Am., 151 p.

- Vozoff, K., Ellis, R. M., and Burke, M. D., 1964, Telluric currents and their use in petroleum exploration: Am. Assoc. Petroleum Geologists Bull., v. 48, no. 12, p. 1890 - 1901.
- Weaver, J. T., 1963, The electromagnetic field within a discontinuous conductor with reference to geomagnetic micropulsations near a coast line: Jour. Physics, v. 41, p. 484 - 495.
- Yungul, S. H., 1961, Magneto-telluric three-layer sounding curves: Geophysics, v. 26, no. 4, p. 465 - 473.
- Zaborovskii, A. I., 1943, Elektrorazvedka (Electric prospecting): GONTI.